Design and Study of Rh(III) Catalysts for the Selective Tail-to-Tail Dimerization of Methyl Acrylate

Elisabeth Hauptman,[†] Sylviane Sabo-Etienne,[†,‡] Peter S. White,[†] Maurice Brookhart,*[,†] J. Michael Garner,[§] Paul J. Fagan,[§] and Joseph C. Calabrese[§]

Contribution from the Department of Chemistry, University of North Carolina, Chapel Hill, North Carolina 27599-3290, and Central Research and Development Department, E. I. DuPont de Nemours and Co., Inc., Experimental Station, P.O. Box 80328, Wilmington, Delaware 19880-0328

Received January 13, 1994[⊕]

Abstract: The development of an efficient, highly selective Rh(III) catalyst system for the tail-to-tail dimerization of methyl acrylate (MA) to dimethyl hexenedioates, precursors to adipic acid, is described. The catalytic cycle is entered by protonation of $Cp^*Rh(C_2H_4)_2$ ($Cp^* = C_5Me_5$) to yield $Cp^*Rh(C_2H_4)(CH_2CH_2\text{-}\mu\text{-}H)^+$ (**7**) followed by reaction with methyl acrylate. The catalyst resting state has been generated by low-temperature protonation of $Cp^*Rh(CH_2CHCO_2CH_3)_2$ (**15**) and identified as $Cp^*Rh(CH_2CH_2COOMe)(\eta^2\text{-}CH_2CHCO_2Me)^+$ (**8**) by ^1H and ^{13}C NMR spectroscopy. Investigation of iridium analogs has led to the isolation and X-ray structural characterization of $Cp^*Ir(CH_2CH_2COOMe)(\eta^2\text{-}CH_2CHCO_2Me)^+$ (**23a**), in which the orientation of the acrylate ligands is that required for tail-to-tail coupling. At −23 °C, complex **8** undergoes β-migratory insertion to give $Cp^*RhCH(CH_2COOMe)(CH_2CH_2COOMe)^+$ (**10**). Complex **10** was independently synthesized by treatment of complex **7** with *trans*-$MeO_2CCH{=}CHCH_2CH_2CO_2Me$ and was characterized by X-ray crystallography. The free energy of activation for the migration reaction is 18.7 kcal/mol and matches that based on the catalytic turnover (TO) frequency (6.6 TO/min at 25 °C, $\Delta G^‡$ = 19 kcal/mol). This observation confirms **8** as the resting state and the C–C coupling reaction as the turnover-limiting step. The catalyst deactivates by formal loss of H_2 from complex **10** to produce $Cp^*Rh(\eta^3\text{-}CH_3OCOCH_2CHCHCHCO_2CH_3)^+$ (**9**). The structure of complex **9** was verified by an X-ray crystallographic study. Exposure of **9** to an atmosphere of H_2 in the presence of MA regenerates the resting state **8**, and dimerization proceeds. Second generation catalysts with increased activity and lifetimes have been developed by replacing the C_5Me_5 ligand by methylated indenyl ligands. Using the catalytic system derived from (1,2,3-trimethylindenyl)$Rh(C_2H_4)_2$ (**11**), conversion of 54 000 equiv of methyl acrylate to dimethyl hexenedioates could be achieved after 68 h at 55 °C under N_2. Details of the mechanism have been elucidated and resemble closely those of the Cp^* system. Similar intermediates to **8** and **10** have been characterized by ^1H and ^{13}C NMR spectroscopy. In contrast, treatment with methyl acrylate of the more electrophilic systems derived from $CpRh(C_2H_4)_2$ (**25**) ($Cp = C_5H_5$) and $Cp'Rh(C_2H_4)_2$ (**30**) ($Cp' = C_5(CH_3)_4CF_3$) results in slow dimerization. Low-temperature protonation of $CpRh(CH_2CHCO_2CH_3)_2$ (**27**) with $H(Et_2O)_2BAr'_4$ yields a mixture of rhodium species which upon warming to 23 °C converge to the bis-chelate complex $CpRhCH(CH_2COOMe)(CH_2CH_2COOMe)^+$ (**28**). Exposure of complex **28** to MA generates the unusual bridged species $CpRh(CH_2CHCOOCH_3)H(CH_2CHCOOCH_3)^+$ (**29**), which serves as the resting state during dimerization. Treatment of complex **30** with $H(Et_2O)_2BAr'_4$ yields $Cp'Rh(C_2H_4)(CH_2CH_2\text{-}\mu\text{-}H)^+$ (**31**), which upon reaction with MA clearly produces $Cp'RhCH(CH_2COOMe)(CH_2CH_2COOMe)^+$ (**33**), and dimerization proceeds. Finally, attempts to catalyze the dimerization of other functionalized olefins including methyl vinyl ketone, methyl crotonate, 2-vinylpyridine, and 1-vinyl-2-pyrrolidinone are presented.

Introduction

The exploration of alternative routes to the Nylon-6,6 intermediates hexamethylenediamine (via adiponitrile hydrogenation) and adipic acid is an active area of industrial research with goals of reducing investment and feedstock costs or improving environmental performance over those of existing manufacturing technologies.[1] Processes utilizing several different feedstocks (C3, C4, and C6) compete for the worldwide production of adiponitrile: (1) Monsanto's electrohydrodimerization of acrylonitrile, (2) DuPont's hydrocyanation of 1,3-butadiene, and (3) dehydrative amination of adipic acid. However, all commercial routes to adipic acid involve C6 feedstocks: (1) oxidative cleavage of cyclohexane and (2) hydration of cyclohexene followed by oxidative cleavage of cyclohexanol.

The linear catalytic dimerization of acrylic esters would represent an alternative route to adipic acid based upon a C3 feedstock. In fact, the literature contains numerous examples of homogeneous and heterogeneous catalysts for the dimerization

‡ Current address: Laboratoire de Chimie de Coordination du CNRS, 31077 Toulouse Cedex, France.
§ DuPont Nylon, Intermediates and Specialties.
† University of North Carolina, Chapel Hill.
⊕ Abstract published in *Advance ACS Abstracts*, July 1, 1994.

(1) Weissermel, K.; Arpe, H.-J. *Industrial Organic Chemistry*, 2nd ed.; Verlag Chemie: Weinheim, Germany, 1993; Chapters 10.1 and 10.2.

0002-7863/94/1516-8038$04.50/0 © 1994 American Chemical Society

Table 1. Examples of Previously Studied Catalysts for the Dimerization of Methyl Acrylate

catalyst	conditions	turnover number[a]	ref
$RhCl_3$	MeOH, 140 °C, 10 h	10	2a,b
$(PhCN)_2PdCl_2$	$AgBF_4$, 23 °C, *p*-benzoquinone, 20 h	340	4m
$Pd(CH_3CN)_4^{2+}$	$LiBF_4$, 40 °C, 30 h	150	4e,g
(COD)(methallyl)Pd^+	PBu_3, 80 °C< 20 h	360	4h,i
$Pd(acac)_2$	HBF_4·Et_2O, PBu_3, 80 °C, 5 h	1040	4o
$(\eta^6\text{-}C_6H_6)Ru(MA)_2$	$NaC_{10}H_8$, 140 °C, 3 h	400	3c
$HRu(CO)Cl[P(iPr)_3]_2$	CF_3SO_3Ag, 85 °C, 24 h	1200	3e
$Ni(\eta^3\text{-}C_3H_5)_2$	PMe_3, HBF_4, CH_2Cl_2, 0 °C, 46 h	700 linear/branched = 9:1	5b

[a] The turnover (TO) number is defined as the number of moles of monomer converted per mole of transition metal catalyst.

of methyl acrylate to dimethyl hexenedioates (eq 1).[2-6] Most of

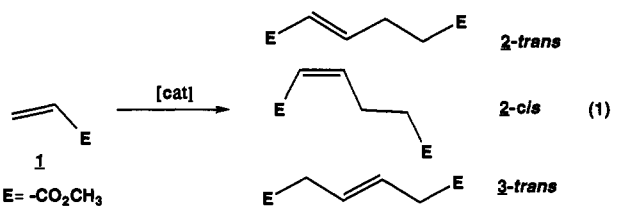

these catalysts are based on late transition metals such as Rh,[2] Ru,[3] Pd,[4] or Ni[5] due to their known compatibility with functional groups. Table 1 lists some examples of the most successful catalysts examined to date. It is clear from this table that each catalyst system suffers from one or more drawbacks which include short catalyst lifetime, low turnover frequencies, formation of branched dimers and oligomers, and a requirement for high temperatures.

In addition, the mixture of catalysts and cocatalysts used has often precluded any detailed mechanistic investigations although several mechanisms have been proposed to account for the selective coupling reaction. One of the most plausible schemes suggested[3e,7b] is a Cossee–Arlman-type mechanism which involves insertion of methyl acrylate (MA) into a metal hydride bond to yield a L_nM–$CH_2CH_2CO_2CH_3$ species followed by a second insertion of methyl acrylate and β-H elimination to release dimer and regenerate a metal hydride species. Mechanistic proposals involving either formation of a metallacyclopentane (derived from oxidative coupling from a bis-acrylate complex)[4p] or formation of a metal hydride via vinyl C–H activation of MA[3b,4d,8] have also been invoked. Bits of evidence supporting each of these mechanisms have emerged, but the overall proposals remain speculative, since, except for the work described below, none of the proposed intermediates have ever been directly observed.

As part of our current studies on the use of electrophilic cationic late transition metal complexes for catalytic dimerization, oligomerization, and polymerization of olefins, we recently reported that complexes of the type $(C_5R_5)Rh(C_2H_4)(L)H^+$ (R = H, CH_3; L = $P(OMe)_3$, PMe_3) act as ethylene dimerization catalysts. The fundamental details of the catalytic mechanism and of the carbon–carbon bond-forming step were investigated.[9] We further realized that these well-defined systems were active for the dimerization of acrylates, which presented an ideal opportunity for catalyst refinement and detailed mechanistic studies.

We describe here the development of a highly efficient and selective Rh(III) catalytic system for the linear dimerization of methyl acrylate which is entered by protonation of $Cp^*Rh(C_2H_4)_2$ (Cp^* = C_5Me_5).[7] An extensive mechanistic analysis of the dimerization reaction is reported. Low-temperature characterization of the catalyst resting state and observation of the carbon–carbon coupling process along with kinetic analyses which demonstrate the key mechanistic features of the catalytic cycle are described. Results using iridium analogs are also reported which offer supporting evidence for the structure of the catalyst resting state. Moreover, replacement of the C_5Me_5 ligand by the methylated indenyl ligands has led to the discovery of second generation catalysts with improved catalytic activities and greatly enhanced lifetimes. Use of C_5H_5- and $C_5(CH_3)_4CF_3$-substituted complexes has generated active catalytic systems which operate via slightly different catalytic cycles and different catalyst resting states and provide clues for the design of other active catalysts. Finally, a description of some of the reactions of other functionalized olefins including methyl vinyl ketone, methyl crotonate, 2-vinylpyridine, and 1-vinyl-2-pyrrolidinone with the active catalytic system will be presented.

Results and Discussion

A. Catalyst Development Studies. 1. The $(C_5Me_5)P(OMe)_3$-$Rh(C_2H_4)H^+$ System. The successful dimerization of ethylene with various Rh(III) catalysts of the type $(C_5R_5)(L)Rh(C_2H_4)$-H^+,[9] coupled with the compatibility of late transition metal complexes with functional groups, led us to examine these systems

(2) For reports of Rh-based acrylate dimerization catalysts, see: (a) Alderson, T. U.S. Patent 3 013 066, 1961. (b) Alderson, T.; Jenner, E. L.; Lindsey, R. V. *J. Am. Chem. Soc.* **1965**, *87*, 5638. (c) Nugent, W. A.; McKinney, R. J. *J. Mol. Catal.* **1985**, *29*, 65. (d) Singleton, D. M. U.S. Patent 4 638 084, 1987. For related vinyl ketone dimerization, see: (e) Kovalev, I. P.; Kolmogorov, Y. N.; Strelenko, Y. A.; Ignatenko, A. V.; Vinogradov, M. G.; Nikishin, G. I. *J. Organomet. Chem.* **1991**, *420*, 125. (f) Nikishin, G. I.; Kovalev, I. P.; Klimova, T. E.; Ignatenko, A. V. *Tetrahedron Lett.* **1991**, *32*, 1077.

(3) For reports of Ru-based acrylate dimerization catalysts, see: (a) McKinney, R. J. U.S. Patent 4 485 256, 1986. (b) McKinney, R. J.; Colton, M. C. *Organometallics* **1986**, *5*, 1080. (c) McKinney, R. J. *Organometallics* **1986**, *5*, 1752. (d) Ren, C. Y.; Cheng, W. C.; Chan, W. C.; Yeung, C. H.; Lau, C. P. *J. Mol. Catal.* **1990**, *59*, L1. (e) Sustmann, R.; Hornung, H. J.; Schupp, T.; Patzke, B. *J. Mol. Catal.* **1993**, *85*, 149. For related acrolein dimerization, see: (f) Ohgomori, Y.; Ichikawa, S.; Yoneyama, T.; Sumitani, N. Eur. Patent 0 537 625 A2, 1993. For related acrylonitrile dimerization, see: (g) Billig, E.; Strow, C. B.; Pruett, R. L. *J. Chem. Soc., Chem. Commun.* **1968**, 1307.

(4) For reports of Pd-based acrylate dimerization catalysts, see: (a) Barlow, M. G.; Bryant, M. J.; Haszeldine, R. N.; Mackie, A. G. *J. Organomet. Chem.* **1970**, *21*, 215. (b) Oehme, G.; Pracejus, H. *Tetrahedron Lett.* **1979**, 343. (c) Pracejus, H.; Krause, H.; Oehme, G. *Z. Chem.* **1980**, *20*, 24. (d) Oehme, G.; Pracejus, H. *J. Prakt. Chem.* **1980**, *322*, 798. (e) Nugent, W. A.; Hobbs, F. W. *J. Org. Chem.* **1983**, *48*, 5364. (f) Oehme, G. *J. Prakt. Chem.* **1984**, *326*, 779. (g) Nugent, W. A. U.S. Patent 4 451 665, 1984. (h) Tkatchenko, I.; Neibecker, D.; Grenouillet, P. FR patent 2 524 341, 1983. (i) Tkatchenko, I.; Neibecker, D.; Grenouillet, P. *Organometallics* **1984**, *3*, 1130. (j) See ref 2c. (k) Oehme, G.; Grassert, I.; Baudisch, H.; Mennenga, H. *J. Mol. Catal.* **1986**, *37*, 53. (l) Grenouillet, P.; Neibecker, D.; Tkatchenko, I. FR Patent 2 596 390, 1987. (m) Oehme, G.; Pracejus, H. *J. Organomet. Chem.* **1987**, *320*, C56. (n) Perron, R.; Mutez, S. Eur. Patent 305 302, 1989. (o) Grenouillet, P.; Neibecker, D.; Tkatchenko, I. U.S. Patent 4 889 949, 1989. (p) Guibert, I.; Neibecker, D.; Tkatchenko, I. *J. Chem. Soc., Chem. Commun.* **1989**, 1850.

(5) For reports of Ni-based acrylate dimerization catalysts, see: (a) Wilke, G.; Sperling, K.; Stehling, L. U.S. Patent 4 594 447, 1986. (b) Wilke, G. *Angew. Chem., Int. Ed. Engl.* **1988**, *27*, 185. For related acrylonitrile dimerization, see: (c) Nomura, K.; Ishino, M. *J. Mol. Catal.* **1991**, *68*, L5. (d) Nomura, K.; Ishino, M. *J. Mol. Catal.* **1992**, *73*, L15.

(6) For miscellaneous metal-based dimerizations of acrylic olefins, see: (a) Cornforth, D. A.; Waddan, D. Y.; Williams, D. S. African 67 02,130, 1968. (b) Kanai, H.; Ishii, K. *Bull. Chem. Soc. Jpn.* **1981**, *54*, 1015.

(7) Part of this work has been previously reported, see: (a) Brookhart, M.; Sabo-Etienne, S. *J. Am. Chem. Soc.* **1991**, *113*, 2777. (b) Brookhart, M.; Hauptman, E. *J. Am. Chem. Soc.* **1992**, *114*, 4437.

(8) Kawamoto, K.; Tatani, A.; Imanaka, T.; Teranishi, S. *Bull. Chem. Soc. Jpn.* **1971**, *44*, 1239.

(9) Brookhart, M.; Hauptman, E.; Lincoln, D. M. *J. Am. Chem. Soc.* **1992**, *114*, 10394.

for catalytic dimerization of acrylates. The complex Cp*-$(P(OCH_3)_3)Rh(C_2H_4)H^+$ (**4**) is the most efficient ethylene dimerization catalyst in the series and was initially studied. Treatment of **4** with excess methyl acrylate in CH_2Cl_2 at 23 °C resulted in the rapid and clean formation of the chelate complex $Cp^*(P(OCH_3)_3)Rh(CH_2CH_2C(O)OCH_3)$ (**5**) (eq 2). Complex

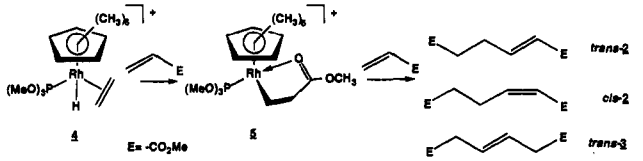

(2)

5 presumably arises from acrylate displacement of ethylene followed by migratory insertion into the rhodium hydride bond. Following formation of **5**, acrylate dimerization ensues to give exclusively the linear diesters dimethyl (*E*)-2-hexenedioate (*trans*-**2**) (93%), dimethyl (*Z*)-2-hexenedioate (*cis*-**2**) (ca. 6%), and dimethyl (*E*)-3-hexenedioate (*trans*-**3**) (ca. 1%).

While selective tail-to-tail coupling is observed, the dimerization is slow, taking 100 h to convert 16 equiv of methyl acrylate to dimer. No intermediates are observed by ^1H NMR monitoring of the dimerization reaction. Complex **5** was independently prepared by protonation of $Cp^*(P(OCH_3)_3)Rh(CH_2{=}CHCO_2Me)$ (**6**) in CH_2Cl_2 (eq 3).

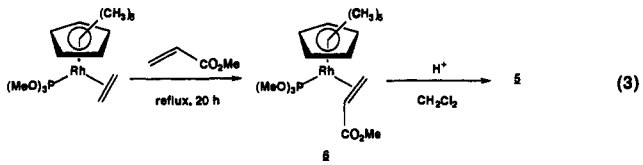

(3)

On the basis of the mechanism of ethylene dimerization by complex **4**, a possible turnover-limiting step for acrylate dimerization was dechelation of the ester carbonyl oxygen of **5** to open a free coordination site for binding external acrylate. This led us to examine the catalytic activity of $Cp^*(C_2H_4)Rh(CH_2CH_2\text{-}\mu\text{-}H)^+$ (**7**), in which $P(OMe)_3$ has been replaced by the much more labile C_2H_4 ligand. This strategy could allow π-complexation of a second acrylate monomer and thus presents the possibility of C–C coupling in a complex containing both a chelating moiety and a π-bound acrylate. The following section describes the successful execution of this approach.[7]

2. $(C_5Me_5)(C_2H_4)Rh(CH_2CH_2\text{-}\mu\text{-}H)^+$ System. Protonation of $Cp^*Rh(C_2H_4)_2$ with $H(Et_2O)_2BAr'_4$ ($Ar' = 3,5\text{-}(CF_3)_2C_6H_3$) in CH_2Cl_2 generates $Cp^*(C_2H_4)Rh(CH_2CH_2\text{-}\mu\text{-}H)^+$ (**7**).[10] Treatment of **7** with methyl acrylate results in efficient catalytic dimerization with an initial turnover frequency of 6.6 min^{-1} (the turnover frequency is defined as the number of moles of monomer converted per mole of rhodium catalyst per unit of time. One catalytic cycle converts 2 equiv of monomer to 1 equiv of dimer). ^1H NMR monitoring of solutions showed formation of only tail-to-tail dimers with *trans*-**2** as the major product (ca. 92%); *cis*-**2** and *trans*-**3** are minor products (the dimer ratios vary somewhat with percent conversion, see below). Some typical results are summarized in eq 4. With monomer-to-catalyst ratios less than 1000, essentially complete conversion of monomer to dimers can be achieved. At higher ratios (e.g. 1600:1 and 2600:1, eq 4), a maximum conversion of ca. 1200–1400 equiv of monomer to dimer is observed.

A gas chromatographic analysis confirmed these NMR observations and provided additional quantitative data. A catalytic reaction which employed pure methyl acrylate as solvent and a catalyst-to-MA ratio of 1:2300 was monitored over 1290

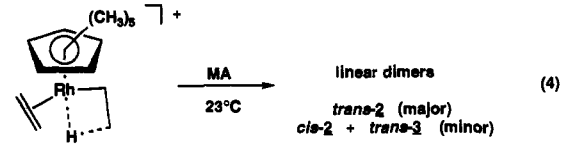

(4)

equiv MA : 7	time	conversion	TO
140	45 min	98%	137
1600	5 h 40 min	88%	1400
2600	22 h	47%	1200

min. After 240 min, 41% conversion of MA had been achieved (940 TO) while, at 360 min, 52% conversion (1200 TO) was noted. After 1290 min only an additional ca. 1% conversion is observed, indicating that catalytic activity had essentially ceased after 360 min. At 360 min, the major products are *trans*-**2** (85%) and *cis*-**2** (14%) with trace amounts of *trans*- and *cis*-**3**. Branched diesters constitute ca. 0.2% of the dimer products, indicating that the selectivity for tail-to-tail versus head-to-tail coupling is >99.7% (additional GC results including rate data are reported below).

The number and fate of the rhodium species present during catalysis could be monitored by ^1H NMR spectroscopy using the Cp* signals. These resonances occur in a region (1.5–1.9 ppm) separate from bands for monomer and dimers and allow analysis even in the presence of large excesses of monomer and dimers. Treatment of complex **7** (δ Cp* = 1.85 ppm) with methyl acrylate (1630 equiv, 23 °C, CH_2Cl_2) results in the immediate formation of a new species (**8**) with a Cp* ^1H NMR signal at 1.6 ppm. We will designate this species as the catalyst "resting state". As the dimerization proceeds, the resting state (**8**) slowly disappears and a new complex **9** with a Cp* ^1H NMR resonance at 1.7 ppm is concomitantly formed. As **9** is formed the turnover rate drops, and once complex **8** has been completely depleted and only complex **9** remains, the dimerization stops (ca. 88% conversion). Complex **9** will be designated as the "deactivated" catalyst. When less than 100 equiv of methyl acrylate is used, an additional species (**10**) with a Cp* resonance at 1.53 ppm appears at the end of the reaction (100% conversion of MA to dimers). Treatment of complex **10** with MA results in its conversion to **8**, and dimerization again proceeds until deactivation and formation of **9** occurs. These results are summarized in Scheme 1.

To fully understand the dimerization reaction, the structural identities of **8**–**10** were sought. Since the experiments described above indicate **8** is not stable at 23 °C in the absence of methyl acrylate, initial efforts were focused on isolation and characterization of **9** and **10**. Treatment of complex **7** in CH_2Cl_2 (23 °C,

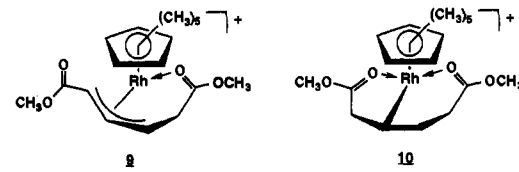

15 h) with 7 equiv of *trans*-**2** dimer yields a mixture of complexes **9** and **10** in a ca. 1:1 ratio. Fractional recrystallization of the residue after removal of the solvent and excess dimer gives complexes **9** and **10** as analytically pure compounds. Complex **9** could also be isolated from solutions of dimers plus MA at the end of catalytic runs. Complex **10** was initially identified as the bis-chelate complex $Cp^*RhCH(CH_2COOCH_3)(CH_2CH_2COOCH_3)^+$ by ^1H and ^{13}C NMR spectroscopy. The ^1H NMR spectrum is particularly informative since it shows seven different proton signals, suggesting a locked conformation around a chiral metal center (each methylene group bears diastereotopic protons). The presence of two acrylate moieties is indicated by two different methoxy signals at 3.93 and 3.84 ppm. The signal corresponding to the single proton on the carbon σ-bound to the metal center

(10) Brookhart, M.; Lincoln, D. M.; Bennett, M. A.; Pelling, S. *J. Am. Chem. Soc.* **1990**, *112*, 2691.

Table 2. Crystallographic Data, Collection Parameters, and Refinement Parameters for **10**, **9**, **23a**, and $Cp^*Rh(MA)_2$

	10	**9**	**23a**	$Cp^*Rh(MA)_2$
molecular formula	$RhF_{24}O_4C_{50}BH_{40}$	$RhF_{24}O_4C_{50}BH_{38}$	$IrF_{24}O_4C_{50}BH_{40}$	$RhO_4C_{18}H_{27}$
fw	1274.53	1272.51	1363.88	410.32
crystal dim. (mm)	0.20 × 0.20 × 0.20	0.20 × 0.20 × 0.30	0.25 × 0.08 × 0.47	0.25 × 0.10 × 0.49
space group	$P\bar{1}$	$P\bar{1}$	$P\bar{1}$	Cc
cell param				
a (Å)	14.347(4)	12.646(8)	13.079(2)	18.889(6)
b (Å)	14.515(4)	13.819(6)	13.125(2)	8.755(1)
c (Å)	14.209(5)	15.650(6)	17.257(2)	13.961(6)
α (deg)	115.055(20)	77.57(4)	84.93(1)	
β (deg)	94.32(3)	84.35(4)	81.90(1)	128.37(3)
γ (deg)	94.91(3)	83.39(5)	67.07(1)	
V (Å^3)	2650.3(14)	2645.5(23)	2699.3	1810.1
Z	2	2	2	4
D_c (g/cc)	1.597	1.597	1.678	1.505
temp (°C)	20	20	−70	−55
radiation (wavelength, Å)	Mo Kα (0.709 30)	Mo Kα (0.709 30)	Mo Kα (0.7107)	Mo Kα (0.7107)
monochromator	graphite	graphite	graphite	graphite
linear abs coeff (mm^{-1})	0.44	0.44	2.584	0.943
scan mode	$\theta/2\theta$	$\theta/2\theta$	ω	ω
2θ limits (deg)	$6 \le 2\theta \le 45$	$6 \le 2\theta \le 45$	$2.4 \le 2\theta \le 48.0$	$0.0 \le 2\theta \le 60.0$
octants collcd	+++, −++, −+−, ++−	+++, −++, −+−, ++−	+++, +−+, −++, −+	+++, −++
total no. unique reflns	6963	6438	8565	3051
data with $I \ge x\sigma(I)$	4752 (x = 2.5)	4953 (x = 2.5)	4739 (x = 3)	1802 (x = 3)
R	0.072	0.062	0.055	0.021
R_w	0.089	0.076	0.046	0.020
GoF	2.00	2.32	1.44	0.85
no. params	721	722	749	312
max Δ/σ	0.120	0.175	0.02	0.10
largest res dens (e/Å^3)	0.900	0.840	1.15	0.29

Scheme 1

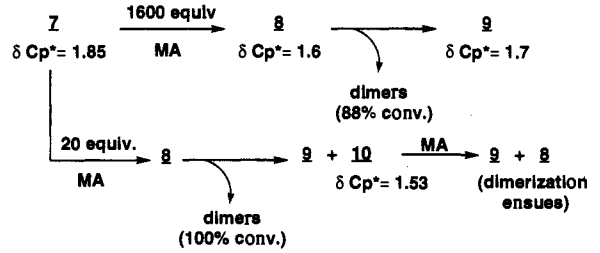

(Rh–C*H*) appears at 3.35 ppm as a ddddd coupled inequivalently to four vicinal hydrogens and ^{103}Rh. In the ^{13}C NMR spectrum, the downfield shift of the carbonyl carbons (190.4 and 183.0 ppm) compared to that of the carbonyl of free methyl propionate (175.0 ppm) indicates that both carbonyl groups are chelated.

i. X-ray Structural Analysis of 10. The structure of complex **10** was verified by an X-ray structure determination. Single crystals of **10** were grown by slow solvent evaporation from a concentrated solution of complex **10** and *trans*-**2** dimer (50 equiv) in CH_2Cl_2 at 23 °C. An ORTEP diagram is shown in Figure 1. Crystallographic data, collection parameters, and refinement parameters are listed in Table 2; selected interatomic distances and angles are summarized in Tables 3 and 4, respectively. The X-ray analysis confirms the presence of two chelate rings with both ester carbonyl groups coordinated to rhodium (Rh(1)–O(1) = 2.132(7) Å, Rh(1)–O(8) = 2.149(7) Å). The coordination geometry at rhodium is approximately octahedral; the bite angle of the six-membered ring (O(1)–Rh(1)–C(5)) is 91.1(4)° while the corresponding angle in the five-membered ring (C(5)–Rh(1)–O(8)) is somewhat smaller at 81.0(4)°. The O(1)–Rh(1)–O(8) angle is 87.8(3)°. In both chelated esters the methyl group and the carbonyl oxygen are *syn* to one another.

Complex **9**, the deactivated catalyst, was identified as the allyl complex $Cp^*Rh(\eta^3\text{-}CH_3OC(O)CH_2CHCHCHCO_2CH_3)^+$ by ^1H and ^{13}C NMR spectroscopy. The most characteristic feature in the ^1H NMR spectrum of complex **9** is the central allylic proton at 4.7 ppm (ddd, J_{trans} = 11 Hz, J_{cis} = 8 Hz and J_{Rh-H} = 2 Hz). Also noticeable in the ^1H NMR spectrum is the presence of two distinct resonances for the diastereotopic methylenic hydrogens at 3.42 ppm (dd, J_{gem} = 21 Hz, ^3J = 7.5 Hz) and 2.61 ppm (dd, J_{gem} = 21 Hz, ^3J = 2 Hz). The ^{13}C NMR spectrum shows two carbonyl resonances, one corresponding to a coordinated carbonyl group (186.8 ppm) and one to an uncoordinated carbonyl group (170 ppm), as well as three resonances at 102.5 ppm (dd, J_{Rh-C} = 5 Hz, J_{C-H} = 170 Hz), 71.6 ppm (dd, J_{Rh-C} = 9 Hz, J_{C-H} = 160 Hz) and 67.8 ppm (dt, J_{C-H} = 170 Hz, $J_{Rh-C} = {}^2J_{C-H}$ = 10 Hz), corresponding to the allylic carbons. Unambiguous proof of the structure of complex **9** was provided by an X-ray crystallographic analysis.

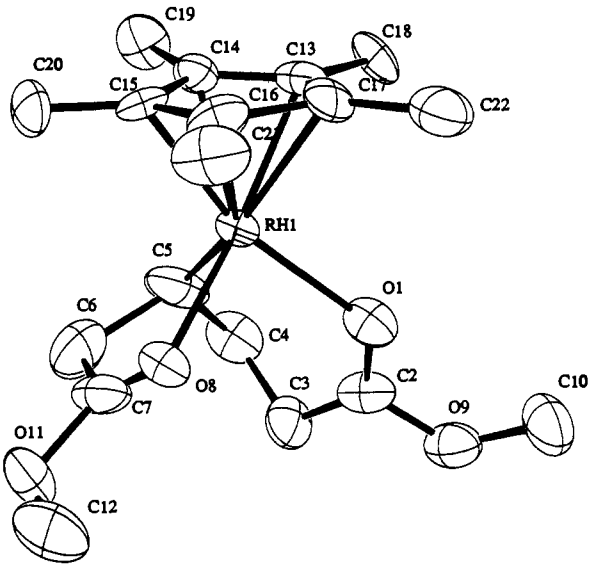

Figure 1. ORTEP drawing of $Cp^*Rh[CH(CH_2COOCH_3)(CH_2CH_2COOCH_3)]^+$ (**10**). The counterion $[(CF_3)_2C_6H_3]_4B^-$ as well as hydrogen atoms have been omitted.

ii. X-ray Structural Analysis of Complex 9. Single crystals of **9** were obtained by slow evaporation of CD_2Cl_2. An ORTEP diagram is shown in Figure 2. Crystallographic data and collection and refinement parameters are listed in Table 2; selected

Table 3. Selected Interatomic Distances (Å) for $Cp^*Rh(CH(CH_2COOCH_3)(CH_2CH_2COOCH_3))^+$ (10)[a]

Rh(1)–O(1)	2.132(7)	C(2)–C(3)	1.467(16)
Rh(1)–C(5)	2.084(11)	C(2)–O(9)	1.322(15)
Rh(1)–O(8)	2.149(7)	C(3)–C(4)	1.512(21)
Rh(1)–C(13)	2.114(9)	C(4)–C(5)	1.480(19)
Rh(1)–C(14)	2.124(9)	C(5)–C(6)	1.578(19)
Rh(1)–C(15)	2.092(9)	C(6)–C(7)	1.527(21)
Rh(1)–C(16)	2.227(9)	C(7)–O(8)	1.207(17)
Rh(1)–C(17)	2.248(9)	C(7)–O(11)	1.284(15)
O(1)–C(2)	1.205(13)		

[a] Numbers in parentheses are the estimated standard deviations.

Table 4. Selected Bond Angles (deg) for $Cp^*Rh(CH(CH_2COOCH_3)(CH_2CH_2COOCH_3))^+$ (10)[a]

O(1)–Rh(1)–C(5)	91.1(4)	Rh(1)–C(5)–C(4)	114.7(8)
O(1)–Rh(1)–O(8)	87.8(3)	Rh(1)–C(5)–C(6)	105.6(7)
C(5)–Rh(1)–O(8)	81.0(4)	C(4)–C(5)–C(6)	111.4(10)
O(1)–C(2)–C(3)	124.9(11)	C(5)–C(6)–C(7)	109.8(10)
O(1)–C(2)–O(9)	122.5(10)	C(6)–C(7)–O(8)	121.2(11)
C(3)–C(2)–O(9)	112.5(10)	C(6)–C(7)–O(11)	113.3(13)
C(2)–C(3)–C(4)	112.4(10)	O(8)–C(7)–O(11)	125.5(14)
C(3)–C(4)–C(5)	117.2(10)	Rh(1)–O(8)–C(7)	113.4(7)

[a] Numbers in parentheses are the estimated standard deviations.

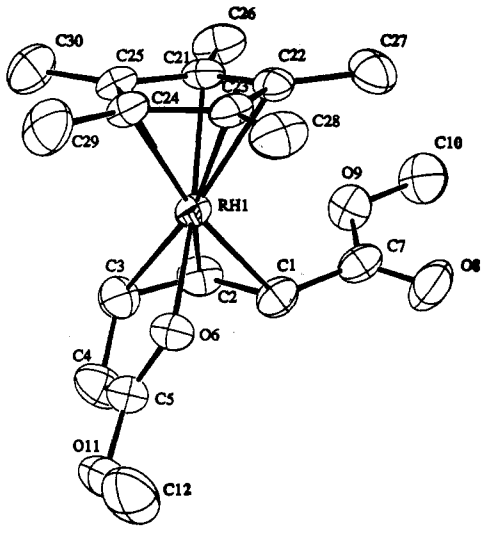

Figure 2. ORTEP drawing of $Cp^*Rh(\eta^3\text{-}CH_3OC(O)CH_2CHCHCHCO_2CH_3)^+$ 9. The counterion $[(CF_3)_2C_6H_3]_4B^-$ as well as hydrogen atoms have been omitted.

Table 5. Selected Interatomic Distances (Å) for $Cp^*Rh(\eta^3\text{-}CH_3OC(O)CH_2CHCHCHCO_2CH_3)^+$ (9)[a]

Rh(1)–C(1)	2.211(8)	Rh(1)–C(24)	2.171(7)	C(5)–O(6)	1.232(10)
Rh(1)–C(2)	2.165(7)	Rh(1)–C(25)	2.197(7)	C(5)–O(11)	1.311(10)
Rh(1)–C(3)	2.214(8)	C(1)–C(2)	1.417(11)	C(7)–O(8)	1.215(10)
Rh(1)–O(6)	2.146(5)	C(1)–C(7)	1.476(12)	C(7)–O(9)	1.315(10)
Rh(1)–C(21)	2.148(7)	C(2)–C(3)	1.410(13)	O(9)–C(10)	1.443(12)
Rh(1)–C(22)	2.218(8)	C(3)–C(4)	1.529(13)	O(11)–C(12)	1.428(12)
Rh(1)–C(23)	2.184(8)	C(4)–C(5)	1.471(13)		

[a] Numbers in parentheses are the estimated standard deviations.

interatomic distances and angles are summarized in Tables 5 and 6, respectively. As for **10**, the X-ray structure clearly shows the presence of a chelated carbonyl group; the Rh(1)–O(6) distance of 2.146(5) Å is analogous to that observed for **10**. The allyl plane (C(1), C(2), C(3)) is nearly coplanar with the Cp* plane with the dihedral angle between these planes being 7.8°. The noncoordinated ester group attached to C(1) is conjugated with the allyl unit with the dihedral angle between the allyl and O(9)–C(7)–O(8) planes being 16.6°. The C(4) carbon is pulled well

Table 6. Selected Bond Angles (deg) for $Cp^*Rh(\eta^3\text{-}CH_3OC(O)CH_2CHCHCHCO_2CH_3)^+$ (9)[a]

C(1)–Rh(1)–C(2)	37.8(3)	Rh(1)–C(3)–C(4)	106.9(5)
C(1)–Rh(1)–C(3)	67.4(3)	C(2)–C(3)–C(4)	122.1(8)
C(1)–Rh(1)–O(6)	86.7(3)	C(3)–C(4)–C(5)	114.3(7)
C(2)–Rh(1)–C(3)	37.5(3)	C(4)–C(5)–O(6)	123.4(7)
C(2)–Rh(1)–O(6)	99.8(3)	C(4)–C(5)–O(11)	114.8(8)
C(3)–Rh(1)–O(6)	80.1(3)	O(6)–C(5)–O(11)	121.8(8)
Rh(1)–C(1)–C(2)	69.4(4)	Rh(1)–O(6)–C(5)	115.0(5)
Rh(1)–C(1)–C(7)	119.6(6)	C(1)–C(7)–O(8)	123.1(8)
C(2)–C(1)–C(7)	122.2(7)	C(1)–C(7)–O(9)	113.2(7)
Rh(1)–C(2)–C(1)	72.9(4)	O(8)–C(7)–O(9)	123.6(8)
Rh(1)–C(2)–C(3)	73.1(5)	C(7)–O(9)–C(10)	116.0(7)
C(1)–C(2)–C(3)	120.6(7)	C(5)–O(11)–C(12)	117.4(7)
Rh(1)–C(3)–C(2)	69.3(4)		

[a] Numbers in parentheses are the estimated standard deviations.

Scheme 2

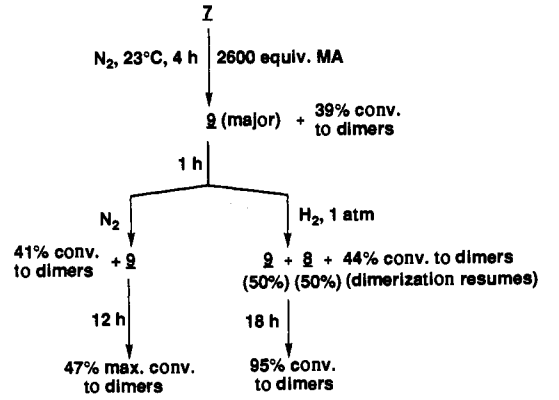

out of the allyl plane by the requirement for chelation of O(6); the dihedral angle between the C(1)–C(2)–C(3) and C(2)–C(3)–C(4) planes is 40.0°. Similar to the case of **10**, both ester units exhibit a *syn* relationship between the methyl groups and the carbonyl oxygens.

Catalyst deactivation by formation of the π-allyl complex **9** must be the result of dehydrogenation of an intermediate in the catalytic cycle. It seemed plausible that reactivation of the catalyst might be possible by exposing the deactivated catalyst (**9**) to H_2. This proved to be the case, and an informative sequence of reactions, as monitored by ^1H NMR spectroscopy, is shown in Scheme 2. Complex **7** was treated with 2600 equiv of MA under N_2 at 23 °C; after 4 h an aliquot (1) was withdrawn and showed that 1000 equiv (39%) of MA had been converted to dimers and the major rhodium species (>85%) in solution was the inactive π-allyl complex **9**. At the same time, the initial solution was exposed to 1 atm of H_2; after 1 h an aliquot (2) was withdrawn and showed that 44% conversion had been achieved and complex **8**, the catalyst resting state, had now increased from ca. 15% to ca. 50% of the rhodium species in solution. After an additional 18 h under H_2, 95% conversion to dimers had been reached. The sample withdrawn after 4 h (aliquot 1) was kept under N_2, and the reaction was followed in parallel and revealed that a maximum of 47% conversion (1200 equiv) was obtained after 13 h and the only observable rhodium species by ^1H NMR spectroscopy was complex **9**: catalytic activity had ceased. These observations support a mechanism in which catalytic activity is restored by regeneration of **8** when the deactivated catalyst **9** is exposed to 1 atm of H_2 in the presence of methyl acrylate.

Carrying out the dimerization reaction under 1 atm of H_2 produces a continuously running long-lived catalyst system. For example, using a MA/catalyst ratio of 6500:1 at 23 °C under 1 atm of H_2, 79% conversion to dimers (85% *trans*-**2**, 15% *cis*-**2**) after 13 h, 97% conversion after 20 h, and >99% conversion (94% *trans*-**2**, 6% *cis*-**2**) after 36 h were observed (isomerization of *cis*-**2** to *trans*-**2** occurs at high conversions). A second experiment

Table 7. Dimerization of Methyl Acrylate (77.24 mmol) under 1 atm of H_2 by **7** (0.034 mmol)[a]

time (min)	60	180	300	420	540
MA (mmol)	65.1	40.2	17.9	4.37	0.45
MP[b] (mmol)	0.06	0.16	0.30	0.50	0.76
cis-**3** (mmol)	0.02	0.05	0.07	0.09	0.10
cis-**2** (mmol)	0.88	2.41	3.23	2.83	1.80
trans-**3** (mmol)	0.07	0.29	0.40	0.32	0.32
trans-**2** (mmol)	4.6	14.7	24.5	31.6	34.6
MA conversion (%)	15.7	48.0	76.8	94.3	99.4
TO rate (min^{-1})	5.9	6.1	5.8	5.5	4.2

[a] No dimethyl adipate (hydrogenated dimer) is observed, and branched dimers account for ca. 0.3% of total dimers at the end of the reaction (540 min). [b] Methyl acrylate (MA) is initially contaminated with 0.01 mmol of methyl propionate (MP).

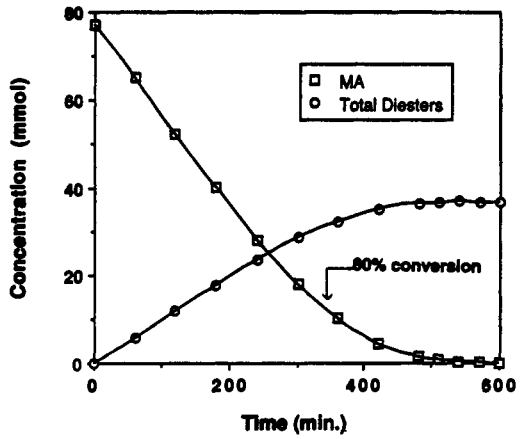

Figure 3. Reaction profile for run 2 (0.034 mmol of Rh, 25 °C, 1 atm H_2).

demonstrates the reaction can be run at higher temperatures. Treatment of **7** with 6500 equiv of MA at 60 °C under 1 atm of H_2 results in 65% conversion after 1 h (70 TO/min) and 94% conversion after 3 h. Adding an additional 6500 equiv of MA at 3 h and monitoring at 6 h indicates 70% conversion of total acrylate. Examination of the solution after 22 h reveals >99% conversion of MA. Under these conditions a total of 13 000 TOs were achieved, but since at the end of the reaction the catalyst is still active, this number represents a lower limit on the maximum TO number which can be achieved. A potential problem with carrying out the reaction under H_2 is hydrogenation of methyl acrylate (MA) to methyl propionate (MP). Examination of solutions by ^1H NMR spectroscopy after complete conversion to MA in fact showed that methyl propionate is formed to the extent of 1–2% (see below for additional details).

Since operating under H_2 clearly produces a highly efficient, very long-lived catalyst system, a thorough GC analysis of the course of three catalytic reactions was carried out. Reactions were run at 25 °C under 1 atm of H_2 with initial Rh/MA ratios of 1:940 (run 1), 1:2270 (run 2), and 1:7000 (run 3). Full GC results are tabulated in the supplementary material; Table 7 displays representative data for run 2.

The reaction profile for run 2 is shown in Figure 3. Over the 0–75% MA conversion range, the rate of formation of the diester was zero-order in MA concentration and first-order in rhodium concentration (0.011–0.084 mmol range, Figure 4). These kinetic results are consistent with carbon–carbon coupling in **8** being the rate-determining step in the major catalytic cycle. As conversion increased, the rate slowly decreased, most likely reflecting a change in the concentration of active rhodium complex **8**. All three runs show essentially equal turnover frequencies up to ca. 75% conversion of 6 mmol of MA converted/mmol of Rh/min. This rate corresponds to a free energy of activation of 19 kcal/mol. Figure 4 illustrates the dependence of the rate of dimer production on the concentrations of Rh in the 0–75% MA conversion range. This plot clearly shows that the rate is first-order in total Rh concentration, as anticipated from earlier results.

Several other minor features of the reaction are evident from examination of the GC data. At low MA conversion (16%), the ratio of *cis*-**2** to *trans*-**2** was ca. 15:81. But as the reaction proceeded, this ratio slowly changed to 4:92 at 99.9% conversion. Evidently, the kinetically controlled diester mixture from **8** was converted to the thermodynamic mixture via a metal-catalyzed isomerization process. Like the diester formation rate, under H_2, the MA hydrogenation rate to methyl propionate was zero-order in MA concentration and first-order in rhodium concentration over the 0–75% conversion range. The decrease in the rate of production of diester at higher MA conversion (≥75–80%, Figure 3) was accompanied by an accelerated MA hydrogenation rate (Figure 5). As the solvent composition became primarily diesters (95% MA conversion), the catalyst began producing small amounts of triester products. Table 8 shows that the linear coupling selectivity was constant over the 0–100% MA conversion range and relatively insensitive to temperature (25–60 °C).

While the above experiments establish that the inactive catalyst system can be reactivated with H_2, it is not clear how the original dehydrogenation occurs which leads to formation of π-allyl complex **9**, nor is the fate of the H_2 "released" known. Complex **9**, at first sight, seems to derive from complex **10** by a formal loss of hydrogen. However, no H_2 in solution can be observed when the reaction is monitored by ^1H NMR spectroscopy.[11] Furthermore, heating a solution of complex **10** at 63 °C resulted in very slow conversion to complex **9** (57% in 22 h). This conversion follows first-order kinetics with $k = 7.4 \times 10^{-6}$ s^{-1}, $\Delta G^{\ddagger}$ ca. 28 kcal/mol. This rate is far too slow to account for the deactivation of the catalyst during the catalytic runs by simple thermolysis of **10**.

Noting that the deactivation of the catalyst occurs when dimers appear, we looked at the effect of the presence of dimers on the conversion of **10** to **9**. Protonation of $Cp^*Rh(C_2H_4)_2$ in CD_2Cl_2 followed by treatment at 23 °C with 14 equiv of dimers (ca. 95% *trans*-**2**, 5% *cis*-**2**) gives, within 15 min, a mixture of complexes **10** and **9** in a 3:2 ratio. Heating the sample to 45 °C for 2 h results in nearly complete conversion of the bis-chelate complex **10** to the π-allyl complex **9** (9:1 ratio).[12] The dramatic increase in this rate of conversion in the presence of dimer strongly suggested a catalyst deactivation pathway in which hydrogen is transferred during the catalysis to either dimer or monomer rather than being released as H_2.

Gas chromatographic analyses of a catalytic run under N_2 indeed do establish that deactivation occurs by transfer of hydrogen to methyl acrylate to form methyl propionate (MP). Results are summarized in Table 9. A MA/Rh mmol ratio of 77.2:0.034 (2270:1) was used. The methyl acrylate was contaminated initially with 0.013% or 0.010 mmol of methyl propionate (see T = 0 entry). As shown in Table 9, MP slowly increases during the catalytic run and, after conversion of 1200 equiv of MA and complete catalyst deactivation (1290 min), 0.040 mmol are present. This indicates 0.030 mmol of MP were formed during the run, which corresponds within experimental error to the number of mmol of catalyst initially employed (0.034). Analysis of these solutions reveals no formation of dimethyl adipate (hydrogenated dimer). We conclude that MA serves as a much better hydrogen acceptor than the unsaturated diesters and the deactivation process to form **9** can be quantitatively accounted

(11) The insolubility of hydrogen gas in solution at ambient temperature and the small amounts expected make the absence of a signal corresponding to H_2 in the ^1H NMR spectra rather inconclusive.

(12) A new rhodium species with a Cp^* signal at δ 1.8 ppm also is formed (ca. 15–20%). Exposure of this solution to H_2 (1 atm) results in rapid disappearance of the latter species and slow formation of hydrogenated dimer dimethyl adipate. The ratio of **10** to **9** changes to a value of ca. 1:5, which remains constant over several hours. In a separate experiment, treatment of the bis-chelate complex **10** with dimers results in the formation of dimethyl adipate, as determined by gas chromatography.

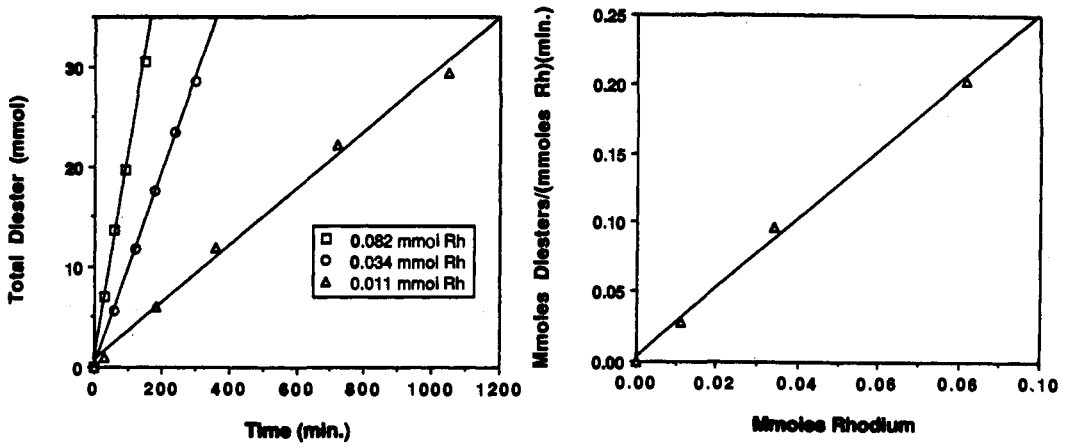

Figure 4. Effect of Rh concentration on diester production rate (0–75% MA conversion range under 1 atm of H_2).

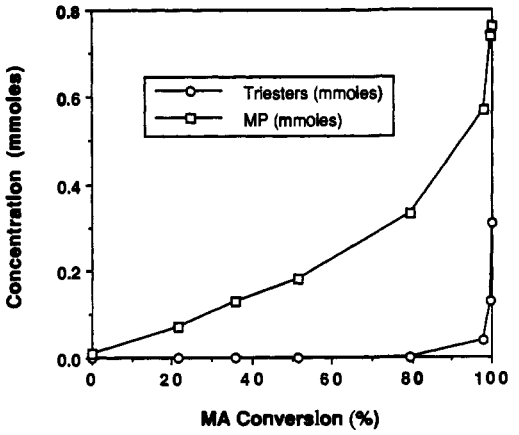

Figure 5. Concentration of methyl propionate (MP) and triesters versus methyl acrylate (MA) conversion.

Table 8. Temperature Dependence on Dimerization Selectivity for 8 and 11

			selectivity (mol %)			
				diesters		
catalyst	temp (°C)	MA conv	MP	linear	branched	triesters
8	25	27.2	0.8	99.0	0.2	0.0
		59.9	0.9	98.8	0.2	0.0
		100.0	2.5	97.0	0.2	0.3
8	60	34.6	0.6	99.0	0.4	0.0
		44.8	0.6	98.8	0.5	0.1
		99.8	3.3	95.4	0.5	0.7
11	25	100.0	0.0	99.5	0.02	0.5
11	60	100.0	0.0	98.8	0.2	1.0

Table 9. Hydrogenation of MA during Catalysis under N_2

time (min)	Rh (mmol)	MA (mmol)	TO no.	MP (mmol)
0	0.034	77.2	0	0.010
60	0.034	68.7	250	0.018
180	0.034	52.2	735	0.027
240	0.034	45.8	924	0.033
1290	0.034	36.5	1197	0.040

for by hydrogenation of MA. While reasonable mechanisms can be written for this reaction, no further experimental evidence is available regarding the details of this process.

3. Catalysts Based on Methylated Indenyl Ligands. Several derivatives of **7** were examined with the goal of increasing both the catalyst activity and lifetime. Since two labile ethylene ligands are required and they are both displaced, the only ligand which can be modified to generate new catalysts is the cyclopentadienyl ligand. We have examined catalytic systems derived from both the C_5H_5 and $C_5(CH_3)_4CF_3$ ligands. These systems show reduced turnover frequencies, but they have provided instructive mechanistic details regarding the dimerization reaction. These will be discussed in the next section.

The most promising new catalyst systems discovered to date are those derived from protonation of η^5-(1,2,3-trimethylindenyl)-$Rh(C_2H_4)_2$ (**11**) and η^5-(1,2,3,4,5,6,7-heptamethylindenyl)Rh-$(C_2H_4)_2$ (**12**). Complexes **11** and **12** have previously been reported by Marder and co-workers.[13]

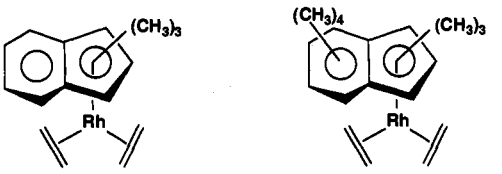

11 12

Protonation of either **11** or **12** in the presence of MA results in a catalyst system which exhibits turnover frequencies of ca. 11 TO/min, which is nearly twice the turnover frequency of the Cp* system. A GC analysis was carried out under N_2 using the trimethylindenyl system **11** with a Rh/MA ratio of 1:2300 (see Experimental Section). Several interesting contrasts between this system and the Cp* system can be noted. First, >99% conversion of MA to dimers is seen after 240 min, indicating a catalytic system which deactivates much less rapidly than the Cp* system. Furthermore, through 99.5% conversion (255 min), the ratio of *trans*-**2** and *cis*-**2** isomers remains steady and constitutes 96% and 3% of dimer products, respectively. The fraction of *trans*-**3** isomer slowly increases and is ca. 1% of the diester product at 99.5% conversion; less than 0.1% *cis*-**3** is present. At 255 min there is 0.15% branched diesters, indicating a selectivity for tail-to-tail coupling of >99.8%. No noticeable increase in methyl propionate through 99.5% conversion is observed, and only traces of triesters are detected.

Results in Table 10 illustrate the dramatic increase in catalyst lifetime of the trimethylindenyl system. Catalysis was initiated by protonation of **11** with $H(Et_2O)_2BAr'_4$ in the presence of 60 000 equiv of MA. The solution was warmed to 55 °C; aliquots were withdrawn, and the reaction was monitored by ^1H NMR spectroscopy. Initial turnover frequencies were 60/min. As shown in Table 10, 70% conversion (42 000 TO) is achieved after 33 h and catalytic activity ceases after 54 000 turnovers (recall the upper limit in the Cp* system was 1200 turnovers). Exposure of this solution to H_2 results in conversion of the remaining MA to dimer.

Since the catalyst is reactivated by exposure to H_2, we assume deactivation occurs by formation of a π-allyl complex analogous

(13) Frankcom, T. M.; Green, J. C.; Nagy, A.; Kakkar, A. K.; Marder, T. B. *Organometallics* **1993**, *12*, 3688.

Table 10. Dimerization of MA by the Catalyst System Generated from Protonation of **11**

time (h)	TO	*trans*-**2**	*cis*-**2**
	1 atm of N_2		
5	17 000	85%	15%
33	42 000	95%	5%
57	51 000	95%	5%
68	54 000	95%	5%
80	54 000	95%	5%
	N_2 replaced by 1 atm of H_2		
81	56 000	95%	5%
84	58 000	95%	5%
86	60 000 (100% conv)	95% + traces of *trans*-**3** and hydrogenated monomer	5%

to **9**.[14] However, due to the large quantity of dimer which is produced together with deactivated catalyst, its recovery was not attempted. NMR monitoring of the solution containing 0.002% catalyst was also not feasible.

When catalytic reactions were carried out using much lower MA/catalyst ratios (e.g. 30:1, see the Experimental Section), complex **13**, the analog of the bis-chelate **10**, was isolated as the only rhodium species in good yields (90%). Details of the reaction of this species with MA will be presented in the next section.

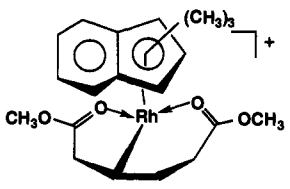

13

B. Mechanistic Studies. Catalytic System Based on the C_5Me_5 Ligand. The results described above established that a long-lived catalyst system can be operated under H_2 using both the C_5Me_5 and the tri- and heptamethylindenyl series of complexes. However, at this point, little is known concerning the mechanistic details of the catalytic cycle, in particular the structure of the catalyst resting state and the nature of the turnover-limiting step. This is not surprising, since catalytic runs have to be conducted at high acrylate concentrations which renders the identification of low concentrations of rhodium species difficult. With the hope of detecting and identifying some catalytically significant intermediates, a series of low-temperature NMR experiments was carried out. The agostic complex **7** was treated with 5 equiv of methyl acrylate at −78 °C in CD_2Cl_2, and the reaction was monitored by low-temperature ^1H NMR spectroscopy. At this temperature, immediate formation of the chelate–ethylene complex $Cp^*Rh(CH_2CH_2C(O)OCH_3)(C_2H_4)^+$ (**14**) occurred (eq 5). Complex **14** results from displacement of ethylene by methyl

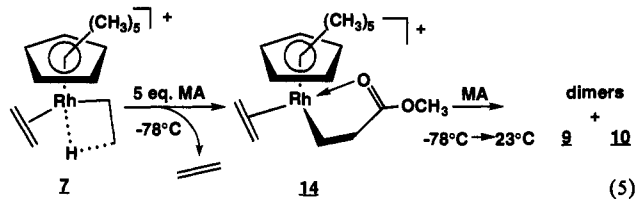

7 **14** (5)

acrylate followed by insertion into the rhodium hydride bond. Support for structure **14** was provided by characteristic signals in the ^1H NMR spectrum (δ 3.93 ppm, m, 2H, CH_2CH_2; 3.63 ppm, s, 3H, OCH_3; 2.6–3.0 ppm, 4H, $C_2H_4CO_2CH_3$). All signals remain sharp until 10 °C, where significant broadening of the ethylenic protons and free ethylene takes place. This fluxional process presumably results from exchange between free ethylene and coordinated ethylene. During acrylate dimerization, which is initiated above −20 °C, complex **14** is the only rhodium species observed. However, the chemical shift for the Cp* resonance in the ^1H NMR spectrum for complex **14** appears at 1.52 ppm and does not correspond to the one observed for the catalyst resting state **8** (1.6 ppm) during bulk dimerization. Once all 5 equiv of MA have been consumed, a mixture of the bis-chelate complex **10** and the deactivated catalyst **9** is obtained. The formation of the chelate–ethylene complex is informative, since it indicates that, at comparable ratios of ethylene and acrylate, ethylene is a sufficiently good ligand to compete with acrylate for coordination at rhodium. However, the bound ethylene never couples to acrylate, suggesting some unique feature inherent to methyl acrylate (this aspect is discussed in more detail below).

Since structural information could not be obtained for the catalyst resting state **8** by treatment of **7** with either high or low concentrations of methyl acrylate, an independent preparation of **8** in the absence of ethylene and MA was sought. We reasoned that complex **8** must exhibit ligation of 2 equiv of acrylate and thus might be prepared by protonation of the bis-acrylate complex $Cp^*Rh(CH_2CHCO_2CH_3)_2$.

Thermolysis of $Cp^*Rh(C_2H_4)_2$ in neat methyl acrylate (130 °C, 4 h) produces a mixture of two isomers **15** and **16** in a 6:4 ratio. In these compounds, rotation of the η^2-acrylate ligands is slow on an NMR time scale and thus all six possible bis-acrylate isomers could potentially be detected. Of these six isomers, two possess a plane of symmetry, two possess a C_2 axis of symmetry, and two are unsymmetrical and thus possess no symmetry elements (symmetry analyses here assume rapid rotation of the Cp* ring, and thus in "symmetrical" isomers the two sets of acrylate protons are magnetically equivalent). The two complexes isolated possess no symmetry and thus must correspond to isomers **15** and **16**, as drawn in eq 6. One pure isomer whose structure was unknown

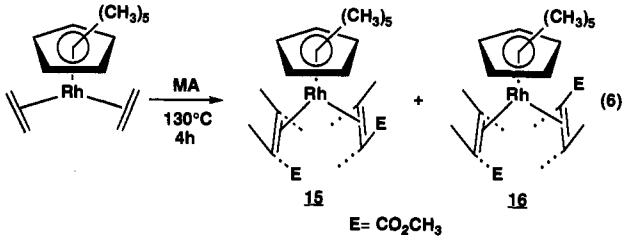

could be isolated by fractional recrystallization. On the basis of subsequent work (see below), the pure isomer was assigned to complex **15**, but no additional data have been obtained to corroborate this assignment.

Protonation of complex **15** at low temperatures (−78 °C) with $H(Et_2O)_2BAr'_4$ in CD_2Cl_2 results in the formation of a new complex whose ^1H chemical shift for the $C_5(CH_3)_5$ ring appears at 1.6 ppm. This shift corresponds precisely to the one observed for the catalyst resting state (**8**), and we assume these are one and the same species (see below for additional supporting evidence). Complex **8** is formulated as an η^2-methyl acrylate chelate complex, as shown in eq 7. The presence of an η^2-methyl acrylate moiety is confirmed by a typical ^1H NMR pattern for the olefinic protons (4.67 ppm, dd, J_{trans} = 13 Hz, J_{cis} = 9 Hz, H_1; 3.95 ppm, d, J_{trans} = 13 Hz, H_3; 3.30 ppm, d, J_{cis} = 9 Hz, H_2) and ^{13}C signals at 72.9 ppm (dd, J_{C-Rh} = 8 Hz, J_{C-H} = 164 Hz, C_α) and 69.0 ppm (dt, J_{C-Rh} = 10 Hz, J_{C-H} = 164 Hz, C_β). The chelate structure is verified by ^{13}C resonances at 22.2 ppm (dt, J_{C-Rh} = 18 Hz, J_{C-H} = 150 Hz) for C_2 and 39.6 ppm (t, J_{C-H} = 127 Hz) for C_1.

When complex **8** is slowly warmed to ca. −50 °C, the ^1H NMR signals broaden, indicating a fluxional behavior. At this

(14) These systems also dimerize methyl vinyl ketone, but in this case the deactivation process is rapid and an allylic species could be clearly detected by ^1H NMR spectroscopy; details of the reactivity of methyl vinyl ketone with the rhodium systems are provided in a following section.

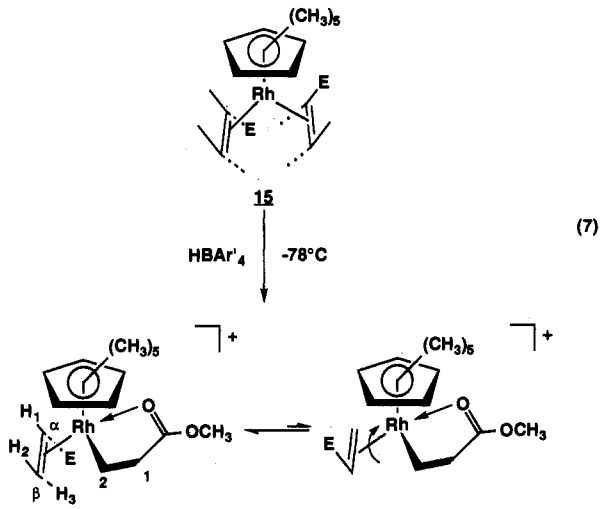

temperature, signals corresponding to traces of free methyl acrylate are sharp (free MA likely results from some decomposition). On the basis of these observations coupled with the behavior of the iridium analog described below, the fluxional process likely reflects interconversion of major and minor isomers **8** and **8'**. However, the minor isomer could not be detected either by ^1H or ^{13}C NMR spectroscopy and probably represents less than 5% of the Rh species. Complex **8** rearranges before coalescence can be reached. The spectroscopic data for the major isomer do not indicate the relative orientations of the η^2-acrylate and the chelate ligands. Structure **8** is tentatively proposed on the basis of the X-ray structure of an analogous iridium complex (see below) and the fact that the acrylate moieties are properly aligned for C–C coupling; i.e., C_2 and C_β are *cis* to each other.

At temperatures above –50 °C, complex **8** isomerizes cleanly to complex **10**. The formation of **10** can be envisioned as occurring via migration of the σ-bound carbon of the chelate to C_β of the η^2-acrylate to give complex **17**. Complex **17** can then yield complex **10** by β-hydride elimination and readdition (see Scheme 3).

The first-order rate constant for isomerization of complex **8** to complex **10** was measured at –23 °C and found to be 2.4×10^{-4} s^{-1}, $\Delta G^\ddagger$ = 18.7 kcal/mol. This free energy of activation matches that of the one obtained earlier from the turnover frequency during bulk dimerization: 6.6 TO/min at 25 °C, $\Delta G^\ddagger$ = 19 kcal/mol. The correspondence of these barriers clearly supports the identity of the resting state as complex **8** and that of the turnover-limiting step in the cycle as the C_2–C_β coupling. It is interesting to note that the barrier for β-migratory insertion in **8** is somewhat lower than the one previously reported for $(C_5(CH_3)_5)Rh(P(OCH_3)_3)(C_2H_4)(C_2H_5)^+$, 22.3 kcal/mol.[9] It is plausible to attribute this rate increase to participation of the carbonyl group of the η^2-methyl acrylate to form an 18-electron oxaallyl complex, **18**. That is, as migration of C_2 to C_β occurs,

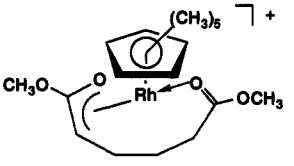

18

the developing open coordination site is synchronously occupied by the carbonyl group, thus avoiding formation of a 16-electron species.[15] The formation of complex **18** would also account for the regioselective tail-to-tail coupling and the fact that ethylene does not couple to the acrylate moiety in the chelate–ethylene complex **14** described above. Treatment of complex **10** with methyl acrylate (30 equiv) at low temperatures (–20 °C) results in displacement of dimer and regeneration of the resting state **8**, which provides further proof that **8** is the catalyst resting state during bulk dimerization.

Scheme 3. Formation of the Bis-Chelate Complex **10**

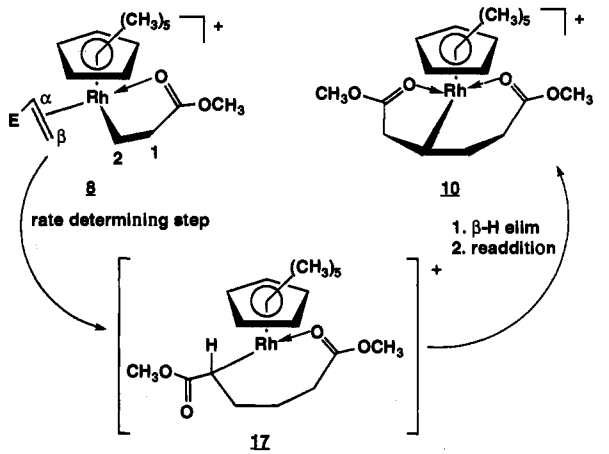

The results described thus far do not indicate whether complex **10** is part of the major catalytic cycle or whether an intermediate formed *prior* to formation of **10** (e.g., **17** or **18**) is intercepted by methyl acrylate to yield dimers and regenerate the resting state **8**. Careful monitoring of the structure of the dimers formed from complexes **8** and **10** upon treatment with MA clearly suggests that complex **10** is *not* part of the major catalytic cycle (see Scheme 4).

When complex **8** is exposed to 86 equiv of MA in CD_2Cl_2 at –78 °C and the solution warmed, *only cis*-**2** and *trans*-**2** dimers are formed up to nearly complete conversion of MA. Small amounts of *trans*-**3** appear only at the end of the reaction presumably due to a metal-catalyzed isomerization process. This experiment implies that the resting state **8** releases almost exclusively *trans*-**2** and *cis*-**2**. In contrast, when **10** is treated with MA (30 equiv) in CD_2Cl_2 at –78 °C and warmed, the first equivalent of dimer released is *trans*-**3**. This is evident from the ratio of *trans*-**3** to *trans*- and *cis*-**2** of ca. 1:2.5 after 2 equiv of dimers are formed.[16] Thereafter, the amount of *trans*-**3** remains constant through nearly complete conversion of MA (none is formed and its percent of total dimers drops). At complete conversion, a ratio of diesters similar to that of the previous experiment is observed. If **10** releases almost exclusively *trans*-**3** but bulk dimerization through **8** as the resting state forms only traces of *trans*-**3**, then **10** cannot be on the major catalytic cycle.[17]

The information provided now allows the construction of a fairly complete catalytic cycle which is illustrated in Scheme 5.

(15) The proposal of participation of a "neighboring group" is well-known for metal acetates. See for example: (a) Maitlis, P. M.; Bailey, P. M.; Isobe, K. *J. Chem. Soc., Dalton Trans.* **1981**, 2003. (b) Bassetti, M.; Monti, D.; Maitlis, P.; Ellis, P.; Sunley, G. J. *Organometallics* **1991**, *10*, 4015. (c) Darensbourg, D. J.; Joyce, J. A.; Bischoff, C. J.; Reibenspies, J. H. *Inorg. Chem.* **1991**, *30*, 1137. (d) Hawthorne, M. F.; Kang, H. C. *Organometallics* **1990**, *9*, 2327.

(16) After formation of 2 equiv of dimer only 70% of **10** has reacted (2.5/3.5 × 100). Thus, knowing the resting state **8** produces only *trans*- and *cis*-**2** dimers and assuming **10** releases only *trans*-**3**, the predicted ratio of *trans*-**3** to *trans*- and *cis*-**2** is ca. 0.7:1.3 (35:65). This ratio is within experimental error of the 30:70 ratio observed.

(17) The release of *trans*-**3** dimer from **10** can be rationalized as follows. Dechelation of an ester carbonyl group is required to generate a vacant coordination site *prior* to β-hydride elimination. The six-membered chelate ring is more strained than the five-membered chelate ring and thus may open preferentially. The flexible three carbon arm produced can then adopt the correct geometry for β-elimination which will result in formation of the nonconjugated double bond.

Scheme 4. Observation of the Structures of Dimers Formed from Complexes **8** and **10**

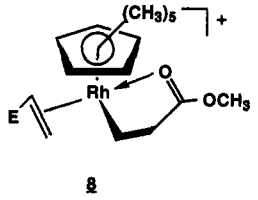

8

MA (86 equiv)
-78°C → 23°C

Equivalents of dimers formed	Dimers: *trans*-3	Dimers: *trans*- & *cis*-2
ca. 2	none	75% 25%
ca. 3	none	90% 10%
ca. 9	none	90% 10%
100% conv. (12 h at 23°C)	5%	90% 5%

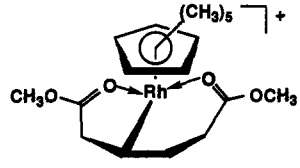

10

MA (30 equiv)
-78°C → 23°C

Equivalents of dimers formed	Dimers: *trans*-3	Dimers: *trans*- & *cis*-2	10:8
ca. 2	30%	70%	1:2.5
ca. 3.5	20%	80%	1:7
ca. 7.5	10%	90%	traces **10**
100% conv.	5%	91% 4%	only **10**

Scheme 5. Catalytic Cycle of the Dimerization of Methyl Acrylate

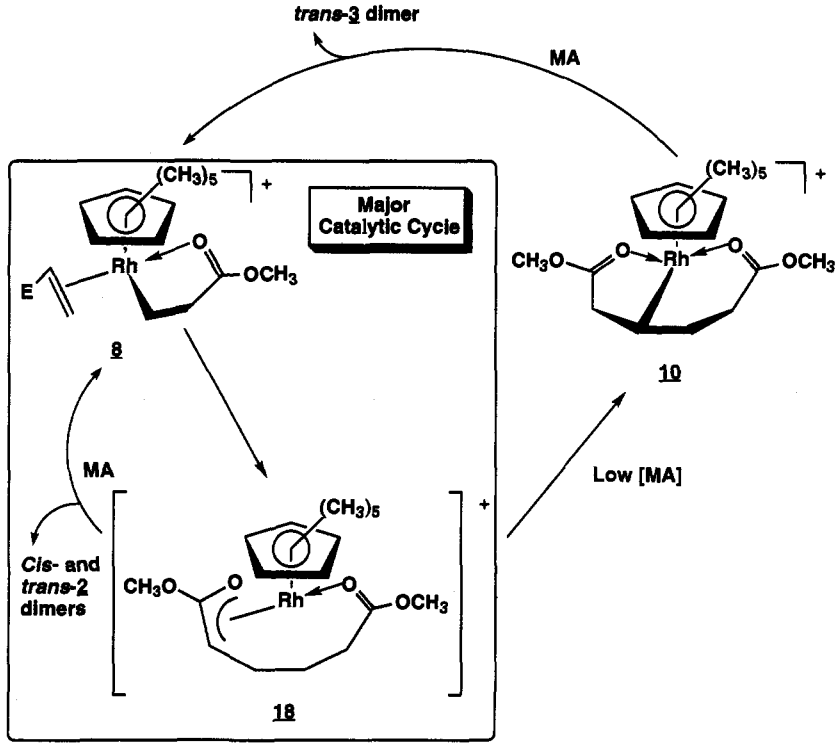

The resting state at high MA concentrations is complex **8**. The turnover-limiting step is carbon–carbon coupling via a migratory insertion reaction to yield an intermediate which we propose is the 18-electron oxaallyl species **18**; but it is not observed, and its precise structure is not known. This intermediate is intercepted by MA to regenerate **8** and produce an ca. 5:1 ratio of *trans*-**2** to *cis*-**2** diesters. At low MA concentrations, the intermediate **18** has sufficient lifetime to isomerize to the bis-chelate **10**. Complex **10** reacts with MA to release *trans*-**3** diester and regenerate **8**. Catalyst deactivation occurs by transfer hydrogenation between some intermediate in the cycle, probably either **10** or **18**, and MA to produce the inactive π-allyl complex **9** and methyl propionate.

2. Catalytic System Based on the 1,2,3-Trimethylindenyl Ligand. As discussed in the Catalyst Development Studies section, the indenyl systems have an increased activity and are longer-lived under N_2 than their C_5Me_5 counterpart. We reasoned that the former system might exhibit somewhat different mechanistic features and thus initiated a brief mechanistic investigation to uncover any differences between the two systems. Protonation of (1,2,3-trimethylindenyl)Rh(C_2H_4)$_2$ (**11**) at −78 °C in CD_2Cl_2 followed by addition of small amounts of methyl acrylate (ca. 5 equiv) results, as in the Cp* system, in the formation of a chelate–ethylene complex (1,2,3-trimethylindenyl)Rh(CH$_2$CH$_2$C(O)OCH$_3$)(C_2H_4)$^+$ (**19**) (δ(−20 °C) 3.72, m, 2H, C_2H_4; 3.58, m, 2H, C_2H_4; 2.2–2.7, m, 3H, $C_2H_4CO_2CH_3$; 1.91, m, 1H, $C_2H_4CO_2CH_3$; complete ^{1}H NMR data are listed in the Experimental Section). All ^{1}H NMR signals are sharp until 0 °C, where significant broadening of the ethylenic protons and free ethylene occurs. This fluxional process, as in the Cp* system, presumably results from exchange between free ethylene and coordinated ethylene. During conversion of these few equivalents to dimers, complex **19** is the resting state but ultimately rearranges to the

bis-chelate complex **13** at the end of the catalysis. On a preparative

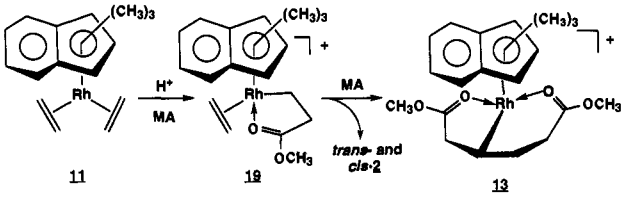

scale, protonation of (1,2,3-trimethylindenyl)$Rh(C_2H_4)_2$ in the presence of a large excess of methyl acrylate yields cleanly the bis-chelate complex **13**, which can be isolated as an analytically pure compound. In an NMR experiment, complex **13** was treated with methyl acrylate (ca. 100 equiv) in CD_2Cl_2 and warmed for brief periods of time (ca. 1 min) to ambient temperature (23 °C). After each warming interval, the sample was quenched at −78 °C and characterized by low-temperature ^1H NMR spectroscopy. As the dimerization proceeds, two new complexes form in a 1:1 ratio.

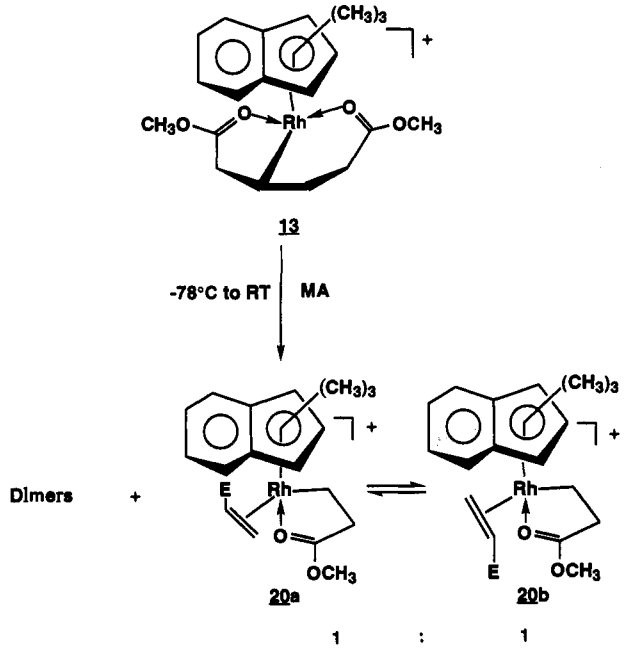

Evidence for two species is provided by the presence of six methyl signals (δ 2.07, 1.93, 1.84, 1.79, 1.56, and 1.28) and the ^1H NMR spectrum at −80 °C. The structures of these compounds have been assigned to the rotational isomers **20a** and **20b** by analogy to the Cp* complex **8**. In the ^1H NMR spectrum at −80 °C, the olefinic region contains two sets of signals attributed to each isomer which have typical ^1H patterns for an η^2-methyl acrylate complex (Complex **20a** or **20b**: 4.46 ppm, dd, J = 14 and 8.6 Hz; 4.08 ppm, d, J = 14 Hz. Complex **20a** or **20b**: 4.27 ppm, dd, J = 13 and 7.9 Hz; 4.03 ppm, d, J = 13 Hz. For both complexes the *cis* olefinic protons are presumably hidden by the methoxy resonances).

Exposure of **20** to MA followed by analysis of the ratio of **20** to **13** as a function of turnover number yields information concerning the catalytic cycle. Again, reactions were run at 23 °C, quenched at −80 °C, and monitored by ^1H NMR spectroscopy at this temperature. Treatment of **13** with 85 equiv of MA in CD_2Cl_2 shows after ca. 50 turnovers an ca. 50:50 mixture of **13** and **20**. This clearly indicates that release of dimer from **13** is substantially slower than formation of dimer via a catalytic cycle involving **20**. These observations also support conclusions drawn above for the Cp* system that the bis-chelate complex is not on the major catalytic cycle. After complete conversion of MA, **20** isomerizes to the more stable **13**, which is the only rhodium species detected. Using higher ratios of MA to **13**, complete conversion to **20** can be achieved before total conversion of MA to dimers. For example, exposure of **13** to 220 equiv of MA results in detection of only **20** after ca. 130 turnovers. As mentioned above, complexes **20a** and **20b** were characterized at −80 °C, at which temperature all ^1H signals are sharp. However, upon warming to ca. −30 °C, broadening of the two sets of three methyl signals occurs, which is reminiscent of the dynamic process exhibited by the catalyst resting state (**8**) in the Cp* system (see eq 7). When the temperature reaches ca. 0 °C, the dimerization is almost complete and the olefinic resonances of the remaining methyl acrylate (ca. 20–25 equiv) are slightly broadened. Since free MA exhibits some broadening, it is not clear whether the dynamic process which interconverts **20a** and **20b** involves acrylate dissociation or acrylate rotation or a combination of each.

3. Iridium Analogs. To gain additional information regarding the intermediates in the catalytic cycle and the precise structure of the resting state, the iridium analogs were investigated. Protonation of $Cp^*Ir(C_2H_4)_2$ (**21**) (CH_2Cl_2, 23 °C) in the presence of methyl acrylate leads sequentially to **22** and then to **23**, both of which could be isolated (eq 8).

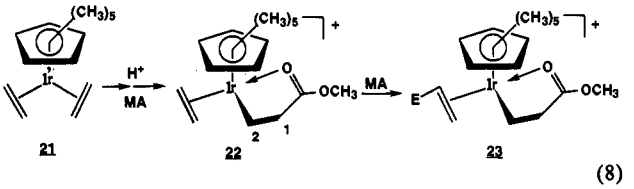

(8)

Complex **22** results from protonation of complex **21** followed sequentially by displacement of one ethylene by methyl acrylate and migratory insertion. This complex could be prepared as an analytically pure material by conducting the reaction at 0 °C and isolating the product after a short reaction time (10 min). Variable-temperature ^1H and ^{13}C NMR spectra reveal that complex **22** is fluxional. Key spectroscopic features at −80 °C include the observation of four ethylene protons (δ 3.59, 3.15, 2.96, and 2.76) in the ^1H NMR spectrum and two characteristic ^{13}C resonances for the ethylenic carbons at 55.9 and 48.9 ppm. At 23 °C, the ethylenic signals average to two signals at 3.50 and 2.89 ppm in the ^1H NMR spectrum and one signal at 54.8 ppm in the ^{13}C NMR spectrum. These spectroscopic data suggest that the fluxional process exhibited by complex **22** is ethylene rotation (if the dynamic process was due to ethylene dissociation, all ^1H NMR resonances of the bound ethylene would average to a *single* band). In addition, evidence for a chelate structure is verified by ^{13}C signals at 38 ppm (t, J_{C-H} = 129 Hz, C_1) and −0.8 ppm (dd, J_{C-H} = 135 and 143 Hz, C_2).

Complex **23** could be prepared analytically pure by protonation of complex **21** at −78 °C followed by addition of methyl acrylate and warming to 23 °C for 1 h. Variable-temperature ^1H and ^{13}C NMR spectroscopies show that complex **23** consists of a mixture of two major isomers **23a,b** (80%, 1:1 ratio) and one minor isomer **23c** (20%) (see Scheme 6). Isomers **23a** and **23b** are in rapid equilibrium, presumably via acrylate rotation, by analogy to the chelate–ethylene complex **22**. Line-shape analysis yields a rate constant for rotation of ca. 132 s^{-1} at 20 °C, $\Delta G^{\ddagger}$ = 14.3 kcal/mol. This free energy of activation is slightly higher (ca. 3 kcal/mol) than the ones observed for ethylene rotation in complexes of the type $(C_5R_5)Rh(C_2H_4)(L)H^+$.[9]

Crystallization at −30 °C of **23** from diethyl ether/hexane gives light-yellow plates as well as traces of orange needles. Single-crystal X-ray analysis of the trapezoidal plates indicates the presence of a single isomer (**23a**) whose ORTEP structure is shown in Figure 6. Crystallographic data, collection parameters, and refinement parameters are listed in Table 2; selected interatomic distances and angles are summarized in Tables 11 and 12, respectively. Angles involving the Cp*(centroid) are as follows: Cp*(centroid)–Ir(1)–C(8) = 122.3°, Cp*(centroid)–

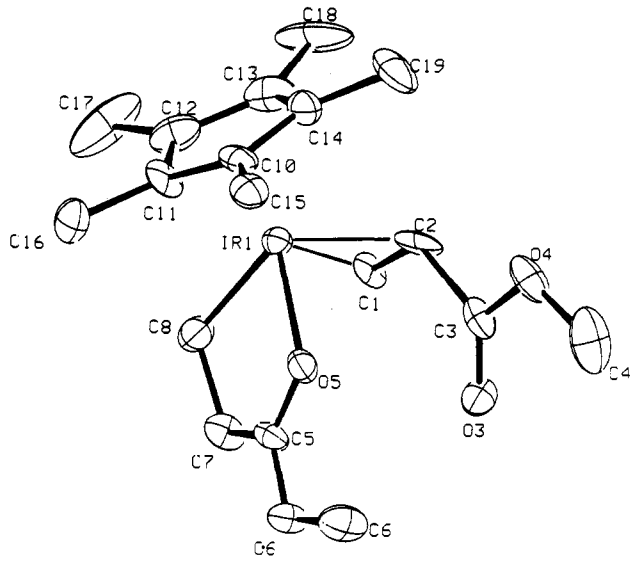

Figure 6. ORTEP drawing of $Cp^*Ir\overline{CH_2CH_2C(O)}OCH_3(\eta^2\text{-}CH_2\text{-}CHCO_2CH_3)^+$ (**23a**). The counterion $[(CF_3)_2C_6H_3]_4B^-$ as well as hydrogen atoms have been omitted.

Scheme 6. Iridium Isomers of **23**

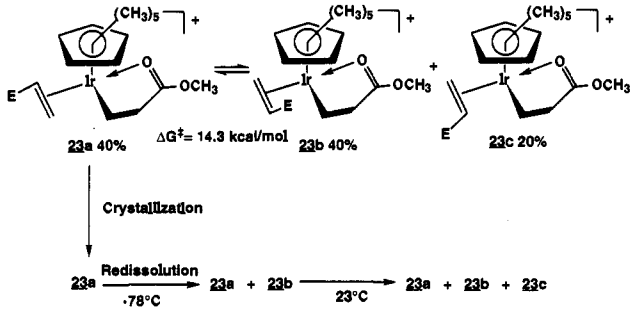

Table 11. Selected Interatomic Distances for $Cp^*Ir\overline{(CH_2CH_2COOCH_3)}(\eta^2\text{-}CH_2CHCO_2CH_3)^+$ (**23a**) (Å)[a]

Ir(1)–O(5)	2.128(8)	O(3)–C(3)	1.184(13)
Ir(1)–C(1)	2.168(13)	O(4)–C(3)	1.345(13)
Ir(1)–C(2)	2.126(14)	O(5)–C(5)	1.251(12)
Ir(1)–C(8)	2.088(14)	O(6)–C(5)	1.307(13)
Ir(1)–C(10)	2.261(11)	C(1)–C(2)	1.335(18)
Ir(1)–C(11)	2.135(14)	C(2)–C(3)	1.600(19)
Ir(1)–C(12)	2.173(16)	C(5)–C(7)	1.452(17)
Ir(1)–C(13)	2.154(14)	C(7)–C(8)	1.513(17)
Ir(1)–C(14)	2.258(13)		

[a] Numbers in parentheses are the estimated standard deviations.

Table 12. Selected Bond Angles for $Cp^*Ir\overline{(CH_2CH_2COOCH_3)}(\eta^2\text{-}CH_2CHCO_2CH_3)^+$ (**23a**) (deg)[a]

Ir(1)–O(5)–C(5)	114.1(8)	O(3)–C(3)–C(2)	123(1)
Ir(1)–C(1)–C(2)	70.2(8)	O(4)–C(3)–C(2)	111(1)
Ir(1)–C(2)–C(1)	74(1)	O(5)–C(5)–C(7)	122(1)
Ir(1)–C(2)–C(3)	112.9(7)	O(6)–C(5)–C(7)	118(1)
Ir(1)–C(8)–C(7)	110(1)	C(1)–C(2)–C(3)	118(1)
O(3)–C(3)–O(4)	126(1)	C(5)–C(7)–C(8)	110(1)
O(5)–C(5)–O(6)	120(1)		

[a] Numbers in parentheses are the estimated standard deviations.

Ir(1)–O(5) = 126.7°, Cp*(centroid)–Ir(1)–C(1) = 132.8°, Cp*-(centroid)–Ir(1)–C(2) = 117.9°. The Cp*(centroid)–Ir distance is 1.830 Å. The atoms Ir(1), O(5), C(5), C(7), O(6), and C(6) are coplanar to within 0.049 Å. This is similar to the case of the complex $Cp^*Ru\overline{(NO)(CH(CH_3)CH_2COOCH_3)}^+$ (**24**), in which the analogous portion of the molecule is coplanar to within 0.008 Å.[18] Puckering of the metallacycle ring is observed, with the plane defined by Ir(1), C(8), and C(7) forming an angle of 159.7° with the Ir(1), O(5), C(5), and C(7) plane (C(8) is displaced toward the Cp* ligand by 0.32 Å from the latter plane). This puckering is smaller than observed in **24** (144.6°), where the carbon attached to ruthenium is displaced by 0.61 Å. Methyl acrylate is coplanar to within 0.066 Å. The torsional angle Cp*-(centroid)–Ir(1)–C(1)–C(2) is 79.3°. The C(1)–C(8) distance is 2.74 Å and is presumably similar to the distance between C_2 and C_β in the rhodium resting state analog **8** (eq 7).

Isomer **23a** must be one of the major isomers which selectively crystallizes from solution, since dissolution of the plates in CD_2Cl_2 at −78 °C gives only the rapid equilibrating pair (**23a**, **23b**). When the solution is warmed to 23 °C, the minor isomer **23c** grows in (see Scheme 6). Complex **23a** is very likely isostructural with the rhodium resting state just prior to C–C coupling, since the orientation of the chelate and MA ligands in **23a** is that required for tail-to-tail coupling. Although the iridium system is an excellent structural model of the rhodium system, when complex **23** was heated at 125 °C for 2 h in neat methyl acrylate (950 equiv), no catalytic activity was observed.

C. C_5H_5 and $C_5(CH_3)_4CF_3$ Systems. In order to gain a better understanding of the steric and electronic factors governing the activity and selectivity of the $C_5(CH_3)_5$ (Cp*) system, we decided to examine the effects on the catalysis of replacing the $C_5(CH_3)_5$ ring by the closely related η^5-ligands C_5H_5 (Cp) and $C_5(CH_3)_4CF_3$ (Cp‡). The Cp ligand is not as sterically demanding as the Cp* ligand and is much less electron donating; in view of these differences, disparities in the catalytic behavior of these two systems might be difficult to interpret. However, the $C_5(CH_3)_4CF_3$ ligand (Cp‡), recently reported by Gassman,[19] was shown to possess the same electronic properties as Cp but a steric bulk comparable with that of Cp*. Therefore, in this system electronic contributions could be studied independent of steric factors. Both systems, Cp and Cp‡, are discussed below.

When $(C_5H_5)Rh(C_2H_4)_2$ (**25**) was protonated in CD_2Cl_2 with 1 equiv of $H(Et_2O)_2BAr'_4$ in the presence of methyl acrylate (20 equiv), a complex mixture of rhodium species was observed and slow tail-to-tail dimerization of MA occurred (ca. 0.1 TO/min).

$$\underset{\mathbf{25}}{CpRh(C_2H_4)_2} \xrightarrow[MA]{H^+} \text{dimers} + \text{mixture of rhodium species} \quad \text{ca. 0.1 TO/min} \qquad (9)$$

By monitoring the Cp signals, at least six rhodium complexes could be detected by ^{1}H NMR spectroscopy during catalysis. One of these could be assigned to the chelate–ethylene complex $Cp\overline{Rh(CH_2CH_2C(O)OCH_3)}(C_2H_4)^+$ (**26**) by comparison of characteristic signals in the ^{1}H NMR spectrum (4.62 ppm, m, 2H, C_2H_4; 3.1–2.8 ppm, m, 4H, $C_2H_4CO_2CH_3$) with those of the analogous species (**14** and **19**) in the Cp* and 1,2,3-trimethylindenyl systems, respectively. Initially, none of the other species could be identified.

Assuming a mechanism similar to that of the Cp* system, the TO rate, which should reflect the rate of C–C bond formation, was surprisingly low for the more electrophilic Cp system. It was not certain how many of the above species belong to the catalytic cycle and how many were species outside the cycle or were the result of a deactivation process. Clearly, under these conditions, with both ethylene and MA present, the multiplicity of species generated precluded detailed analysis. In an alternative approach, we turned to the synthesis of $CpRh(MA)_2$ (**27**) with the hope that its low-temperature protonation in the absence of ethylene and MA would result in the formation of identifiable intermediates

(18) Hauptman, E.; Brookhart, M.; Fagan, P. J.; Calabrese, J. C. *Organometallics* **1994**, *13*, 774.
(19) Gassman, P. G.; Mickelson, J. W.; Sowa, J. R. *J. Am. Chem. Soc.* **1992**, *114*, 6942.

Scheme 7. Possible Isomers of $C_5H_5Rh(CH_2CHCO_2CH_3)_2$ (27)[a]

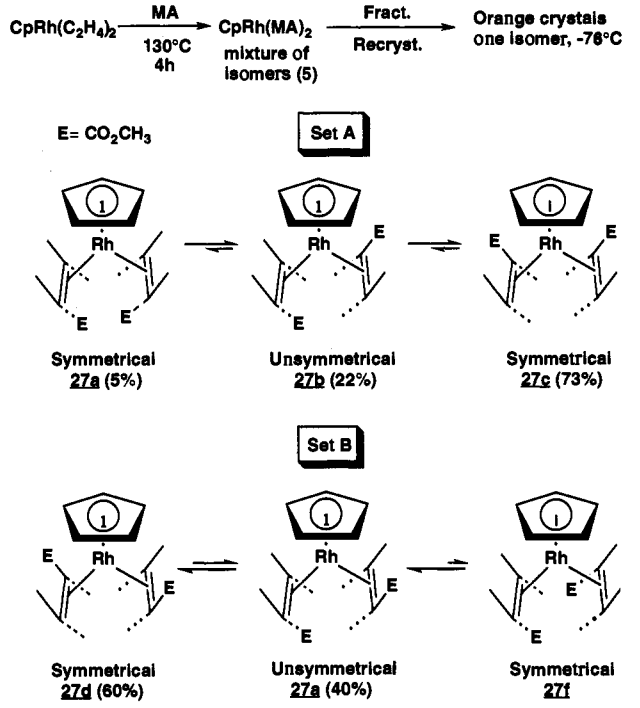

[a] Symmetry analyses here assume rapid rotation of the Cp* ring, and thus in "symmetrical" isomers the two sets of acrylate protons are magnetically equivalent.

perhaps resembling those observed in the Cp* system such as the resting state **8** and the bis-chelate complex **10**.

Treatment of complex **25** with neat methyl acrylate (MA) at 130 °C for 3 h results in the quantitative formation of $CpRh(MA)_2$ as a mixture of five isomers **27a–e** (88% yield). Depending on which face of the acrylate is coordinated and its orientation (ester group "inside" or "outside"), there are six possible isomers. Their structures, which are pictured in Scheme 7, can be grouped into two independent sets, A and B. Within each set, the isomers can interconvert via acrylate rotation, but this dynamic process does not connect set A and set B. (Acrylate rotation is slow on an NMR time scale at 23 °C.)

Fractional recrystallization of the mixture of isomers yields orange crystals whose dissolution in CD_2Cl_2 at −78 °C gives a single symmetrical isomer; upon warming to 23 °C an unsymmetrical isomer grows in and at equilibrium is 40% of the mixture. As shown in Scheme 7, the symmetrical and unsymmetrical isomers were assigned to **27d** and **27e**, respectively. Experiments which support each structural assignment will be offered below.

Protonation at −78 °C in CD_2Cl_2 of the original mixture of isomers of the orange crystals obtained from fractional recrystallization gives numerous rhodium complexes whose structures could not be assigned. However, upon warming to 23 °C, these compounds all converge and form a single cyclic complex **28** (eq 10). Complex **28** is analogous to complex **10** in the Cp* system and results from coupling of the two acrylates, followed by β-H elimination and readdition.

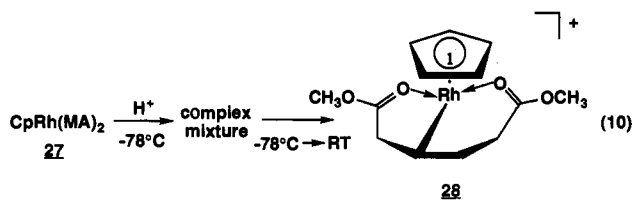

Complex **28** was treated with methyl acrylate (8 equiv) at −78 °C and slowly warmed to −10 °C, at which temperature internal dimer (*trans*-**3**) is released, catalytic dimerization starts, and a new rhodium complex is cleanly formed. The low-temperature (−78 °C) ^1H NMR spectrum of this new species is surprisingly simple and supports the unusual symmetrical structure **29** (Scheme 8), in which a proton bridges the two acrylate carbonyls. The chemical shift of the bridged proton comes at δ 18.0 ppm, comparable with other bridged protons such as the enolic proton of acetylacetone (δ 15.0 ppm) or that of dibenzoylmethane (δ 16.6 ppm). Evidence for a symmetrical structure is confirmed by the presence of only three sets of signals for the vinylic protons (δ 4.20, ddd, 2H, J = 8.9, 3.6, and 2 Hz, H_2; 3.98, ddd, 2H, J = 11.5, 8.9, and 2.6 Hz, H_1; 1.46, ddd, 2H, J = 11.5, 3.6, and 1.3 Hz, H_3) and one methoxy singlet (δ 3.92, 6H). Complete ^1H and ^{13}C NMR data can be found in the Experimental Section. At 23 °C the bridged proton is too broad to be observed presumably because of fast exchange with diethyl ether and traces of water.[20] Complex **29** is the resting state during the catalysis and at very low concentrations of methyl acrylate rearranges to the initial cyclic compound **28** (see Scheme 8).

The structure of **29** was also probed by chemical means. Indeed, deprotonation of complex **29** could be accomplished with bases such as proton sponge, pyridine, and even methanol. Monitoring the deprotonation by ^1H NMR spectroscopy was most informative (see Scheme 9). Deprotonation of **29** with pyridine (5 equiv) occurs rapidly at −85 °C to give first a kinetic symmetrical product (**27a**). Upon warming to −60 °C, complex **27a** isomerizes to an unsymmetrical complex (**27b**) via rotation of one acrylate ligand. Finally, at −40 °C complex **27b** isomerizes via a second acrylate rotation to a symmetrical complex (**27c**). At 23 °C, a thermodynamic equilibrium is established with a ratio of **27a** to **27b** to **27c** of 5:22:73.

The assignments given above derive from examination of the X-ray structure of one isomer of $Cp^*Rh(CH_2CHCO_2CH_3)_2$. Single crystals of this complex were grown from CH_2Cl_2/hexane at −30 °C. An ORTEP diagram is shown in Figure 7. Crystallographic data and collection and refinement parameters are listed in Table 2; selected interatomic distances and angles are summarized in Tables 13 and 14, respectively. The Cp*(centroid)–Rh distance is 1.889 Å. The atoms C(1), C(2), C(3), O(3), O(4), and C(4) are coplanar within 0.026 Å while C(1′), C(2′), C(3′), O(3′), O(4′), and C(4′) are coplanar within 0.053 Å. The torsional angle defined by C(2), C(1) and C(2′), C(1′) is 30.1°. It is interesting to note that the distance C(1)–Rh(1) (C(1′)–Rh(1)), 2.116(5) (2.119(5)) Å, is slightly shorter than the distance C(2)–Rh(1) (C(2′)–Rh(1)), 2.132(6) (2.143(5)) Å. The ORTEP diagram also clearly shows that in the bridged species **29** the ester groups have to be oriented "inside" in order for a proton to act as a bridge between the two carbonyl groups. It is also reasonable to assume that the ester groups are head-to-head, and thus the structure of **29** shown in Scheme 8 seems the most likely. If the assignments are correct, it is not surprising to find that, for this set, the most thermodynamically favored neutral isomer **27c** is one in which the two ester groups are head-to-head and point "outside" away from each other where steric interactions are minimal. In addition, it is interesting to note

(20) In our studies of other functionalized olefins which are partly described in a following section, we observed the same type of bridged species by protonation of (1,2,3-trimethylindenyl)$Rh(C_2H_4)_2$ in the presence of *N*,*N*-dimethyl acrylamide (CH_2=$CHC(O)N(CH_3)_2$). Partial ^1H and ^{13}C NMR data for this symmetrical species follow: ^1H NMR (CD_2Cl_2, 250 MHz, 23 °C): δ 7.5–7.2 (m, 4H, aromatic), 3.65 (ddd, J_{trans} = 11.3 Hz, J_{cis} = 8.7 Hz, J_{Rh-H} = 2.5 Hz, 2H), 3.11 (s, 6H, $N(CH_3)_2$), 2.19 (d, J_{Rh-H} = 1.5 Hz, 3H, CH_3), 1.95 (s, 3H, CH_3), 1.81 (s, 3H, CH_3), 1.53 (ddd, J_{trans} = 11.3 Hz, J_{Rh-H} = 2.4 Hz, J_{gem} = 1.4 Hz, 2H). ^{13}C NMR (CD_2Cl_2, 100 MHz, 23 °C): δ 175.5 (s, C=O), 52.0 (dt, J_{C-Rh} = 13.6 Hz, J_{C-H} = 160 Hz, $CH_2CHC(O)NMe_2$), 46.4 (dd, J_{C-Rh} = 13.3 Hz, J_{C-H} = 157 Hz, $CH_2CHC(O)NMe_2$), 39.2 (q, J_{C-H} = 140 Hz, $N(CH_3)_2$), 38.2 (q, J_{C-H} = 140 Hz, $N(CH_3)_2$), 11.3 (q, J_{C-H} = 129 Hz, CH_3), 8.9 (q, J_{C-H} = 128 Hz, CH_3), 11.3 (q, J_{C-H} = 129 Hz, CH_3), 7.0 (q, J_{C-H} = 128 Hz, CH_3). This experiment was effected at 23 °C prior to our Cp results, and at this time the bridged proton had not been observed. This complex could not be separated from monomer and traces of dimer (ca. 1.1 TO after 2 days at 23 °C).

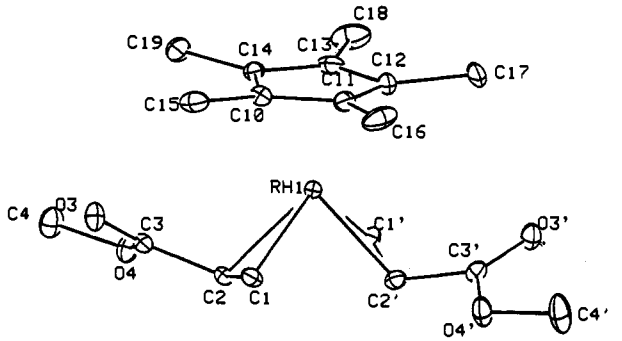

Figure 7. ORTEP drawing of one symmetrical isomer of $C_5(CH_3)_5Rh(CH_2CHCO_2CH_3)_2$.

Scheme 8. Generation of the Catalyst Resting State **29**

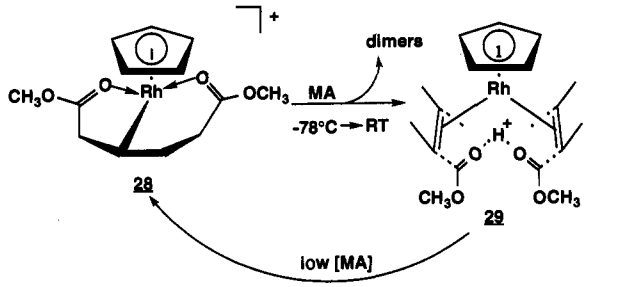

Scheme 9. Deprotonation of Complex **29**

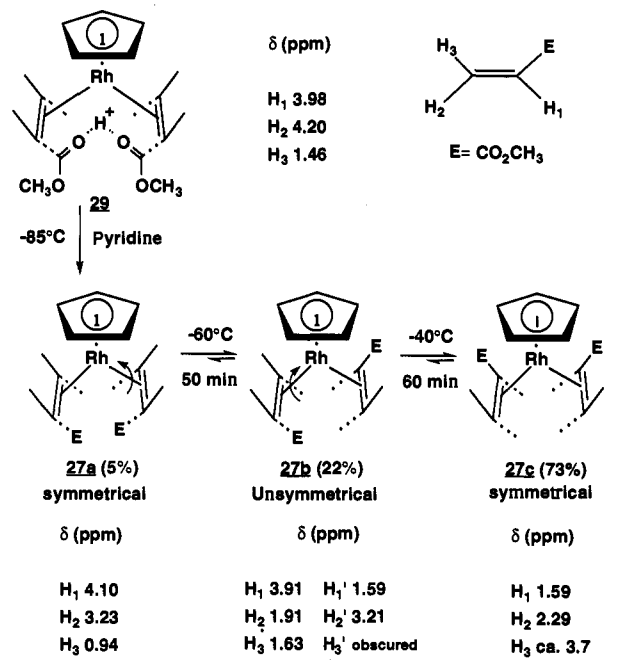

that the ^1H chemical shifts of the vinylic protons are correlated with their "inside" or "outside" orientation: "inside" protons are shielded and appear upfield compared to the "outside" ones. Scheme 9 lists observable vinylic ^1H chemical shifts for complexes **29**, **27a**, **27b**, and **27c**. All assignments are secure on the basis of coupling patterns, and as can be seen, the shift trend noted above is followed in every case.

The deprotonation of complex **29** leads to one set of three isomers which is different from the set obtained from fractional recrystallization (orange crystals). The set from recrystallization must be set B, as assigned in Scheme 7. The unsymmetrical isomer is unique and must be **27e**. The symmetrical isomer is assigned to **27d** on the basis of the relative chemical shifts of H_1, H_2, and H_3. From these data, structural assignments can be made for all of the five isomers obtained from the thermolysis of $CpRh(C_2H_4)_2$ in methyl acrylate.

Table 13. Selected Interatomic Distances for $Cp^*Rh(CH_2CHCO_2CH_3)_2$ (Å)[a]

Rh(1)–C(1)	2.116(5)	O(3)–C(3)	1.204(5)
Rh(1)–C(1′)	2.119(5)	O(3′)–C(3′)	1.193(5)
Rh(1)–C(2)	2.132(6)	O(4)–C(3)	1.331(5)
Rh(1)–C(2′)	2.143(5)	O(4′)–C(3′)	1.340(6)
Rh(1)–C(10)	2.213(4)	C(1)–C(2)	1.416(8)
Rh(1)–C(11)	2.238(6)	C(1′)–C(2′)	1.409(7)
Rh(1)–C(12)	2.238(6)	C(2)–C(3)	1.483(7)
Rh(1)–C(13)	2.265(6)	C(2′)–C(3′)	1.483(7)
Rh(1)–C(14)	2.261(6)		

[a] Numbers in parentheses are the estimated standard deviations.

Table 14. Selected Bond Angles for $Cp^*Rh(CH_2CHCO_2CH_3)_2$ (deg)[a]

C(1)–Rh(1)–C(1′)	110.0(2)	Rh(1)–C(2′)–C(1′)	69.8(3)
C(1)–Rh(1)–C(2)	39.0(2)	Rh(1)–C(2′)–C(3′)	114.3(3)
C(1)–Rh(1)–C(2′)	85.8(2)	O(3)–C(3)–O(4)	122.6(4)
C(1′)–Rh(1)–C(2)	86.9(2)	O(3′)–C(3′)–O(4′)	123.0(4)
C(1′)–Rh(1)–C(2′)	38.6(2)	O(3)–C(3)–C(2)	126.5(5)
C(2)–Rh(1)–C(2′)	85.3(2)	O(4)–C(3)–C(2)	110.8(4)
Rh(1)–C(1)–C(2)	71.1(3)	O(3′)–C(3′)–C(2′)	126.8(4)
Rh(1)–C(1′)–C(2′)	71.6(3)	O(4′)–C(3′)–C(2′)	110.2(4)
Rh(1)–C(2)–C(1)	69.9(3)	C(1)–C(2)–C(3)	121.2(5)
Rh(1)–C(2)–C(3)	113.8(4)	C(1′)–C(2′)–C(3′)	122.1(4)

[a] Numbers in parentheses are the estimated standard deviations.

After these studies which established the nature of the resting state, we decided to reinvestigate the protonation of $CpRh(C_2H_4)_2$ in the presence of methyl acrylate (eq 9). Among the numerous rhodium species observed, we noticed the presence of at least two *neutral* complexes **27d** and **27c** (see Scheme 7). Signals corresponding to the resting state could not be clearly detected. It occurred to us that in the presence of a large excess of MA under catalytic conditions methyl acrylate could act as a base and deprotonate the resting state thus deactivating the catalyst. To examine this possibility, $CpRh(C_2H_4)_2$ was protonated with an excess of acid (4 equiv) in the presence of 20 equiv of methyl acrylate and the reaction monitored by ^1H NMR spectroscopy. Again, the chelate–ethylene complex **26** is formed, but now signals corresponding to the bridged species **29** are also visible and those of the neutral species are greatly reduced. These observations support our proposed deactivation pathway through deprotonation. This finding might be relevant to possible deactivation pathways of the Cp* and indenyl systems when catalytic runs are carried out with extremely large ratios of MA to catalyst.

As noted above, the $C_5(CH_3)_4CF_3$ ($Cp^\ddagger$) ligand has similar electronic properties to the C_5H_5 ligand but comparable steric bulk to the C_5Me_5 ligand. This presented an opportunity to study electronic factors independent of steric considerations. Increased electrophilicity at the metal center was expected to accelerate the rate of migratory insertion. We consequently expected the $C_5Me_4CF_3$ catalyst system to be more active, since migratory insertion is the turnover-limiting step in the Cp*-based system. The bis-ethylene complex **30** was prepared in fair yield (54%) by mild reduction of $[Cp^*RhCl_2]_2$ under ethylene (Na_2CO_3, EtOH, 70 °C) (eq 11). This synthesis was modeled after one reported for $Cp^*Rh(C_2H_4)_2$.[21]

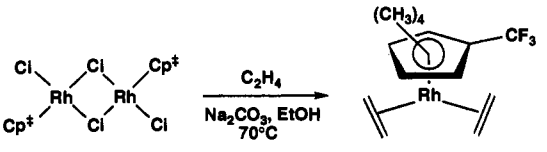

(11)

$Cp^\ddagger = C_5(CH_3)_4CF_3$ **30**

Protonation of complex **30** in CD_2Cl_2 at −78 °C yields the

(21) Booth, B. L.; Haszeldine, R. N.; Hill, M. *J. Chem. Soc. A* **1969**, 1299.

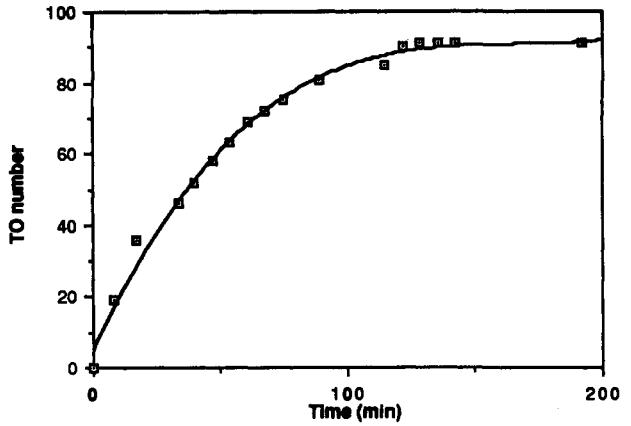

Figure 8. Equivalents of methyl acrylate consumed versus time at 23 °C for $(C_5(CH_3)_4CF_3)Rh(C_2H_4)(CH_2CH_2\text{-}\mu\text{-}H)^+$ (**31**) (0.025 mmol of Rh, 92 equiv of MA, CD_2Cl_2).

agostic complex $Cp^*Rh(C_2H_4)(CH_2\text{–}CH_2\text{–}\mu\text{-}H)^+$ (**31**).[22] ^1H NMR shift values of **31** are similar to those of $Cp^*Rh(C_2H_4)(CH_2\text{–}CH_2\text{–}\mu\text{-}H)^+$ (**7**) and support the assigned structure. For example, the agostic hydrogen H_a appears at –8.76 ppm (–100 °C) for **31** relative to –8.6 ppm (–110 °C) for **7**.[10] Complex **31** is unstable at ambient temperatures, but when it is treated immediately at –78 °C with methyl acrylate followed by warming to 23 °C, slow dimerization occurs. A typical plot representing the reaction profile is pictured in Figure 8.

In contrast to the Cp* and 1,2,3-trimethylindenyl systems, the rate of dimerization drops rapidly with time. Unexpectedly, a much lower activity is observed (ca. 1 TO/min) for this electrophilic $Cp^\ddagger$ system, which led us to examine the details of the mechanism by ^1H NMR spectroscopy.

In close analogy to the C_5Me_5 and 1,2,3-trimethylindenyl systems, addition of a few equivalents (ca. 5) of methyl acrylate to complex **31** at –78 °C in CD_2Cl_2 results in immediate formation of the chelate–ethylene complex $Cp^*Rh(CH_2CH_2COOCH_3)(C_2H_4)^+$ (**32**).

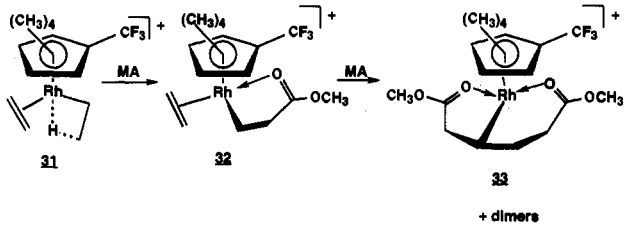

Once complete conversion of MA has occurred, the bis-chelate complex **33** is formed. ^1H and ^{13}C NMR data of complex **33** are consistent with the data reported for the analogous C_5H_5, C_5Me_5, and 1,2,3-trimethylindenyl systems (see the Experimental Section for spectroscopic characterization of **32** and **33**).

Treatment of complex **33** with methyl acrylate (42 equiv) results in slow dimerization (27 TO after 13 h at 23 °C). In contrast to the case of the previously described systems, no reaction takes place below 23 °C and the only observable species during catalysis is the bis-chelate complex **33**.

This result indicates that **33** is the catalyst resting state under these conditions. We presume that the major catalytic cycle for this system is similar to that for Cp*,[23] but once the bis-chelate **33** is formed release of dimer and reentry into the catalytic cycle must occur much more slowly than the analogous process in the Cp* system. This can be attributed to stronger interactions of the chelating carbonyl groups in **33** due to the enhanced electrophilicity of the metal center induced by the CF_3 substituent. Thus, while the migratory insertion reaction may be faster in the $C_5Me_4CF_3$ system (we have no evidence on this point), the overall catalytic activity is decreased relative to that of the Cp* system due to the enhanced stability and decreased reactivity of **33**, a species outside the major catalytic loop. Although the C_5H_5 and $C_5Me_4CF_3$ ligands are proposed to have similar electronic properties, the behavior of the catalytic systems derived from these ligands is quite different, as described above. We presume this difference must be attributed to steric factors, but cannot offer any explicit rationalization.

D. Attempted Catalytic Dimerization of Other Functionalized Olefins. In order to determine the scope of the dimerization reaction, various functionalized olefins were investigated which could potentially form chelate structures such as those in the catalyst resting states for the Cp* and 1,2,3-trimethylindenyl systems **8** and **20**. The reactions of methyl vinyl ketone, methyl crotonate, 2-vinylpyridine, and 1-vinyl-2-pyrrolidinone are described below.

1. Methyl Vinyl Ketone (MVK). Treatment of $Cp^*Rh(C_2H_4)(CH_2\text{–}CH_2\text{–}\mu\text{-}H)^+$ (**7**) with MVK resulted in the immediate formation of the allylic species $Cp^*Rh(\eta^3\text{-}CH_3COCH_2CHCHCHCOCH_3)^+$ (**34**). No dimers were detected after 12 h at 55 °C. Spectroscopic data for complex **34** match those of the closely related deactivated catalyst **9** formed from methyl acrylate. For example, in the ^1H NMR spectrum, allylic hydrogens appear at 5.46 ppm (ddd, J = 11, 8, and 2 Hz), 4.85 ppm (ddd, 2 J = 8 Hz and J = 2 Hz), and 3.07 ppm (d, J = 11 Hz) while in the ^{13}C NMR spectrum two carbonyl resonances appear at 230.2 ppm (chelated) and 198.9 ppm (free) (see the Experimental Section for complete NMR data). Similar to complex **9**, complex **34** must arise from dehydrogenation of an intermediate analogous to the bis-chelate complex **10** or the oxaallyl **18**. However, attempts to generate an active system by running the reaction (35 equiv of MVK) under an atmosphere of H_2 at 23 °C were not successful. After 3 days only ca. 2 equiv of dimers had been formed along with ca. 5 equiv of 2-butanone (hydrogenated MVK).

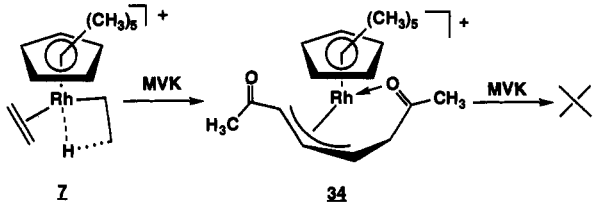

In contrast to the C_5Me_5 results, protonation of (trimethyl- or (heptamethylindenyl)$Rh(C_2H_4)_2$ in the presence of MVK produced dimers.[24] However, rates of coupling are much lower than those for MA. Initial turnover frequencies are in the ranges 0.1–0.2 min^{-1} and 1–3 min^{-1} for the trimethyl- and heptamethylindenyl systems, respectively. In addition, the catalyst lifetime is greatly reduced and a maximum of 120 TO could be achieved with this best catalyst system. The conjugated *trans*-**2′** dimer is the major product (ca. 98%). At the end of the reaction isomerization occurs, yielding small amounts of *trans*-**3′** (ca. 2%); no *cis*-**2′** can be detected by ^1H NMR spectroscopy. The deactivated catalyst, as in the Cp* system, is an allylic species $[Ind]Rh(\eta^3\text{-}CH_3COCH_2CHCHCHCOCH_3)^+$ (**35**). When [Ind] = 1,2,3-trimethylindenyl, this species was clearly observed by ^1H

(22) When 1 equiv of acid is used, low-temperature ^1H NMR spectroscopy reveals the presence of both neutral and cationic complexes **30** and **31**. Ratios of **30** to **31** vary from sample to sample, and an excess of acid favors the agostic complex **31**. This can be rationalized by the poor basicity of the rhodium center in complex **31** coupled with the presence of other bases such as diethyl ether or adventitious water which compete for the proton.

(23) In support of this contention, *trans*-**2** (ca. 99%) is the major isomer formed with only ca. 1% of *trans*-**3**, in analogy with the Cp* system.

(24) Rhodium-catalyzed dimerization of methyl vinyl ketone has been reported: see ref 2e.

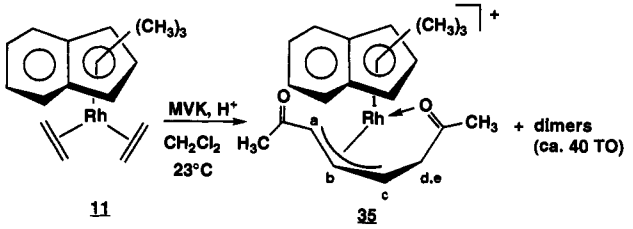

11 35

NMR spectroscopy but could not be separated from product dimers. The structure of complex **35** was established by characteristic ^{1}H NMR signals (CD_2Cl_2, 23 °C) at δ 5.70 (ddd, J = 10.5, 7.5, and 2.7 Hz, H_b), 4.93 (ddd, 2 J = 7.5 Hz, J = 2.3 Hz, H_c), and 3.44 (dd, J_{gem} = 21 Hz, J_{Hd-Hc} = 7.5 Hz, H_d). These chemical shifts and coupling patterns are consistent with the ones observed for the allylic species in the Cp* system **34**. The catalyst lifetime could not be prolonged by running the reaction under H_2; slow hydrogenation of MVK occurred instead.

In order to understand this dramatic loss in activity and possibly observe new intermediates, the reaction of MVK with the 1,2,3-trimethylindenyl system was monitored by low-temperature ^{1}H NMR spectroscopy. Protonation of (1,2,3-trimethylindenyl)-$Rh(C_2H_4)_2$ in CD_2Cl_2 followed by addition of MVK (40 equiv) at −78 °C resulted in the formation of a complex mixture of rhodium species. Upon warming to −20 °C, a major species (**36**) emerges. Complex **36** has characteristic signals corresponding to

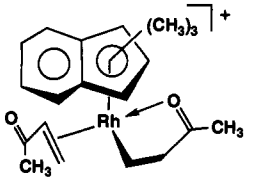

36

an η^2-methyl vinyl ketone moiety (δ 3.82 [dd, J_{cis} = 7 Hz, J_{trans} = 13 Hz], 3.55 [d, J_{trans} = 13 Hz], 2.87 [d, J_{cis} = 7 Hz]) and is thus tentatively assigned as the analog of **20** although no additional resonances can be clearly assigned. When this solution is warmed to 23 °C, dimerization occurs, and after 2 h and 20 min, ca. 26 TO have been achieved. After 26 h, the dimerization is complete and the major species in solution is the deactivated catalyst **35**.

2. Methyl Crotonate. Treatment of $Cp^*Rh(C_2H_4)(CH_2CH_2$-μ-H)$^+$ (**7**) with excess *trans*-methyl crotonate ($CH_3CH{=}CHCO_2CH_3$) in CD_2Cl_2 does not produce any dimers after 12 h at 23 °C. However, a single rhodium species (**37**) is generated. Also noticeable early in the reaction is the presence of ethane. Complex **37** was characterized by ^{1}H and ^{13}C NMR spectroscopy as well as elemental analysis and is formulated as the oxaallyl complex shown below.

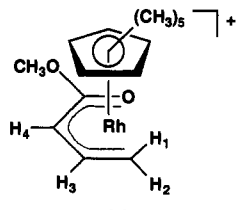

37

The presence of only one crotonate moiety in complex **37** is suggested by the observation of only one methoxy signal integrating for three protons in the ^{1}H NMR spectrum (3.83 ppm) and single resonances for *C*=O (171.4 ppm) and CO_2CH_3 (52.1 ppm) in the ^{13}C NMR spectrum. In the ^{1}H NMR spectrum, the downfield chemical shift (5.42 ppm) and dddd pattern (J = 7, 10, 12 Hz and J_{Rh-H} = 2.2 Hz) of H_3 are also very characteristic. All the other protons appear as doublets (δ 4.38, J = 7 Hz, H_4; 3.12, J = 10 Hz, H_2; 2.84, J = 12 Hz, H_1).

The formation of **37** can be rationalized by a transfer hydrogenation reaction which results in dehydrogenation of methyl crotonate to produce complex **37** and hydrogenation of ethylene to give ethane. Attempts to run the dimerization reaction under 1 atm of H_2 resulted in hydrogenation of methyl crotonate to yield methyl butyrate ($CH_3(CH_2)_2CO_2CH_3$) rather than dimerization. For example, purging a solution of **7** in CD_2Cl_2 with H_2 at 23 °C in the presence of methyl crotonate (40 equiv) gave 43% conversion of methyl crotonate to methyl butyrate after 30 min.

3. 2-Vinylpyridine. Treatment of $Cp^*Rh(C_2H_4)(CH_2CH_2$-μ-H)$^+$ (**7**) with 2-vinylpyridine results in the clean formation of a new species (**38**) but no dimer formation (36 h, 23 °C). Spectroscopic data reveal that complex **38** has structural features resembling those of the deactivated catalysts **9** and **34** (see below). When the reaction is monitored by ^{1}H NMR spectroscopy, ethane production is observed (δ 0.8 ppm in CD_2Cl_2), which suggests again that complex **38** is derived from dehydrogenation of an intermediate containing the coupled product of 2-vinylpyridine and that ethylene acts as an hydrogen acceptor. However, in contrast to the deactivated compounds obtained earlier from the reaction of the Cp* system with methyl acrylate or methyl vinyl ketone (**9** and **34**, respectively), complex **38** is not an allylic species. It is best formulated as a σ-bound bis-chelate complex as drawn below.

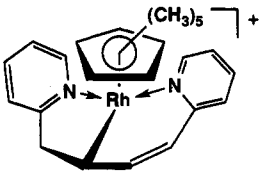

38

The most definitive proof of the structure of **38** is given by the ^{13}C chemical shift of the σ-bound carbon at 45.0 ppm and its large ^{103}Rh coupling of 22 Hz. This chemical shift and Rh–C coupling constant are very similar to the ones observed for the σ-bound carbon in the bis-chelate complex **10** derived from reaction of **7** with MA (δ 43.2 ppm, J_{C-Rh} = 25 Hz). In contrast, for the allylic species **9** and **34** chemical shifts for the corresponding carbons are 71.6 and 78.6 ppm, respectively, and in both cases J_{Rh-C} coupling constants are low (9 Hz). Exposing complex **7** to an excess of 2-vinylpyridine (ca. 500 equiv) in CH_2Cl_2 at 23 °C under 1 atm of H_2 did not result in any dimerization after 5 days.

4. 1-Vinyl-2-pyrrolidinone. Treatment of $Cp^*Rh(C_2H_4)(CH_2$-CH_2-μ-H)$^+$ (**7**) or the analogous 1,2,3-trimethylindenyl complex with 1-vinyl-2-pyrrolidinone ($CH_2{=}CH$–[N–C(O)–$(CH_2)_3$]) results in the slow formation of dimers (ca. 35 TO after 1 week for the indenyl system at 23 °C). In contrast to the methyl acrylate and methyl vinyl ketone dimers, the dimer formed here is a branched, head-to-tail isomer (eq 12). The dimer was not isolated

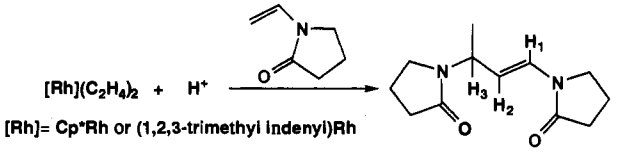

(12)

free of catalyst. However, ^{1}H and ^{13}C NMR data are consistent with the above structure. For example in the ^{1}H NMR spectrum the vinylic protons H_1 and H_2 appear at 6.92 ppm (d, J = 14 Hz) and 4.88 ppm (dd, J = 14 and 6 Hz), respectively. The methine proton H_3 comes at 4.77 ppm as a multiplet while a doublet at 1.23 ppm (J = 7 Hz) corresponds to CH_3 (a complete set of NMR data is given in the Experimental Section). We postulate

Scheme 10. Preferential Formation of Head-to-Tail over Tail-to-Tail Dimers

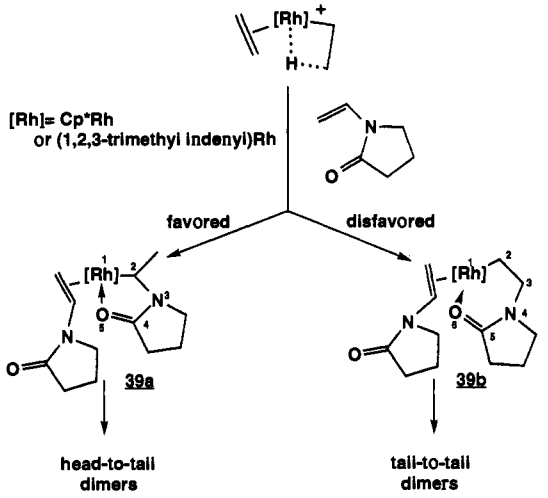

a mechanism similar to that of methyl acrylate in which an η^2-vinylpyrrolidinone–chelate complex (**39**) is formed. The selective formation of head-to-tail dimers can be rationalized by the preferential formation of a five-membered ring over a six-membered ring chelate in the presumed resting state **39**. This proposal is pictured in Scheme 10. However, no additional experiments have been carried out to detect any of the proposed intermediates. The decreased activity of the catalytic system toward 1-vinyl-2-pyrrolidinone compared to methyl acrylate might be electronic in origin (amides are better donor ligands), but no direct evidence on this point has been obtained.

Summary

The development of highly efficient Rh(III) catalysts for the selective tail-to-tail dimerization of methyl acrylate (MA) has been described. Protonation of $Cp^*Rh(C_2H_4)_2$ in the presence of MA provides a route into the catalytic cycle. Mechanistic details of this cycle have been elucidated. The catalyst resting state has been generated by protonation of $Cp^*Rh(MA)_2$ at −78 °C and identified as $Cp^*Rh(CH_2CH_2COOCH_3)(\eta^2\text{-}CH_2CHCO_2CH_3)^+$ (**8**). The analogous $Cp^*Ir(CH_2CH_2COOCH_3)(\eta^2\text{-}CH_2CHCO_2CH_3)^+$ (**23a**) was synthesized; X-ray analysis of this complex strongly suggests, by comparison, a structure of **8** in which the orientation of the acrylate ligands is that required for tail-to-tail coupling. Complex **8** undergoes β-migratory insertion to give $Cp^*RhCH(CH_2COOCH_3)(CH_2CH_2COOCH_3)^+$ (**10**). The free energy of activation for this process is 18.7 kcal/mol and matches that based on the catalytic turnover frequency (6.6 TO/min at 25 °C), which confirms **8** as the resting state and the C–C coupling reaction as the turnover-limiting step. This catalytic system, however, deactivates after ca. 1400 TO, resulting in the formation of $Cp^*Rh(\eta^3\text{-}CH_3OCOCH_2CHCHCHCO_2CH_3)^+$ (**9**). The production of complex **9** occurs through formal loss of H_2 from **10**. This deactivation process is reversible under H_2, and thus a very long-lived catalytic system can be operated under 1 atm of H_2.

Second-generation catalysts have been produced by replacing the $C_5(CH_3)_5$ ligand by methylated indenyl ligands. Although both systems operate via a similar mechanism, the indenyl catalysts have greater activities and much longer lifetimes. For example, using the catalytic system derived from (1,2,3-trimethylindenyl)-$Rh(C_2H_4)_2$ (**11**), conversion of 54 000 equiv of MA to dimethyl hexenedioates could be achieved after 68 h at 55 °C under N_2. In contrast, substitution of the $C_5(CH_3)_5$ ligand by the C_5H_5 or $C_5(CH_3)_4CF_3$ ligands generates electrophilic systems with low activities. The former systems operate via somewhat different catalytic cycles with different catalyst resting states: the bridged species $CpRh(CH_2CHCOOCH_3)H(CH_2CHCOOCH_3)^+$ (**29**) and the bis-chelate complex $Cp^*RhCH(CH_2COOCH_3)(CH_2CH_2COOCH_3)^+$ (**33**), respectively.

Finally, the scope of the dimerization reaction was examined by employing other olefins. Catalytic systems derived from protonation of (trimethylindenyl)$Rh(C_2H_4)_2$ or (heptamethylindenyl)$Rh(C_2H_4)_2$ slowly dimerize methyl vinyl ketone to tail-to-tail dimers. Reaction of $Cp^*Rh(C_2H_4)(CH_2CH_2\text{-}\mu\text{-}H)^+$ (**7**) with methyl crotonate results in formal loss of H_2 and production of the oxaallyl complex $Cp^*Rh(\eta^5\text{-}CH_2CHCHCO_2CH_3)^+$ (**37**). Treatment of complex **7** with 2-vinylpyridine results in stochiometric coupling followed by formal dehydrogenation to yield the bis-chelate complex $Cp^*Rh[(C_5H_5N)CHCHCHCH_2(C_5H_5N)]^+$ (**38**). Finally, slow catalytic head-to-tail dimerization occurs when 1-vinyl-2-pyrrolidinone is employed using $Cp^*Rh(C_2H_4)_2$ or (trimethylindenyl)$Rh(C_2H_4)_2$ as catalyst precursors. The disparities observed in the catalytic cycles, the catalyst activities, and the lifetimes associated with changing the steric or/and electronic features of either the ligands or the substrates offer insight into the design of other active catalytic systems.

Experimental Section

General Information. All complexes were manipulated under an atmosphere of dry, oxygen-free nitrogen within a Vacuum Atmospheres drybox, on a high-vacuum line, or on a standard Schlenk line. Methylene chloride was distilled in an N_2 atmosphere from phosphorus pentaoxide prior to use. Tetrahydrofuran, dimethoxyethane, toluene, diethyl ether, and hexane was distilled in an N_2 atmosphere from sodium/benzophenone. Methanol was distilled from $Mg(OMe)_2$. ^1H and ^{13}C NMR spectra were recorded on either a Varian XL-400, a Bruker WM-200, -250, or -300, or a General Electric 300 spectrometer. Chemical shifts were reported by reference to protonated residues of solvents. Ethylene was purified by passing over an oxygen-scavenging copper catalyst (BASF catalyst R 3-11) and water-scavenging molecular sieves (4 Å). Elemental analyses were performed by Oneida Research Services, Inc. The following preparations were based on standard literature procedures: $H(Et_2O)_2BAr'_4$,[25] $[(C_2H_4)_2RhCl]_2$,[26] (1,2,3-trimethylindenyl)$Rh(C_2H_4)_2$,[13] (1,2,3,4,5,6,7-heptamethylindenyl)$Rh(C_2H_4)_2$,[13] $[C_5(CH_3)_4(CF_3)RhCl_2]_2$,[19] $CpRh(C_2H_4)_2$,[27] $Cp^*Rh(C_2H_4)_2$,[21] $Cp^*Ir(C_2H_4)_2$,[28] and $Cp^*(P(OCH_3)_3)Rh(C_2H_4)$.[29] Methyl acrylate was purchased from Aldrich, stored over 4-Å molecular sieves at −30 °C, and degassed with an N_2 purge just prior to use. Methyl vinyl ketone, methyl crotonate, 2-vinylpyridine, and 1-vinyl-2-pyrrolidinone were purchased from Aldrich and used as received.

^1H and ^{13}C NMR data attributed to the counteranion BAr'_4 (Ar' = 3,5-$(CF_3)_2C_6H_3$) follow. These are consistent for all examined cationic complexes and are not included in each compound characterized below. ^1H NMR (CD_2Cl_2): δ 7.72 (8H, Ar'), 7.56 (4H, Ar'). ^1H NMR chemical shifts are accurate to within ±0.02 ppm. ^{13}C NMR (CD_2Cl_2): δ 162.1 (q, J_{C-B} = 50 Hz, $C_{1'}$), 135.2 (d, J_{C-H} = 160 Hz, $C_{2'}$), 129.3 (q, $^2J_{C-F}$ = 31 Hz, $C_{3'}$), 125.0 (q, J_{C-F} = 272 Hz, CF_3), 117.8 (dq, J_{C-H} = 164 Hz, $^3J_{C-F}$ = 4 Hz, $C_{4'}$). ^{13}C NMR chemical shifts and coupling constants are accurate to within ±1 ppm and ±2 Hz, respectively.

Kinetics of Methyl Acrylate Dimerization Followed by ^1H NMR Spectroscopy. The following general procedure is typical. A round-bottomed flask was charged with the catalyst precursor dissolved in a minimum amount of CH_2Cl_2. It was then cooled to −0 °C, and a solution of $H(Et_2O)_2BAr'_4$ in CH_2Cl_2 was added. After complete dissolution of the solids, methyl acrylate was syringed into the solution. At this stage,

(25) Brookhart, M.; Grant, B.; Volpe, A. F., Jr. *Organometallics* **1992**, *11*, 3920.
(26) Cramer, R. *Inorg. Synth.* **1974**, *15*, 14.
(27) King, R. B. *Inorg. Chem.* **1963**, *2*, 528.
(28) Maitlis, P. M.; Moseley, K.; Kang, J. W. *J. Chem. Soc. A* **1970**, 2875. For an improved procedure for the preparation of $(Cp^*IrCl_2)_2$, see: Heinekey, D. M.; Ball, R. G.; Graham, W. A. G.; Hoyano, J. K.; McMaster, A. D.; Mattson, B. M.; Michel, S. T. *Inorg. Chem.* **1990**, *29*, 2023.
(29) Jones, W. D.; Feher, F. J. *Inorg. Chem.* **1984**, *23*, 2376.

when runs were conducted under H_2, the solution was purged with H_2 for 15 min and then exposed to 1 atm of hydrogen. The flask was then either placed in a water bath at 23 °C or heated to a designated temperature under N_2 or H_2. Samples were taken at regular intervals, and the extent of dimerization was checked by ^1H NMR spectroscopy. NMR signals corresponding to the methoxy groups of dimers *trans*-**2**, *cis*-**2**, and *trans*-**3** were integrated versus the methoxy signal of methyl acrylate. The relative percentage of each dimer was calculated using signals at 3.09 ppm for *trans*-**3**, 2.93 ppm for *cis*-**2**, and 2.47 ppm for *trans*-**2** (see below for complete NMR data).

Typical Example: Dimerization of 60 000 equiv of MA by the Catalyst System Derived from Protonation of 11 (see Table 10). Under N_2, a two-neck 500-mL round-bottomed flask fitted with a condenser was charged with 8.6 mg (0.027 mmol) of (1,2,3-trimethylindenyl)$Rh(C_2H_4)_2$ (**11**). The flask was cooled to 0 °C, and 150 mL (1666 mmol) of methyl acrylate was added. One equivalent of $H(Et_2O)_2BAr'_4$ (28.3 mg, 0.028 mmol) dissolved in 10 mL of CH_2Cl_2 was transferred to the solution via cannula. The solution turned immediately from yellow to orange. Finally, the polymerization inhibitor, 4-methoxyphenol (19.6 mg, 0.158 mmol) dissolved in CH_2Cl_2 (5 mL) was added. The flask was then heated to 55 °C, and samples were withdrawn at regular intervals. ^1H NMR spectroscopy was used to monitor the reaction (see above). Analysis of the data showed the following conversion versus time: 285 min (27.9%), 1275 min (56.6%), 1965 min (68.9%), 2740 min (79.4%), 3375 min (83.2%), and 4065 min (88.4%). The solution was then exposed to 1 atm of H_2, and complete conversion was achieved after an additional 360 min.

When >99% MA conversion was achieved, ^1H and ^{13}C NMR data could be obtained for the three major diester products in catalytic runs. These data are summarized below.[30]

Dimethyl (*E*)-2-Hexenedioate (*trans*-2). ^1H NMR (250 MHz, $CDCl_3$, 23 °C): δ 6.92 (m, 1H, $MeCO_2CH{=}CHR$), 5.83 (dt, 1H, J_{trans} = 16 Hz, ^4J = 1.5 Hz, $MeCO_2CH{=}CHR$), 3.70 (s, 3H, OCH_3), 3.66 (s, 3H, OCH_3), 2.47 (m, 4H, $R'(CH_2)_2CO_2CH_3$). ^{13}C NMR (100 MHz, CD_2Cl_2, 23 °C): δ 172.7 (s, C=O), 166.6 (s, C=O), 147.2 (d, J_{C-H} = 155 Hz, *C*H), 121.9 (d, J_{C-H} = 162 Hz, *C*H), 51.6 (q, J_{C-H} = 147 Hz, OCH_3), 51.3 (q, J_{C-H} = 147 Hz, OCH_3), 32.3 (t, J_{C-H} = 130 Hz, CH_2), 27.4 (t, J_{C-H} = 130 Hz, CH_2).

Dimethyl (*Z*)-2-Hexenedioate (cis-2). ^1H NMR (250 MHz, $CDCl_3$, 23 °C): δ 6.23 (m, 1H, $MeCO_2CH{=}CHR$), 5.80 (dt, J_{cis} = 11 Hz, ^4J = 1.6 Hz, $MeCO_2CH{=}CHR$), 3.69 (s, 3H, OCH_3), 3.65 (s, 3H, OCH_3), 2.96 (dd, *J* = 7 and 1.6 Hz, CH_2), 2.90 (dd, *J* = 7 and 1.6 Hz, CH_2). ^{13}C NMR (100 MHz, CD_2Cl_2, 23 °C): δ 173.0 (s, C=O), 166.4 (s, C=O), 148.3 (d, J_{C-H} = 166 Hz, *C*H), 120.5 (d, J_{C-H} = 163 Hz, *C*H), 51.5 (q, J_{C-H} = 147 Hz, OCH_3), 51.0 (q, J_{C-H} = 147 Hz, OCH_3), 33.2 (t, J_{C-H} = 129 Hz, CH_2), 24.5 (t, J_{C-H} = 131 Hz, CH_2).

Dimethyl (*E*)-3-Hexenedioate (trans-3). ^1H NMR (300 MHz, CD_2Cl_2, 23 °C): δ 5.63 (m, 2H, CH), 3.09 (m, CH_2, 4H). The methoxy signal is obscured by the methoxy bands of the *trans*- and *cis*-**2** isomers.

Kinetics of Methyl Acrylate Dimerization Followed by Gas Chromatography. Quantitative organic analyses were obtained with an Hewlett Packard 5890A gas chromatograph using a J&W Scientific DB-5 capillary column (30 M, 0.25-mm i.d., 0.25-mm film thickness), the following temperature program (35 °C for 4 min; 35–220 °C at 7 °C/min; 220 °C for 2 min), and flame ionization detection. For organic products identified by GC-MS, the following elution order was observed: MA, MP, *cis*-**3**, *cis*-**2**, dimethyl adipate (DMA), branched diester, *trans*-**3**, *trans*-**2**, dimethyl muconate (DMM), triester. The *cis*/*trans* assignments were based upon intensities and the normal tendency of *cis* isomers to elute before *trans* isomers on this column. With *o*-dichlorobenzene (ODCB) internal standard (5.00 wt %), GC response factors were obtained with multilevel calibrations over the entire concentration range observed in kinetic experiments. MA (Spectrum Chemical) and MP (Aldrich) were calibrated from pure samples. A sample of mixed diester products was obtained from a reaction solution via distillation and calibrated by assuming each diester component had the same response factor. The response factor for triester products was assumed to be equivalent to that of the diesters.

In a typical kinetic experiment, $H(OEt_2)BAr'_4$ (1.1 equiv) and $Cp^*Rh(C_2H_4)_2$ or (1,2,3-trimethylindenyl)$Rh(C_2H_4)_2$ were weighed into separate vials in the drybox and then dissolved in 0.2 mL of CH_2Cl_2 and placed in a freezer at −40 °C. As the solutions cooled, 6.650 g of freshly distilled MA (stabilized with 1 wt % 3,5-di-*tert*-butyl-4-hydroxyanisole) was weighed into a bottle containing 0.350 g of ODCB and a magnetic stir bar. The bottle was capped with a septum. The cold solution of $H(OEt_2)_2$-BAr'_4 was added dropwise to the $Cp^*Rh(C_2H_4)_2$ solution. A few drops of MA were added to the (1,2,3-trimethylindenyl)$Rh(C_2H_4)_2$ solution prior to acid addition to prevent precipitation of purple crystals. The resulting catalyst solution was placed into a gas-tight syringe and diluted to 0.50 mL with fresh CH_2Cl_2. The septum bottle and syringe were removed from the drybox, and the MA solution was stirred and thermostated at 25.0 ± 0.1 °C (water bath heated with a recirculating bath) in a hood. Nitrogen or hydrogen was bubbled through the MA solution for 5 min; then the catalyst was added with the syringe. Ten-microliter samples were withdrawn from the resulting catalyst solution at the indicated times and immediately added to 2 mL of acetonitrile, which quenched all Rh-catalyzed reactions. The acetonitrile solution was then analyzed by GC.

Because the GC analysis described above was only capable of detecting one of potentially several different branched diester isomers, hydrogenation studies were performed to more accurately determine tail-to-tail versus head-to-tail coupling selectivity. In these studies, 1-mL samples were withdrawn and immediately added to Bu_4NCl (2 mol/mol of Rh) dissolved in toluene (5 mL), which also quenched all Rh-catalyzed reactions. Adding 10% Pd on activated carbon (100 mg) and heating the toluene solution to reflux under 1 atm of H_2 for 4–5 h converted all the unsaturated diester isomers to dimethyl adipate (DMA) and dimethyl 2-methylglutarate. The relative amounts of these saturated diester products could be analyzed with the same GC column and temperature program described above. The head-to-head coupling product dimethyl 2,3-dimethylsuccinate was never detected in any hydrogenation experiment.

Raw GC data are tabulated in the supplementary material. See also Tables 7–9 in the text.

$[Cp^*Rh(CH_2CH_2C(O)OCH_3)(P(OCH_3)_3)]^+[BAr'_4]^-$ (5). A 50-mL round-bottomed flask was charged with 71 mg (0.18 mmol) of $Cp^*P(OCH_3)_3Rh(C_2H_4)$ and 185 mg (0.18 mmol) of $H(Et_2O)_2BAr'_4$. The solids were cooled to −78 °C and dissolved in 10 mL of CH_2Cl_2. Then, 100 μL (1.11 mmol) of methyl acrylate was syringed into the solution. The orange solution was allowed to reach room temperature, and after the reaction mixture was stirred for 3 h, the solvent and excess methyl acrylate were removed under reduced pressure. The residue was washed with hexane (3 × 3 mL), and the resulting orange powder was dried under vacuo (181 mg, 79%). Anal. Found (calcd): C, 44.97 (44.84); H, 3.21 (3.30). ^1H NMR (CD_2Cl_2, 400 MHz, 23 °C): δ 3.74 (s, CO_2CH_3), 3.68 (d, J_{P-H} = 12 Hz, $P(OCH_3)_3$), 2.9 (m, CH_2), 2.2 (m, CH_2), 1.64 (d, J_{P-H} = 4 Hz, $C_5(CH_3)_5$. ^{13}C NMR (CD_2Cl_2, 100 MHz, 23 °C): δ 191.0 (s, CO_2CH_3), 101.3 (d, J_{C-Rh} or J_{C-P} = 5 Hz, $C_5(CH_3)_5$), 55.4 (q, J_{C-H} = 150 Hz, CO_2CH_3), 53.1 (dq, J_{P-C} = 4 Hz, J_{C-H} = 148 Hz, $P(OCH_3)_3$), 39.1 (t, J_{C-H} = 129 Hz, $CH_2CO_2CH_3$), 13.1 (tt, J_{Rh-C} = J_{P-C} = 18 Hz, J_{C-H} = 139 Hz, Rh-CH_2), 9.2 (q, J_{C-H} = 129 Hz, $C_5(CH_3)_5$).

$Cp^*Rh(CH_2{=}CHCO_2CH_3)(P(OCH_3)_3)$ (6). Methyl acrylate (20 mL) was added to $Cp^*(P(OMe)_3)Rh(C_2H_4)$ (120 mg, 0.31 mmol). The mixture was heated for 20 h under reflux. After filtration, methyl acrylate was removed under reduced pressure. Recrystallization from 2-methylbutane at −78 °C gave orange-yellow crystals of complex **6** (80% yield). Anal. Found (calcd): C, 45.76 (45.74); H, 6.70 (6.70). ^1H NMR (C_6D_6, 400 MHz, 23 °C): δ 3.59 (s, CO_2CH_3), 3.20 (d, J_{P-H} = 12 Hz, $P(OCH_3)_3$), 3.1 (ddd, J_{Rh-H} or J_{P-H} = 2.4 Hz, J_{trans} = 10 Hz, J_{cis} = 7 Hz, H_1), 2.43 (dd, J_{trans} = 10 Hz, J_{gem} = 2 Hz, H_3), 2.19 (brt, J_{P-H} = J_{cis} = 7 Hz, H_2), 1.83 (d, J_{P-H} = 4 Hz, $C_5(CH_3)_5$). ^{13}C NMR (C_6D_6, 400 MHz, 23 °C): δ 175.5 (s, CO_2CH_3), 97.6 (s, $C_5(CH_3)_5$), 50.3 (q, J_{C-H} = 144 Hz, CO_2CH_3), 50.0 (q, J_{C-H} = 145 Hz, $P(OCH_3)_3$), 38.9 (ddd, J_{Rh-C} and J_{P-C} are either 4 and 14 Hz or 14 and 4 Hz, respectively, J_{C-H} = 158 Hz, $CHCO_2CH_3$), 31.5 (ddd, J_{Rh-C} and J_{P-C} are either 4 and 15 Hz or 15 and 4 Hz, respectively, J_{C-H} = 155 Hz, CH_2), 9.8 (q, J_{C-H} = 126 Hz, $C_5(CH_3)_5$).

Generation and Spectroscopic Characterization of $[Cp^*RhCH_2CH_2C(O)OMe(\eta^2\text{-}CH_2CHCO_2Me)]^+[BAr'_4]^-$ (8). An NMR tube was charged with $Cp^*Rh(CH_2{=}CHCO_2Me)_2$ (**15**) (11 mg, 0.027 mmol) and cooled to −78 °C. $BAr'_4H(Et_2O)_2$ (30 mg, 0.030 mmol) dissolved in 0.6 mL of CD_2Cl_2 was slowly syringed into the NMR tube. Once the solution was homogeneous, the NMR tube was introduced into a precooled (−78 °C) NMR probe. ^1H NMR (400 MHz, CD_2Cl_2, −78 °C): δ 4.67 (dd, J_{trans} = 13 Hz, J_{cis} = 9 Hz, H_1), 3.95 (d, J_{trans} = 13 Hz, H_3), 3.57 (s, CO_2CH_3), 3.30 (d, J_{cis} = 9 Hz, H_2), 3.06 (m, 1H), 2.87 (m, 3H), 1.56 (s, $C_5(CH_3)_5$). At higher temperatures the Cp* resonance appears at slightly lower field, δ 1.6 ppm. ^{13}C NMR (100 MHz, CD_2Cl_2, −78 °C): δ 189.6 (s, C=O), 168.5 (s, C=O), 103.2 (d, J_{C-Rh} = 6 Hz, $C_5(CH_3)_5$),

(30) ^1H NMR data have been reported for *trans*-**2**, see ref 4e.

72.9 (dd, J_{C-Rh} = 8 Hz, J_{C-H} = 164 Hz, C_α), 69.0 (dt, J_{C-Rh} = 10 Hz, J_{C-H} = 164 Hz, C_β), 55.4 (q, J_{C-H} = 150 Hz, OCH_3), 52.3 (q, J_{C-H} = 150 Hz, OCH_3), 39.6 (t, J_{C-H} = 127 Hz, C_1), 22.2 (dt, J_{C-Rh} = 18 Hz, J_{C-H} = 150 Hz, C_2), 8.0 (q, J_{C-H} = 129 Hz, $C_5(CH_3)_5$).

[Cp*Rh(η³-MeOC(O)CH₂CHCHCHCO₂Me)]⁺[BAr'₄]⁻ (9) and [Cp*RhCH(CH₂CO(O)OMe)(CH₂CH₂C(O)OMe)]⁺[BAr'₄]⁻ (10). 1. Method 1. $H(Et_2O)_2BAr'_4$ (218 mg, 0.22 mmol) in 3 mL of CH_2Cl_2 was added at 0 °C to $Cp^*Rh(C_2H_4)_2$ (49 mg, 0.17 mmol) in 7 mL of CH_2Cl_2. After the mixture was stirred for 10 min, $MeO_2CCH{=}CHCH_2CH_2CO_2Me$ (200 μL) was added. After being stirred overnight at room temperature, the solution was evaporated to dryness. The residue was washed with hexane to eliminate the dimer. The two complexes **9** and **10** were separated by successive recrystallizations in diethyl ether/hexane and isolated as orange crystals.

2. Method 2. $H(Et_2O)_2BAr'_4$ (171 mg, 0.17 mmol) dissolved in 3 mL of CH_2Cl_2 was added at 0 °C to $Cp^*Rh(C_2H_4)_2$ (39 mg, 0.13 mmol) dissolved in 7 mL of CH_2Cl_2. After the mixture was stirred for 10 min, methyl acrylate (240 μL, 2.67 mmol) was added. After being stirred overnight at room temperature, the solution was evaporated to dryness. The residue was washed with hexane to eliminate excess dimer. The two complexes **9** and **10** were separated by successive recrystallizations in diethyl ether/hexane and isolated as orange crystals.

Subsequent to use of these methods, an alternative for the synthesis of complex **10** was derived from Method 1: A 100-mL round-bottomed flask was charged with 108 mg (0.37 mmol) of $Cp^*Rh(C_2H_4)_2$ and 390 mg (0.39 mmol) of $H(Et_2O)_2BAr'_4$. The solids were dissolved at −78 °C in 10 mL of CH_2Cl_2. $MeO_2CCH{=}CHCH_2CH_2CO_2Me$ (1.15 mL of a 0.35 M solution in CH_2Cl_2) was then syringed into the cold solution. The flask was allowed to reach room temperature, and the mixture was stirred for 10 min. The solvent was then removed under reduced pressure. The yellowish solid was washed with 2 × 5 mL of hexane. Complex **10** (380 mg, 81%) is pure by ^1H NMR spectroscopy.

[Cp*Rh(η³-MeOC(O)CH₂CHCHCHCO₂Me)]⁺[BAr'₄]⁻ (9). Anal. Found (calcd): C, 47.97 (47.19); 3.05 (3.05). ^1H NMR (400 MHz, CD_2Cl_2, 23 °C): δ 5.49 (ddd, J_{Ha-Hb} = 11 Hz, J_{Hc-Hb} = 8 Hz, J_{Rh-Hb} = 2 Hz, H_b), 4.70 (ddd, J_{Hb-Hc} = 8 Hz, J_{Hc-Hd} = 7.5 Hz, J_{Hc-He} = 2 Hz, H_c), 3.85 (s, CO_2CH_3), 3.82 (s, CO_2CH_3), 3.42 (dd, J_{Hd-Hc} = 7.5 Hz, J_{Hd-He} = 21 Hz, H_d), 3.11 (d, J_{Ha-Hb} = 11 Hz, H_a), 2.61 (dd, J_{He-Hd} = 21 Hz, J_{He-Hc} = 2 Hz, H_e), 1.70 (s, $C_5(CH_3)_5$). ^{13}C NMR (100 MHz, CD_2Cl_2, 23 °C): δ 186.8 (s, C=O), 170.0 (s, C=O), 102.5 (dd, J_{C-Rh} = 5 Hz, J_{C-H} = 170 Hz, C_2), 101.3 (d, J_{C-Rh} = 7 Hz, $C_5(CH_3)_5$), 71.6 (dd, J_{C-Rh} = 9 Hz, J_{C-H} = 160 Hz, C_3), 67.8 (dt, $^2J_{C-H}$ = J_{C-Rh} = 10 Hz, J_{C-H} = 161 Hz, C_1), 56.6 (q, J_{C-H} = 151 Hz, OCH_3), 52.5 (q, J_{C-H} = 148 Hz, OCH_3), 36.5 (t, J_{C-H} = 130 Hz, C_4), 8.9 (q, J_{C-H} = 129 Hz, $C_5(CH_3)_5$).

[Cp*RhCH(CH₂C(O)OMe)(CH₂CH₂C(O)OMe)]⁺[BAr'₄]⁻ (10). Anal. Found (calcd): C, 46.99 (47.10); H, 3.26 (3.14). ^1H NMR (400 MHz, CD_2Cl_2, 23 °C): δ 3.93 (s, CO_2CH_3), 3.84 (s, CO_2CH_3), 3.35 (m, broad, H_a), 3.00 (dd, $J_{Ha-Hb\ or\ c}$ = 9 Hz, J_{Hb-Hc} = 19 Hz, H_b or H_c), 2.68 (d, J_{Hb-Hc} = 19 Hz, H_c or H_b), 2.40 (ddd, J = 3, 7, and 19 Hz, H_f or H_g), 2.15 (ddd, J = 3, 9, and 19 Hz, H_g or H_f), 1.68 (m, H_d or H_e), 1.53 (s, $C_5(CH_3)_5$), 1.52 (m, H_e or H_d). ^{13}C NMR (100 MHz, CD_2Cl_2, 23 °C): δ 190.4 (s, CO_2CH_3), 183.0 (s, CO_2CH_3), 94.6 (d, J_{C-Rh} = 8 Hz, $C_5(CH_3)_5$), 55.7 (q, J_{C-H} = 150 Hz, CO_2CH_3), 54.9 (q, J_{C-H} = 150 Hz, CO_2CH_3), 44.8 (t, J_{C-H} = 130 Hz, CH_2), 38.7 (dd, J_{C-Rh} = 23 Hz, J_{C-H} = 140 Hz, Rh-CH), 31.6 (t, J_{C-H} = 130 Hz, CH_2), 29.9 (t, J_{C-H} = 130 Hz, CH_2), 8.9 (q, J_{C-H} = 129 Hz, $C_5(CH_3)_5$).

X-ray Structural Analysis of [Cp*Rh(η³-MeOC(O)CH₂CHCHCHCO₂Me)]⁺[BAr'₄]⁻ (9). A single crystal of **9** (parallelopiped, ca. 0.20 × 0.20 × 0.30 mm³) was grown by slow evaporation of CD_2Cl_2. The crystal is triclinic ($P\bar{1}$) with the following cell dimensions determined from 25 reflections (μ(Mo) = 0.44 mm⁻¹): a = 12.646(8), b = 13.819(6), c = 15.650(6) Å; α = 77.57(4), β = 84.35(4), γ = 83.39(5)°; V = 2645.5(23) Å³; Z = 2; FW = 1272.51 ($RhC_{50}H_{38}BF_{24}O_4$); density(calcd) = 1.597 g/cm³.

Data were collected on a Nonius diffractometer with a graphite monochromator using Mo Kα radiation (λ = 0.709 30 Å). A total of 6815 data were collected ($6° \le 2\theta \le 45°$; maximum h, k, l = 11, 14, 16; data octants +++, −++, −+−, ++−; $\theta/2\theta$ scan method, scan width = 2 × 2θ, scan speed = 4 deg/min); three standards were collected every 100 reflections and showed no significant variations during data collection; no absorption correction was applied. There were 6438 unique reflections with $I \ge 2.5\sigma(I)$.

The structure was solved by automated Patterson analysis. Hydrogen atoms were idealized with C–H = 0.96 Å. The structure was refined by full-matrix least squares on F (H atoms fixed, all others anisotropic) with scattering factors from ref 31 including anomalous dispersion terms. There were 722 parameters, and the data to parameter ratio was 8.92; final R = 0.062 (R_w = 0.076). The error of fit was 2.32 with a maximum Δ/σ of 0.175. The highest difference peaks were all in the CF_3 regions, and this fact plus the extremely high anisotropic thermal parameters indicates that there is a high degree of rotational disorder. Attempts to model this disorder by placing multiple CF_3's at each site did not result in any significant improvement in the refinement, especially in view of the additional parameters that were added. The largest residual density = 0.840 e/Å³ near Rh.

X-ray Structural Analysis of [Cp*RhCH(CH₂C(O)OMe)(CH₂CH₂C(O)OMe)]⁺[BAr'₄]⁻ (10). A single orange crystal of **10** (crystal dimensions ca. 0.20 × 0.20 × 0.20 mm³) was grown from ($MeO_2CCH_2CH_2$-CH=$CHCO_2Me$)/CH_2Cl_2 at 23 °C. The crystal is triclinic ($P\bar{1}$) with the following cell dimensions determined from 16 reflections (μ(Mo) = 0.44 mm⁻¹): a = 14.347(4), b = 14.515(4), c = 14.209(5) Å; α = 115.055(20), β = 94.32(3), γ = 94.91(3)°; V = 2650.3(14) Å³; Z = 2; FW = 1274.53 ($RhC_{50}H_{40}BF_{24}O_4$); density(calcd) = 1.597 g/cm³.

Data were collected on a Rigaku diffractometer with a graphite monochromator using Mo Kα radiation (λ = 0.709 30 Å). A total of 6963 data were collected ($6° \le 2\theta \le 45°$; maximum h, k, l = 15, 15, 13; data octants +++, −++, −+−, ++−; $\theta/2\theta$ scan method; scan width = 2 × 2θ; scan speed = 4 deg/min); three standards were collected every 100 reflections and showed no significant variations during data collection; no absorption correction was applied. There were 4752 unique reflections with $I \ge 2.5\sigma(I)$.

The structure was solved by automated Patterson analysis. Hydrogen atoms were idealized with C–H = 0.96 Å. The structure was refined by full-matrix least squares on F (H atoms fixed, all others anisotropic) with scattering factors from ref 31 including anomalous dispersion terms. There were 721 parameters, and the data to parameter ratio was 9.66; final R = 0.072 (R_w = 0.089). The error of fit was 2.00 with a maximum Δ/σ of 0.120. The largest residual density = 0.900 e/Å³ near Rh.

Thermal Rearrangement of 8 to 10 in CD_2Cl_2. Complex **8** was prepared as described above at −78 °C in an NMR tube. In experiment 1 (experiment 2), the tube was warmed to −23 °C (−22 °C). The reaction was monitored with ^1H NMR spectroscopy by following the appearance of the OCH_3 resonances of **10** (using CD_2Cl_2 as an internal standard) every 20 min for 2 h and 20 min. The reaction was determined to follow first-order kinetics from a plot of $\ln([\mathbf{8}_0]/[\mathbf{8}_t])$ versus $1/t$, giving a rate constant of 2.4 × 10⁻⁴ s⁻¹ at −23 °C, $\Delta G^\ddagger$ = 18.7 kcal/mol (4.7 × 10⁻⁴ s⁻¹ at −22 °C, $\Delta G^\ddagger$ = 18.5 kcal/mol).

Thermal Conversion of 10 to 9. An NMR tube was charged with complex **10** dissolved in 0.65 mL of CD_2Cl_2. The tube was then heated to 63 °C and the conversion of **10** to **9** monitored by ^1H NMR spectroscopy using the $C_5(CH_3)_5$ resonance. The reaction was determined to follow first-order kinetics from a plot of $\ln([\mathbf{10}_0]/[\mathbf{10}_t])$ versus $1/t$, giving a rate constant at 63 °C of 7.43 × 10⁻⁶ s⁻¹, $\Delta G^\ddagger$ = 27.7 kcal/mol.

Dimerization of MA using 11 as a Catalyst Precursor. A 100-mL flask was charged with 9.8 mg (0.026 mmol) of **11** and cooled to 0 °C, at which temperature methyl acrylate (7 mL, 77.7 mmol) was added. Then $H(Et_2O)_2BAr'_4$ (27 mg, 0.027 mmol) was syringed into the cold solution, which turned from clear yellow to clear orange. The flask was placed in a water bath at 23 °C and samples were withdrawn at regular intervals. The dimerization reaction was monitored by ^1H NMR spectroscopy (see above). Analysis of the data showed the following conversion versus time: 19 min (0.5%), 34 min (6.2%), 51 min (10.2%), 68 min (12.4%), 85 min (14.4%), 107 min (19.1%), 1.36 min (25.5%), 159 min (33%), 191 min (41.3%), 220 min (51.1%), 248 min (59.7%), 272 min (65.3%), 298 min (74%), 324 min (84.7%), and 354 min (93.4%).

Dimerization of Methyl Vinyl Ketone using 11 as a Catalyst Precursor. Formation of 3-*trans*-2,7-Octenedione (*trans*-2') (Major Isomer). A typical experiment is described. An NMR tube was charged with 6.9 mg (0.022 mmol) of (1,2,3-trimethylindenyl)$Rh(C_2H_4)_2$ and 23 mg (0.023 mmol) of $H(Et_2O)_2BAr'_4$. The tube was cooled to −78 °C, at which temperature CD_2Cl_2 (0.65 mL) was added. Then 300 μL (1.22 mmol) of methyl vinyl ketone was syringed into the solution and the tube warmed

(31) *International Tables for X-Ray Crystallography*; Kynoch Press: Birmingham, England, 1974; Vol. 4.

to 23 °C. A maximum of ca. 44 TO could be achieved after 24 h. The mixture of dimers obtained consists of >98% *trans*-**2′** and ca. 1–2% of *trans*-**3′**. No *cis*-**2′** was detected by ^{1}H NMR spectroscopy. The major *trans*-**2′** dimer has been reported by Kovalev.[2e] For comparison purposes, complete NMR data of this compound follow: ^{1}H NMR (250 MHz, $CDCl_3$, 23 °C): δ 6.71 (m, 1H, $MeCO_2CH$=C*H*R), 5.98 (dt, J_{trans} = 16 Hz, ^4J = 1.3 Hz, $MeCO_2C$*H*=CHR), 2.3–2.7 (m, 4H, R′(CH_2)$_2$-CO_2Me), 2.15 (s, 3H, CH_3), 2.09 (s, 3H, CH_3). ^{13}C NMR (100 MHz, CD_2Cl_2, 23 °C): δ 206.9 (s, C=O), 198.3 (s, C=O), 146.7 (d, J_{C-H} = 153 Hz, *C*H), 131.8 (dt, J_{C-H} = 157 and 5 Hz, *C*H), 41.7 (t, J_{C-H} = 123 Hz, CH_2), 30.0 (q, J_{C-H} = 127 Hz, CH_3), 26.9 (q, J_{C-H} = 127 Hz, CH_3), 26.5 (t, J_{C-H} = 127 Hz, CH_2).

Dimerization of 1-Vinyl-2-pyrrolidinone using 11 as a Catalyst Precursor. A typical experiment is described. An NMR tube was charged with 11 mg (0.035 mmol) of (1,2,3-trimethylindenyl)Rh(C_2H_4)$_2$ and 36 mg (0.036 mmol) of H(Et_2O)$_2$BAr′$_4$. The tube was cooled to −78 °C, at which temperature CD_2Cl_2 (0.65 mL) was added. Then 130 μL (1.22 mmol) of 1-vinyl-2-pyrrolidinone was syringed into the solution and the tube warmed to 23 °C. Complete conversion to dimer occurred over a period of 1 week. Spectroscopic data for the branched dimer follow. ^{1}H NMR (CD_2Cl_2, 300 MHz, 23 °C): δ 6.92 (d, J = 14 Hz, H_1), 4.88 (dd, J = 14 and 6 Hz, H_2), 4.77 (m, H_3), 3.40 (m, 2H, ring), 3.25 (m, 2H, ring), 2.38 (m, 2H, ring), 2.26 (m, 2H, ring), 2.1–1.8 (m, 4H, ring), 1.23 (d, J = 7 Hz, 3H, CH_3). ^{13}C NMR (CD_2Cl_2, 100 MHz, 23 °C): δ 173.9 (s, C=O), 173.3 (s, C=O), 125.3 (d, J_{C-H} = 173 Hz, R′*C*H=CHNR$_2$), 110.7 (d, J_{C-H} = 153 Hz, R′*C*H=CHNR$_2$), 46.4 (d, J_{C-H} = 140 Hz, R′-*C*H(CH_3)R), 45.3 (t, J_{C-H} = 143 Hz, ring CH_2), 42.4 (t, J_{C-H} = 139 Hz, ring CH_2), 31.6 (t, J_{C-H} = 133 Hz, ring CH_2), 31.3 (t, J_{C-H} = 133 Hz, ring CH_2), 18.2 (t, J_{C-H} = 134 Hz, ring CH_2), 17.65 (t, J_{C-H} = 134 Hz, ring CH_2), 17.58 (q, J_{C-H} = 130 Hz, R′CH(*C*H$_3$)-R).

[(1,2,3-Trimethylindenyl)RhCH(CH$_2$C(O)OMe)(CH$_2$CH$_2$C(O)OMe)]$^+$-[BAr′$_4$]$^-$ (13). $C_{12}H_{13}Rh(C_2H_4)_2$ (31 mg, 0.098 mmol) and H(Et_2O)$_2$-BAr′$_4$ (100 mg, 0.099 mmol) were weighed in a drybox and transferred to a Schlenk flask. The solids were dissolved with stirring at −78 °C in 2 mL of methylene chloride. The solution turned immediately orange. Methyl acrylate (260 μL, 2.89 mmol) was added at −78 °C, and the solution was warmed to room temperature with stirring. After the mixture was stirred for 45 min, the solvent was removed under reduced pressure. The residue was washed with hexane (2 × 5 mL) to eliminate the dimer. Complex **13** (114 mg, 90%) was recrystallized from diethyl ether/hexane and isolated as dark-orange crystals. Anal. Found (calcd): C, 48.19 (48.17); H, 2.98 (2.95). ^{1}H NMR (CD_2Cl_2, 400 MHz, 23 °C): δ 7.61 (m, aromatic, 2H), 7.45 (dd, J = 6.6 Hz, J < 2 Hz, 1H), 7.35 (dd, J = 6.2 Hz, J < 2 Hz, 1H), 3.79 (s, 6H, OCH_3), 3.55 (m, broad, H_a), 2.99 (dd, $J_{Ha-Hb\ or\ c}$ = 8 Hz, J_{Hb-Hc} = 18 Hz, H_b or H_c), 2.48 (d, J_{Hb-Hc} = 18 Hz, H_c or H_b), 2.38 (ddd, J = 18.1, 8.4, and 2.9 Hz, H_f or H_g), 2.26 (ddd, J = 18.1, 9.4, and 2.9 Hz, H_f or H_g), 1.98 (d, J_{Rh-H} = 2.9 Hz, central CH_3), 1.49 (s, 3H), 1.42 (s, 3H), 1.13 (m, H_e or H_d). ^{13}C NMR (CD_2-Cl_2, 100 MHz, 23 °C): δ 188.1 (s, *C*O$_2$CH$_3$), 182.8 (s, *C*O$_2$CH$_3$), 132.3 (dd, J = 7.4 Hz, J_{C-H} = 162 Hz, aromatic C-H), 131.9 (dd, J_{C-H} = 163 Hz, $^3J_{C-H}$ = 7.5 Hz, aromatic C-H), 121.5 (dd, $^1J_{C-H}$ = 165 Hz, $^3J_{C-H}$ = 7 Hz, aromatic C-H), 120.9 (dd, $^1J_{C-H}$ = 164 Hz, $^3J_{C-H}$ = 7.6 Hz, aromatic C-H), 117.2 (s, C), 116.5 (s, C), 104.3 (d, J_{C-Rh} = 11 Hz, C), 76.0 (d, J_{C-Rh} = 11 Hz, C), 74.2 (d, J_{C-Rh} = 11 Hz, C), 55.8 (q, J_{C-H} = 140 Hz, CO_2CH_3), 55.2 (q, J_{C-H} = 150 Hz, CO_2CH_3), 45.1 (t, J_{C-H} = 129 Hz, CH_2), 43.2 (dd, J_{C-Rh} = 25 Hz, J_{C-H} = 152 Hz, Rh-*C*H), 31.5 (t, J_{C-H} = 130 Hz, CH_2), 30.1 (t, J_{C-H} = 127 Hz, CH_2), 9.33, 9.29, 9.23 (q, J_{C-H} = 129 Hz, 3CH_3).

Generation and Spectroscopic Characterization of [Cp*Rh(CH$_2$CH$_2$C(O)OCH$_3$)(C$_2$H$_4$)]$^+$[BAr′$_4$]$^-$ (14). An NMR tube was charged with 9.1 mg (0.031 mmol) of Cp*Rh(C_2H_4)$_2$ and 38 mg (0.038 mmol) of H(Et_2O)$_2$BAr′$_4$. The tube was cooled to −78 °C, and CD_2Cl_2 (0.65 mL) was slowly added. After complete dissolution, 14 μL (0.155 mmol) of methyl acrylate was syringed into the tube, which was then introduced into a precooled (−80 °C) NMR probe. Complex **14** was immediately generated. For best signal resolution the tube was warmed to −20 °C. ^{1}H NMR (CD_2Cl_2, 400 MHz, −20 °C): δ 4.01 (m, 2H, C_2H_4), 3.67 (s, 3H, OCH_3), 3.72 (m, 2H, C_2H_4), the other ethylenic signal is masked in the methoxy region, 3–2.6 ppm (m, 4H, $C_2H_4CO_2$-CH_3), 1.54 (s, 15 H, $C_5(CH_3)_5$).

Cp*Rh(CH$_2$=CHCO$_2$Me)$_2$ (15 and 16). To a thick-walled 25-mL flask fitted with a rotoflow stopcock was added 203 mg (0.69 mmol) of Cp*Rh(C_2H_4)$_2$ and 3 mL (33.3 mmol) of methyl acrylate. The flask was degassed by freeze–pump–thawing, the stopcock was closed, and the solution was left under vacuum. It was then heated to 130 °C for 4 h, over which time the initially yellow solution turned orange. Excess methyl acrylate was removed under reduced pressure. The residue was extracted with CH_2Cl_2 and filtered through a plug of Celite. Removal of CH_2Cl_2 under reduced pressure provided 252 mg (90%) of a mixture of isomers (**15** and **16**) as an orange solid (the ratio **15**/**16** was 1.3:1). On subsequent runs an additional minor isomer (15%) could be detected. All of these isomers can be detected by ^{1}H NMR spectroscopy. Complex **15** can be extracted and recrystallized from hexane to yield a pure isomer (unknown structure). The minor isomer must possess either a C_2 axis or a plane of symmetry σ_v on the basis of the observation of only one set of resonances for the two η^2-methyl acrylate ligands. Isomers **15** and **16** are unsymmetrical isomers. Isomer **16** is much less soluble in hexane than complex **15** and the minor isomer, which allows its clean isolation. Isomer **16** could also be separated from the other isomers by chromatography (neutral alumina, CH_2Cl_2/hexane as eluant). NMR data of these three isomers are shown below. Anal. (mixture of isomers). Found (calcd): C, 52.24 (52.69); H, 6.65 (6.63).

Cp*Rh(CH$_2$=CHCO$_2$Me)$_2$ (15). ^{1}H NMR (400 MHz, CD_2Cl_2, 23 °C): δ 3.61 (s, 3H, CO_2CH_3), 3.55 (s, 3H, CO_2CH_3), 2.75 (ddd, 1H, J_{trans} = 11 Hz, J_{cis} = 8 Hz, J_{H-Rh} = 2 Hz), 2.15 (ddd, 1H, J_{H-Rh} = 3 Hz, J_{cis} = 8 Hz, J_{gem} = 2 Hz), 1.78 (ddd, 1H, J_{trans} = 11 Hz, J_{cis} = 8 Hz, J_{H-Rh} = 2 Hz), 2.46 (dd, 1H, J_{trans} = 11 Hz, J_{gem} = 2 Hz), 2.45 (dd, 1H, J_{cis} = 8 Hz, J_{gem} = 2 Hz), 1.67 (s, 15H, $C_5(CH_3)_5$), 1.16 (ddd, 1H, J_{trans} = 11 Hz, J_{gem} = J_{H-Rh} = 2 Hz). ^{13}C NMR (100 MHz, CD_2Cl_2, 23 °C): δ 174.10 (s, C=O), 174.08 (s, C=O), 100.0 (s, $C_5(CH_3)_5$), 55.5 (dd, J_{C-Rh} = 13 Hz, J_{C-H} − 161 Hz, CH_2=$CHCO_2CH_3$), 51.3 (q, J_{C-H} = 146 Hz, OCH_3), 50.3 (q, J_{C-H} = 146 Hz, OCH_3), 47.0 (dd, J_{C-Rh} = 13 Hz, J_{C-H} = 157 Hz, CH_2=*C*HCO$_2$CH$_3$), 46.2 (dt, J_{C-Rh} = 13 Hz, J_{C-H} = 159 Hz, *C*H$_2$=CHCO$_2$CH$_3$), 44.0 (dt, J_{C-Rh} = 13 Hz, J_{C-H} = 159 Hz, *C*H$_2$=CHCO$_2$CH$_3$), 8.6 (q, J_{C-H} = 128 Hz, $C_5(CH_3)_5$).

Cp*Rh(CH$_2$=CHCO$_2$Me)$_2$ (16). ^{1}H NMR (400 MHz, CD_2Cl_2, 23 °C): δ 3.61 (s, 3H, CO_2CH_3), 3.53 (s, 3H, CO_2CH_3), 2.61 (m, 2H), 2.35 (dd, 1H, J = 2 Hz, J_{trans} = 11 Hz), 2.24 (ddd, 1H, J_{Rh-H} = 2 Hz, J_{trans} = 11 Hz, J_{cis} = 8 Hz), 2.05 (m, 1H), 1.43 (dd, 1H, J_{cis} = 7 Hz, J = 2 Hz), 1.66 (s, 15H, $C_5(CH_3)_5$).

Cp*Rh(CH$_2$=CHCO$_2$Me)$_2$ (Minor Isomer). ^{1}H NMR (400 MHz, CD_2Cl_2, 23 °C): δ 3.54 (s, 6H, CO_2CH_3), 2.77 (ddd, 2H, J_{trans} = 11 Hz, J_{Rh-H} = J_{gem} = 1.4 Hz), 2.58 (ddd, 2H, J_{Rh-H} = 2 Hz, J_{trans} = 11 Hz, J_{cis} = 8 Hz), 1.95 (ddd, 2H, J_{cis} = 8 Hz, J_{Rh-H} = 2 Hz, J_{gem} = 1.4 Hz), 1.91 (s, 15H, $C_5(CH_3)_5$).

X-ray Structural Analysis of a Symmetrical Isomer of Cp*Rh(CH$_2$-CHCO$_2$Me)$_2$. (See text.) A single gold crystal of Cp*Rh(CH_2CHCO_2-Me)$_2$ (parallelopiped, ~0.25 × 0.10 × 0.49 mm^3) was grown from hexane/CH_2Cl_2 at −30 °C. The crystal is monoclinic (*Cc*, No. 9) with the following cell dimensions determined from 25 reflections (μ(Mo) = 0.943 mm^{-1}): a = 18.889(6), b = 8.755(1), c = 13.961(6) Å; β = 128.37 (3)°; V = 1810.1 Å^3; Z = 4; FW = 410.32 ($RhC_{18}H_{27}O_4$); density(calcd) = 1.505 g/cm^3.

Data were collected at −55 °C on an Enraf-Nonius CAD4 diffractometer with a graphite monochromator using Mo Kα radiation (λ = 0.7107 Å). A total of 3051 data were collected (0.0° ≤ 2θ ≤ 60°; maximum h, k, l = 19, 12, 21; data octants +++, −++; ω scan method, typical half-height peak width = 0.26ω; scan speed = 2.50–5.00 deg/min); two standards were collected 23 times, 1% fluctuation, corrected for absorption (DIFABS. Walker, N.; Stuart, D. *Acta Crystallogr.* **1983**, *A39*, 158.), range of transmission factors = 0.71–0.95. There were 1802 unique reflections with $I \geq 3.0\sigma(I)$.

The structure was solved by automated Patterson analysis (PHASE). The asymmetric unit consists of one molecule in a general position. Hydrogen atoms were idealized and refined. The structure was refined by full-matrix least squares on F with scattering factors from ref 31 including anomalous terms for Rh (biweight ∝ $[\sigma^2(I) + 0.0009I^2]^{-1/2}$) (excluded 2): refined anisotropic, all non-hydrogen atoms; isotropic, H. There were 312 parameters, and the data to parameter ratio was 5.77; final R = 0.021 (R_w = 0.020). The error of fit was 0.85 with a maximum Δ/σ of 0.10. The largest residual density = 0.29 e/Å near Rh(1).

Generation and Spectroscopic Characterization of [(1,2,3-Trimethylindenyl)Rh(CH$_2$CH$_2$C(O)OMe)(C$_2$H$_4$)]$^+$[BAr′$_4$]$^-$ (19). An NMR tube was charged with 12.2 mg (0.039 mmol) of (1,2,3-trimethylindenyl)-Rh(C_2H_4)$_2$ and 43 mg (0.042 mmol) of H(Et_2O)$_2$BAr′$_4$. The tube was cooled to −78 °C, and CD_2Cl_2 (0.65 mL) was slowly added (the solution turned first orange and then green). After complete dissolution, 17 μL (0.189 mmol) of methyl acrylate was syringed into the tube, which was then introduced into a precooled (−80 °C) NMR probe (the solution

color turned from black to orange). Complex **19** was generated immediately. For best signal resolution the tube was warmed to −20 °C. ^{1}H NMR (CD_2Cl_2, 400 MHz, −20 °C): δ 7.6–7.0 (m, aromatic H), 3.76 (s, 3H, OCH_3), 3.72 (m, 2H, C_2H_4), the other ethylenic signal is masked by the free methyl acrylate methoxy signal (ca. 3.71 ppm), 2.2–2.7 ppm (m, 3H, $C_2H_4CO_2CH_3$), 2.04 (d, J_{Rh-H} = 2.3 Hz, 3H, CH_3), 1.91 (m, 1H, $C_2H_4CO_2CH_3$), 1.82 (s, 3H, CH_3), 1.46 (s, 3H, CH_3).

[Cp*Ir(CH$_2$CH$_2$C(O)OMe)(C$_2$H$_4$)]$^+$[BAr'$_4$]$^-$ (22). Methyl acrylate (291 μL, 3.23 mmol) was added at 0 °C to $Cp^*Ir(C_2H_4)_2$ (62 mg, 0.16 mmol) in 2.5 mL of CH_2Cl_2. After the mixture was stirred for 5 min, $H(Et_2O)_2BAr'_4$ (188 mg, 0.19 mmol) dissolved in 2 mL of CH_2Cl_2 was added. The initially yellow solution turned immediately orange. After the mixture was stirred for 10 min at 0 °C, the solvent and the excess methyl acrylate were removed under reduced pressure. Complex **22** was recrystallized from diethyl ether/hexane and isolated as orange crystals. Anal. Found (calcd): C, 44.58 (44.15); H, 2.85 (2.93). ^{1}H NMR (400 MHz, CD_2Cl_2, 23 °C): δ 3.70 (s, 3H, CO_2CH_3), 3.50 (m, 2H, C_2H_4), 2.91 (m, 3H), overlapping with 2.89 (m, 2H, C_2H_4), 2.71 (m, 1H), 1.59 (s, 15H, $C_5(CH_3)_5$). ^{13}C NMR (100 MHz, CD_2Cl_2, 23 °C): δ 197.9 (s, C), 96.7 (s, $C_5(CH_3)_5$), 56.6 (q, J_{C-H} = 151 Hz, OCH_3), 54.8 (t, J_{C-H} = 163 Hz, C_2H_4), 38.0 (t, J_{C-H} = 129 Hz, C), 8.3 (q, J_{C-H} = 129 Hz, $C_5(CH_3)_5$), −0.8 (dd, J_{C-H} = 135 Hz, J_{C-H} = 143 Hz, C). ^{1}H NMR (400 MHz, CD_2Cl_2, −80 °C): δ 3.64 (s, 3H), 3.59 (m, 1H), 3.15 (m, 1H), 2.96 (m, 1H), 2.90 (m, 2H), 2.76 (m, 1H), 2.62 (m, 1H), 2.51 (m, 1H), 1.54 (s, 15H, $C_5(CH_3)_5$). ^{13}C{H} NMR (100 MHz, CD_2Cl_2, −80 °C): δ 197.0 (s, C=O), 95.3 (s, $C_5(CH_3)_5$), 56.1 (s, OCH_3), 55.9 (broad, C_2H_4), 48.9 (broad, C_2H_4), 37.0 (s, C), 7.7 (s, $C_5(CH_3)_5$), −2.3 (s, C).

[Cp*IrCH$_2$CH$_2$C(O)OMe(η^2-CH$_2$CHCO$_2$Me)]$^+$[BAr'$_4$]$^-$ (23). Methyl acrylate (362 μL, 4.02 mmol) was added at room temperature to $Cp^*Ir(C_2H_4)_2$ (77 mg, 0.20 mmol) in 5 mL of CH_2Cl_2. After the mixture was stirred for 5 min, $H(Et_2O)_2BAr'_4$ (224 mg, 0.22 mmol) dissolved in 5 mL of CH_2Cl_2 was added to the mixture. The solution was stirred for 1 h at room temperature and the solvent removed under reduced pressure. The residue was recrystallized from diethyl ether/hexane to yield 171 mg (62%) of light-yellow crystals. The crystals formed are of mainly one isomer, presumably **23a**, which upon dissolution interconverts rapidly with **23b** (pair of major isomers, see text). A minor isomer **23c** is also detected by NMR spectroscopy at 25 °C. The NMR data for the two major isomers **23a** and **23b** (80%, 1:1) and the minor isomer **23c** (20%) are given below. Anal. Found (calcd): C, 44.07 (44.03); H, 2.85 (2.96).

[Cp*IrCH$_2$CH$_2$C(O)OMe(η^2-CH$_2$CHCO$_2$Me)]$^+$[BAr'$_4$]$^-$ (23a and 23b). ^{1}H NMR (400 MHz, CD_2Cl_2, −78 °C): δ 4.31 and 3.68 (dd, J_{trans} = 11 Hz, J_{cis} = 8 Hz, H_1), 4.09 and 3.83 (d, J_{trans} = 11 Hz, H_3), 2.76 (d, J_{cis} = 8 Hz, H_2), 3.64 (2), 3.58, 3.55 (s, CO_2CH_3), 2–3.6 (m, other protons), 1.54 and 1.53 (s, $C_5(CH_3)_5$). ^{13}C NMR (100 MHz, CD_2Cl_2, −78 °C): δ 197.7 and 197.4 (s, C=O), 169.9 and 169.5 (s, C=O), 98.6 and 97.5 (s, $C_5(CH_3)_5$), 56.5 and 56.4 (q, J_{C-H} = 151 Hz, OCH_3), 52.2 and 52.1 (q, J_{C-H} = 147 Hz, OCH_3), 52.0 (t, J_{C-H} = 162 Hz, C_β) and 46.6 (t, J_{C-H} = 164 Hz, C_β), 50.2 (d, J_{C-H} = 166 Hz, C_α), 38.9 (t, J_{C-H} = 127 Hz, C_1) and 37.5 (t, J_{C-H} = 128 Hz, C_1), 8.0 and 7.4 (q, J_{C-H} = 130 Hz, $C_5(CH_3)_5$), 1.1 and 1.0 (t, J_{C-H} = 139 Hz, C_2). The missing ^{13}C C_α resonance is probably obscured by the CD_2Cl_2 resonance.

[Cp*IrCH$_2$CH$_2$C(O)OMe(η^2-CH$_2$CHCO$_2$Me)]$^+$[BAr'$_4$]$^-$ (23c). ^{1}H NMR (400 MHz, CD_2Cl_2, −78 °C): δ 3.72 (s, CO_2CH_3), 1.59 (s, $C_5(CH_3)_5$). ^{13}C NMR (100 MHz, CD_2Cl_2, −78 °C): δ 197.9 (s, C=O), 173.5 (s, C=O), 97.5 (s, $C_5(CH_3)_5$), 52.3 (q, J_{C-H} = 148 Hz, OCH_3), 35.2 (t, J_{C-H} = 127 Hz, C_1), 7.9 (q, J_{C-H} = 130 Hz, $C_5(CH_3)_5$), −4.9 (t, J_{C-H} = 136 Hz, C_2). The missing ^{13}C OCH_3, C_α, and C_β resonances are probably obscured by the CD_2Cl_2 resonance.

X-ray Structural Analysis of [Cp*IrCH$_2$CH$_2$C(O)OMe(η^2-CH$_2$CHCO$_2$Me)]$^+$[BAr'$_4$]$^-$ (23a). A single light-yellow crystal of **23a** (trapezoidal plate, ~0.25 × 0.08 × 0.47 mm^3) was grown from diethyl ether/hexane at 23 °C. The crystal is triclinic ($P\bar{1}$, No. 2) with the following cell dimensions determined from 25 reflections (μ(Mo) = 25.84 cm^{-1}): a = 13.079(2), b = 13.125(2), c = 17.257(2) Å; α = 84.93(1), β = 81.90(1), γ = 67.07(1)°; Z = 2; V = 2699.3 Å^3; FW = 1363.88 ($IrF_{24}O_4C_{50}BH_{40}$); density (calcd) = 1.678 g/cm^3.

Data were collected at −70 °C on an Enraf-Nonius CAD4 diffractometer with a graphite monochromator using Mo Kα radiation (λ = 0.7107 Å). A total of 8757 data were collected (2.4° ≤ 2θ ≤ 48°; maximum h, k, l = 14, 15, 19; data octants +++, +−+, −++, −+; ω scan method; typical half-height peak width = 0.20ω; scan speed = 1.70–5.00 deg/min); two standards were collected 59 times, and a correction for an 8% decrease in intensity was applied to the data; 17.2% variation in azimuthal scan; an absorption correction was applied (DIFABS. Walker, N.; Stuart, D. *Acta Crystallogr.* **1983**, *A39*, 158.); range of transmission factors = 0.32–1.17. There were 4739 unique reflections with $I \geq 3.0\sigma(I)$.

The structure was solved by automated Patterson analysis (PHASE). The asymmetric unit consists of one ion pair in a general position. Hydrogen atoms were idealized with C–H = 0.95 Å. The structure was refined by full-matrix least squares on F (H atoms fixed, all others anisotropic) with scattering factors from ref 31 including anomalous terms for Ir (biweight ∝ $[\sigma^2(I) + 0.0009I^2]^{-1/2}$). There were 749 parameters, and the data to parameter ratio was 6.33; final R = 0.055 (R_w = 0.046). The error of fit was 1.44 with a maximum Δ/σ of 0.02. In each of the CF_3 groups, there is evidence of rotational disorder. Only the major rotamer was modeled. The coordinated hydrogens were allowed to refine. The curious twist of the π-bonded methyl acrylate hydrogens may be an artifact of the CF_3 disorder. The largest residual density = 1.15 e/Å near Ir(1).

Measurement of the Rate of Interconversion between 23a and 23b. The sample was prepared in a glovebox by loading the iridium complex **23a** (98 mg) and CD_2Cl_2 (0.6 mL) into an NMR tube at ambient temperature. The tube was introduced into a precooled (−78 °C) NMR probe and gradually warmed. The rate of interconversion at the coalescence temperature (20 °C, Varian XL-400 spectrometer) is calculated from the frequency separation of the two $C_5(CH_3)_5$ resonances in the slow-exchange limit using the Gutowsky–Holm approximation, $k = \pi(\nu_A - \nu_X)/\sqrt{2}$ (k = 132 s^{-1} at 20 °C). The free energy of activation obtained from the Eyring equation is 14.3 kcal/mol. Alternatively, line widths of the two $C_5(CH_3)_5$ signals in the slow-exchange region can be used to determine the rate of interconversion using the approximation $k = \pi(\Delta W)$, $\Delta W = W - W_0$, where W_0 is the natural line width (k = 20 s^{-1} at 3 °C, $\Delta G^\ddagger$ = 14.3 kcal/mol).

CpRh(CH$_2$=CHCO$_2$Me)$_2$ (27). To a thick-walled 25-mL flask fitted with a rotoflow stopcock was added 183 mg (0.82 mmol) of $CpRh(C_2H_4)_2$ and 3 mL (33.3 mmol) of methyl acrylate. The flask was degassed by freeze–pump–thawing, the stopcock was closed, and the solution was left under vacuum. It was then heated behind a safety shield to 130 °C for 3 h, over which time the initially yellow solution turned orange. Excess methyl acrylate was removed under reduced pressure, and the residue was extracted with hexane (10 mL) and filtered through a plug of Celite. Removal of hexane under reduced pressure provided 244 mg (88%) of a mixture of isomers **27a–e** as an orange solid (^{1}H NMR spectroscopy). Anal. (mixture of isomers). Found (calcd): C, 46.36 (45.90); H, 4.93 (5.04). All of the isomers have been characterized by ^{1}H NMR spectroscopy (see below).

Generation and Characterization of CpRh(CH$_2$CHCO$_2$CH$_3$)$_2$ (27a–c) from Complex 29. An NMR sample of complex **29** was prepared as described below using 10.0 mg (0.029 mmol) of the mixture of complexes **27** and 31.3 mg (0.031 mmol) of $H(Et_2O)_2BAr'_4$. The NMR tube was cooled to −80 °C, and 10 μL (0.124 mmol) of pyridine was added (proton sponge has also been used and works equally well). The tube was shaken at low temperature to promote mixing and was introduced into a precooled (−85 °C) NMR probe. The first formed, symmetrical isomer **27a** is only stable below −60 °C and rearranges within 1 h at this temperature to yield the unsymmetrical isomer **27b**. Finally warming the solution to −40 °C for an additional hour establishes a thermodynamic equilibrium between **27a,b** and the favored symmetrical isomer **27c** (**27a**/**27b**/**27c** is 5:22:73). NMR data for these isomers appear below.

CpRh(CH$_2$CHCO$_2$CH$_3$)$_2$ (27a) (First Formed Symmetrical Isomer). ^{1}H NMR (CD_2Cl_2, 300 MHz, −85 °C): δ 5.34 (s, 5H, C_5H_5), 4.10 (dd, 2H, J_{cis} = 8.1 Hz, J_{trans} = 11.4 Hz, $CH_2CHCO_2CH_3$), 3.55 (s, 6H, OCH_3), 3.23 (d, 2H, J_{cis} = 8.1 Hz, $CH_2CHCO_2CH_3$), 0.94 (d, 2H, J_{trans} = 11.4 Hz, $CH_2CHCO_2CH_3$).

CpRh(CH$_2$CHCO$_2$CH$_3$)$_2$ (27b) (Unsymmetrical Isomer). ^{1}H NMR (CD_2Cl_2, 300 MHz, −60 °C): δ 5.19 (s, 5H, C_5H_5), 3.91 (ddd, 1H, J_{trans} = 11.0 Hz, J_{cis} = 7.6 Hz, J_{Rh-H} = 2 Hz, $CH_2CHCO_2CH_3$), 3.61 (s, 3H, OCH_3), 3.60 (s, 3H, OCH_3), 3.21 (d, 1H, J_{cis} = 8.1 Hz, $CH_2CHCO_2CH_3$), 1.91 (d, 1H, J_{cis} = 7.6 Hz, $CH_2CHCO_2CH_3$), 1.63 (d, 1H, J_{trans} = 11.0 Hz, $CH_2CHCO_2CH_3$), 1.59 (m, 1H, $CH_2CHCO_2CH_3$). The missing olefinic proton is probably obscured by signals in the methoxy region.

CpRh(CH$_2$CHCO$_2$CH$_3$)$_2$ (27c) (Thermodynamic Symmetrical Isomer). ^{1}H NMR (CD_2Cl_2, 300 MHz, 23 °C): δ 5.12 (d, J_{Rh-H} = 0.6 Hz, 5H, C_5H_5), 3.60 (s, 6H, OCH_3), 2.29 (dd, 2H, J_{cis} = 7.6 Hz, J_{Rh-H} = 1.8 Hz, $CH_2CHCO_2CH_3$), 1.59 (ddd, 2H, J_{trans} = 11.4 Hz, J_{cis} = 7.6 Hz, J_{Rh-H} = 1.8 Hz, $CH_2CHCO_2CH_3$). Decoupling and NOESY experiments showed that the signal corresponding to the two missing protons (*trans*)

$CH_2CHCO_2CH_3$ was obscured by signals in the methoxy region. ^{13}C NMR (CD_2Cl_2, 100 MHz, 23 °C): δ 175.8 (s, CO_2CH_3), 92.4 (dd, J_{C-Rh} = 5 Hz, J_{C-H} = 178 Hz, C_5H_5), 51.5 (q, J_{C-H} = 146 Hz, CO_2CH_3), 50.9 (dd, J_{Rh-C} = 13 Hz, J_{C-H} = 161 Hz, $CH_2CHCO_2CH_3$), 37.8 (dt, J_{Rh-C} = 12 Hz, J_{C-H} = 160 Hz, $CH_2CHCO_2CH_3$).

Generation and Characterization of $CpRh(CH_2CHCO_2CH_3)_2$ (27d and e). The mixture of compounds **27a–e** was recrystallized from hexane at −30 °C. Orange crystals came out of solution along with an orange-yellow powder. The crystals were manually separated and characterized by ^1H NMR spectroscopy. Dissolution of the orange crystals at −78 °C in CD_2Cl_2 yields a single symmetrical isomer (**27d**), which upon warming to 23 °C rearranges to an unsymmetrical isomer (**27e**). The thermodynamic ratio of **27d** to **27e** is ca. 60:40.

$CpRh(CH_2CHCO_2CH_3)_2$ (27d). ^1H NMR (CD_2Cl_2, 300 MHz, −78 °C): δ 5.03 (s, 5H, C_5H_5), 3.62 (s, 6H, OCH_3), 3.43 (d, 2H, J_{trans} = 11 Hz, $CH_2CHCO_2CH_3$), 2.29 (dd, 2H, J_{trans} = 11 Hz, J_{cis} = 7 Hz, $CH_2CHCO_2CH_3$), 1.54 (d, 2H, J_{cis} = 7 Hz, $CH_2CHCO_2CH_3$).

$CpRh(CH_2CHCO_2CH_3)_2$ (27e). ^1H NMR (CD_2Cl_2, 400 MHz, 23 °C): δ 5.22 (s, 5H, C_5H_5), 3.63 (s, 3H, OCH_3), 3.55 (s, 3H, OCH_3), three multiplets integrating each for 1H are obscured in the methoxy region (3.4–3.7 ppm), 2.35 (d, 1H, J_{cis} = 8 Hz, $CH_2CHCO_2CH_3$), 2.27 (ddd, 1H, J_{trans} = 11 Hz, J_{cis} = 8 Hz, J_{Rh-H} = 1.9 Hz, $CH_2CHCO_2CH_3$), 1.22 (dd, 1H, J_{cis} = 8 Hz, J_{Rh-H} = 1.2 Hz, $CH_2CHCO_2CH_3$).

$[CpRhCH(CH_2C(O)OCH_3)(CH_2CH_2C(O)OCH_3)]^+[BAr'_4]^-$ (28). An NMR tube was charged with a mixture of isomers of $C_5H_5Rh(CH_2CHCO_2CH_3)_2$ (**27**) (8.8 mg, 0.026 mmol) and cooled to −78 °C. $H(Et_2O)_2BAr'_4$ (28 mg, 0.027 mmol) dissolved in 0.65 mL of CD_2Cl_2 was slowly syringed into the NMR tube. The tube was then warmed to ambient temperature and kept at this temperature for ca. 1 h and 30 min to generate $CpRhCH(CH_2C(O)OCH_3)(CH_2CH_2C(O)OCH_3)^+$ (**28**). The solvent and diethyl ether were then removed under vacuo from the NMR tube to yield **28** (although the complex is an orange oil, it is pure by ^1H NMR spectroscopy). ^1H NMR (CD_2Cl_2, 400 MHz, 23 °C): δ 5.35 (d, J_{Rh-H} = 1 Hz, C_5H_5), 5.10 (m, broad, H_a), 3.91 (s, 3H, OCH_3), 3.87 (s, 3H, OCH_3), 3.11 (dd, $J_{Ha-Hb\ or\ c}$ = 8.5 Hz, J_{Hb-Hc} = 19 Hz, H_b or H_c), 2.77 (d, J_{Hb-Hc} = 19 Hz, H_c or H_b), 2.47 (ddd, J = 3, 7, and 18 Hz, H_f or H_g), 2.24 (ddd, J = 3, 11, and 18 Hz, H_g or H_f), 1.80 (m, H_d or H_e), 1.46 (m, H_e or H_d). ^{13}C NMR (100 MHz, CD_2Cl_2, 23 °C): δ 191.3 (s, CO_2CH_3), 183.5 (s, CO_2CH_3), 84.4 (dd, J_{C-Rh} = 8 Hz, J_{C-H} = 182 Hz, C_5H_5), 56.4 (q, J_{C-H} = 151 Hz, CO_2CH_3), 55.7 (q, J_{C-H} = 150 Hz, CO_2CH_3), 45.8 (t, J_{C-H} = 130 Hz, CH_2), 31.6 (t, J_{C-H} = 132 Hz, CH_2), 30.8 (dd, J_{C-Rh} = 19 Hz, J_{C-H} = 137 Hz, Rh-CH), 29.4 (t, J_{C-H} = 132 Hz, CH_2).

$[CpRh(CH_2CHC(O)OCH_3)H(CH_2CHC(O)OCH_3)]^+[BAr'_4]^-$ (29). Complex **28** was prepared as described above using 15.1 mg (0.044 mmol) of **27** and 47.2 mg (0.047 mmol) of $H(Et_2O)_2BAr'_4$. Complex **28** was then redissolved in 0.65 mL of CD_2Cl_2 and cooled to −78 °C, at which temperature 32 μL (0.36 mmol) of methyl acrylate was added. The NMR tube was introduced into a precooled (−78 °C) NMR probe and gradually warmed to 15 °C, at which temperature it was kept for 15 min. Over this period of time, ca. 2–3 turnovers of MA to dimers had been achieved and complex **29** was generated cleanly. The tube was then cooled to −50 °C, and the products were characterized at this temperature, where dimerization is extremely slow. ^1H NMR (CD_2Cl_2, 300 MHz, −50 °C): δ 18.0 (sharp singlet at −80 °C, 1H, H), 5.52 (s, 5H, C_5H_5), 4.20 (ddd, 2H, J_{cis} = 8.9 Hz, J_{gem} = 3.6 Hz, J_{Rh-H} = 2 Hz, $CH_2CHCO_2CH_3$), 3.98 (ddd, 2H, J_{trans} = 11.5 Hz, J_{cis} = 8.9 Hz, J_{Rh-H} = 2.6 Hz, $CH_2CHCO_2CH_3$), 3.92 (s, 6H, OCH_3), 1.46 (ddd, 2H, J_{trans} = 11.5 Hz, J_{gem} = 3.6 Hz, J_{Rh-H} = 1.3 Hz, $CH_2CHCO_2CH_3$). ^{13}C NMR (CD_2Cl_2, 100 MHz, −50 °C): δ 184.4 (s, CO_2CH_3), 91.7 (dd, J_{C-Rh} = 5 Hz, J_{C-H} = 181 Hz, C_5H_5), 56.8 (q, J_{C-H} = 151 Hz, CO_2CH_3), 44.6 (dt, J_{Rh-C} = 13 Hz, J_{C-H} = 162 Hz, $CH_2CHCO_2CH_3$), 36.0 (dd, J_{Rh-C} = 13 Hz, J_{C-H} = 166 Hz, $CH_2CHCO_2CH_3$).

$Cp^‡Rh(C_2H_4)_2$ (30). A 500-mL three-neck round-bottomed flask fitted with a condenser was charged with 1.06 g (1.46 mmol) of $[Cp^‡RhCl_2]_2$ and 900 mg (8.49 mmol) of anhydrous sodium carbonate. Degassed ethanol (220 mL) was syringed into the flask, and ethylene was bubbled through the resulting suspension while it was being heated to 70 °C. The initial red suspension turned very dark within 15–20 min and finally to orange-brown (over the course of 1 h). It was kept overnight at 70 °C with an ethylene purge, and then the ethanol was removed under reduced pressure. In a glovebox, the solid residue was extracted three times with 50-mL portions of hexane, each of which was filtered through a plug of Celite. The solvent was removed from the combined extracts in vacuo, and the solid obtained was transferred to a 50-mL round-bottomed flask. On a high-vacuum line, hexane (30 mL) was vacuum transferred into the flask and the resulting solution was cooled to −78 °C to yield 375 mg of **30** as an orange-yellow solid. The solvent was removed from the filtrate and the oily residue sublimed (high vacuum, 60 °C), yielding an additional 375 mg of product (54% overall yield). Anal. Found (calcd): C, 48.67 (48.29); H, 5.74 (5.79). ^1H NMR (300 MHz, CD_2Cl_2, 23 °C): δ 2.08 (br, 4H, C_2H_4), 1.88 (s, 6H, $2CH_3$), 1.66 (q, J_{H-F} = 1.3 Hz, 6H, $2CH_3$), 1.45 (br, 4H, C_2H_4). ^{13}C NMR (100 MHz, CD_2Cl_2, 23 °C): δ 126.4 (q, J_{C-F} = 270 Hz, CF_3), C_{ipso} obscured, 102.5 (d, J_{Rh-C} = 4 Hz, C-CH_3), 95.6 (s, C-CH_3), 46.1 (dt, J_{Rh-C} = 14 Hz, J_{C-H} = 156 Hz, C_2H_4), 9.7 (q, J_{C-H} = 127 Hz, CH_3), 8.6 (q, J_{C-H} = 129 Hz, CH_3).

Generation and Spectroscopic Characterization of $[Cp^‡Rh(C_2H_4)(CH_2CH_2-\mu-H)]^+[BAr'_4]^-$ (31). An NMR tube was charged with 10.7 mg (0.031 mmol) of $Cp^‡Rh(C_2H_4)_2$ and 37.3 mg (0.037 mmol) of $H(Et_2O)_2BAr'_4$. The solids were dissolved at −78 °C in CD_2Cl_2, and the sample was characterized by ^1H NMR spectroscopy at −100 °C. ^1H NMR (400 MHz, CD_2Cl_2, −100 °C): δ 3.01 (br, 2H, C_2H_4), 2.76 (br, 2H, C_2H_4), 2.09 (br, 2H, C_2H_4), 1.81 (6H, $2CH_3$), 1.49 (6H, $2CH_3$), −8.76 (br, 1H, Rh···H). The missing C_2H_4 signal (2H) is presumably masked by the methyl signals. Complex **38** is unstable at 23 °C.

Generation and Spectroscopic Characterization of $[Cp^‡Rh(CH_2CH_2C(O)OCH_3)(C_2H_4)]^+[BAr'_4]^-$ (32). An NMR tube was charged with 9.0 mg (0.026 mmol) of $Cp^‡Rh(C_2H_4)_2$ and 28 mg (0.028 mmol) of $H(Et_2O)_2BAr'_4$. The tube was cooled to −78 °C, and CD_2Cl_2 (0.65 mL) was slowly added. After complete dissolution, 12 μL (0.133 mmol) of methyl acrylate was syringed into the tube, which was then introduced into a precooled (−80 °C) NMR probe. Complex **32** was generated immediately. For best signal resolution the tube was warmed to −20 °C. ^1H NMR (CD_2Cl_2, 400 MHz, −20 °C): δ 4.32 (m, 2H, C_2H_4), the methoxy signal is masked by the methoxy signal of free methyl acrylate at 3.71 ppm, 3.62 (m, 2H, C_2H_4), 3.26 (m, 1H, $C_2H_4CO_2CH_3$), 3.05–2.7 (m, 3H, $C_2H_4CO_2CH_3$), 1.71 (s, 3H, CH_3), 1.63 (s, 3H, CH_3), 1.59 (s, 3H, CH_3), 1.54 (s, 3H, CH_3).

$[Cp^‡RhCH(CH_2C(O)OMe)(CH_2CH_2C(O)OMe)]^+[BAr'_4]^-$ (33). A 50-mL Schlenk flask was charged with 51.4 mg (0.15 mmol) of $Cp^‡Rh(C_2H_4)_2$. The flask was cooled to 0 °C, and a solution of $H(Et_2O)_2BAr'_4$ (165 mg, 0.16 mmol) and methyl acrylate (270 μL, 3.0 mmol) dissolved in 10 mL of freshly distilled methylene chloride was transferred via cannula into the flask. The orange solution was warmed to room temperature with stirring. After 30 min, the solvent was removed under reduced pressure. The residue was washed with hexane (3 × 2 mL) to eliminate the dimer. Complex **33** was recrystallized from diethyl ether/hexane and isolated as orange crystals (142 mg, 72%). Anal. Found (calcd): C, 45.35 (45.20); H, 2.83 (2.81). ^1H NMR (300 MHz, CD_2Cl_2, 23 °C): δ 3.94 (s, 3H, CO_2CH_3), 3.87 (s, 3H, CO_2CH_3), the signal corresponding to H_a is presumably obscured by the methoxy resonance at ~3.90 ppm, 3.11 (dd, J_{Hb-Hc} = 19 Hz, $J_{Ha-Hb\ or\ Hc}$ = 9 Hz, H_b or H_c), 2.76 (d, J_{Hb-Hc} = 19 Hz, H_c or H_b), 2.52 (ddd, J = 18, 7, and 3 Hz, H_f or H_g), 2.21 (ddd, J = 18, 11, and 3 Hz, H_g or H_f), H_d and H_e are obscured by the methyl signals, 1.73 (br, 6H, CH_3), 1.62 (s, 3H, CH_3), 1.60 (s, 3H, CH_3). ^{13}C NMR (100 MHz, CD_2Cl_2, 23 °C): δ 191.2 (s, CO_2CH_3), 183.5 (s, CO_2CH_3), 125.3 (q, J_{C-F} = 272 Hz, CF_3), C_1 might be obscured by the signal at 129.3 (counterion signal), 103.2 (m, C_3), 102.5 (m, C_3), 95.2 (2 doublets, J = 7.4 Hz, C–Rh or C–F coupling, C_2's), 56.4 (q, J_{C-H} = 151 Hz, OCH_3), 55.5 (q, J_{C-H} = 151 Hz, OCH_3), 44.8 (br t, J_{C-H} ~ 127 Hz, CH_2), 41.1 (br dd, J_{C-Rh} = 21 Hz, J_{C-H} ~ 138 Hz, Rh-CH), 31.3 (br t, J_{C-H} = 128 Hz, CH_2), 29.7 (br t, J_{C-H} = 126 Hz, CH_2), 9.5 (q, J_{C-H} = 129 Hz, CH_3), 9.3 (q, J_{C-H} = 129 Hz, CH_3), 8.8 (q, J_{C-H} = 129 Hz, CH_3), 8.7 (q, J_{C-H} = 129 Hz, CH_3).

$[Cp^*Rh(\eta^3\text{-}MeC(O)CH_2CHCHCHCOMe)]^+[BAr'_4]^-$ (34). $Cp^*Rh(C_2H_4)_2$ (98 mg, 0.33 mmol) and $H(Et_2O)_2BAr'_4$ (406 mg, 0.40 mmol) were weighed in a drybox and transferred to a Schlenk flask. The solids were dissolved with stirring at −78 °C in 7 mL of methylene chloride. The solution turned orange immediately. Methyl vinyl ketone (1 mL, 12 mmol) was added at −78 °C, and the solution was warmed to room temperature with stirring. The initially orange solution turned a dark red-orange. After the mixture was stirred overnight at ambient temperature, the solvent and excess methyl vinyl ketone were removed under reduced pressure. The oily residue was washed with hexane (2 × 5 mL). Recrystallization from diethyl ether/hexane yielded 230 mg (56%) of orange crystals. Anal. Found (calcd): C, 48.28 (48.41); H,

3.37 (3.09). ^{1}H NMR (400 MHz, CD_2Cl_2, 23 °C): δ 5.46 (ddd, J_{Ha-Hb} = 11.3 Hz, J_{Hc-Hb} = 7.9 Hz, J_{Rh-Hb} = 2.2 Hz, H_b), 4.85 (ddd, J_{Hb-Hc} = J_{Hc-Hd} = 8.1 Hz, J_{Hc-He} = 2.0 Hz, H_e), 3.64 (dd, J_{Hd-Hc} = 8.1 Hz, J_{Hd-He} = 21.5 Hz, H_d), 3.07 (d, J_{Ha-Hb} = 11.3 Hz, H_a), 2.82 (dd, J_{He-Hd} = 21.5 Hz, J_{Hc-He} = 2 Hz, H_e), 2.29 (s, $COCH_3$) 2.25 (s, $COCH_3$), 1.68 (s, $C_5(CH_3)_5$). ^{13}C NMR (100 MHz, CD_2Cl_2, 23 °C): δ 230.2 (s, C=O), 198.9 (s, C=O), 101.1 (d, J_{C-Rh} = 7 Hz, $C_5(CH_3)_5$), 100.2 (dd, J_{C-Rh} = 5 Hz, J_{C-H} = 169 Hz, C_2), 78.6 (ddd, J_{C-Rh} = $^2J_{C-Hb}$ = 9 Hz, J_{C-H} = 165 Hz, C_3), 75.3 (ddd, J_{C-Rh} = $^2J_{C-Hb}$ = 9 Hz, J_{C-H} = 156 Hz, C_1), 49.1 (t, J_{C-H} = 127 Hz, C_4), 30.8 (q, J_{C-H} = 127 Hz, $COCH_3$), 28.5 (q, J_{C-H} = 132 Hz, $COCH_3$), 8.7 (q, J_{C-H} = 129 Hz, $C_5(CH_3)_5$).

[Cp*Rh(η^5-$CH_2CHCHCO_2CH_3$)]$^+$[BAr′$_4$]$^-$ (37). A 100-mL round-bottomed flask was charged with 73.7 mg (0.25 mmol) of $Cp^*Rh(C_2H_4)_2$ and 279 mg (0.28 mmol) of $H(Et_2O)_2BAr'_4$. The solids were dissolved at −78 °C in 10 mL of CH_2Cl_2, and methyl crotonate (530 μL, 5 mmol) was syringed into the solution. The solution was allowed to reach room temperature and stirred for 30 min. The solvent was then removed under vacuo, leaving an orange powder. After the powder was washed with three 2-mL portions of hexane, an orange powder remained (225 mg, 76%). In contrast to all of the cationic species described here, complex **37** is sparingly soluble in Et_2O and CH_2Cl_2. Anal. Found (calcd): C, 46.25 (46.53); H, 2.53 (2.80). ^{1}H NMR (400 MHz, acetone-d_6, 23 °C): δ 7.78 (8H, Ar′), 7.67 (4H, Ar′), 5.42 (m, H_3), 4.38 (d, J_{H3-H4} = 7.4 Hz, H_4), 3.83 (s, 3H, OCH_3), 3.12 (d, $J_{H3-H1\ or\ H2}$ = 10.4 Hz, H_1 or H_2), 2.84 (d, $J_{H3-H1\ or\ H2}$ = 11.9 Hz, H_1 or H_2), 1.74 (s, 15H, $C_5(CH_3)_5$). ^{13}C NMR (100 MHz, acetone-d_6, 23 °C): δ 171.4 (s, C=O), 162.6 (q, J_{C-B} = 50 Hz, $C_{1'}$), 135.5 (d, J_{C-H} = 159 Hz, $C_{2'}$), 130.0 (q, $^2J_{C-F}$ = 32 Hz, $C_{3'}$), 125.3 (q, J_{C-F} = 272 Hz, CF_3), 118.4 (d, J_{C-H} = 165 Hz, $C_{4'}$), 103.2 (dd, J_{C-Rh} = 5 Hz, J_{C-H} = 165 Hz, C_2), 101.2 (d, J_{C-Rh} = 7 Hz, $C_5(CH_3)_5$), 69.5 (dt, J_{C-Rh} = 9 Hz, J_{C-H} = 161 Hz, C_1), 67.7 (dd, J_{C-Rh} = 9.5 Hz, J_{C-H} = 168 Hz, C_3), 52.1 (q, J_{C-H} = 147 Hz, OCH_3), 8.8 (q, J_{C-H} = 130 Hz, $C_5(CH_3)_5$).

[$C_5(CH_3)_5$Rh[(C_5H_5N)CHCHCHCH$_2$(C_5H_5N)]]$^+$[BAr′$_4$]$^-$ (38). A Schlenk flask was charged with $Cp^*Rh(C_2H_4)_2$ (81.2 mg, 0.28 mmol) and 279 mg (0.28 mmol) of $H(Et_2O)_2BAr'_4$. After the solids were dissolved at −40 °C in 10 mL of CH_2Cl_2, 2-vinylpyridine (445 μL, 4.12 mmol) was added. The orange solution turned almost colorless immediately and then gradually more orange. Upon being warmed to room temperature, the solution turned red-orange. After being stirred overnight, the solvent was removed under vacuo. The residue was washed with hexane (3 × 3 mL). Recrystallization from methylene chloride/hexane yielded 277 mg (77%) of orange crystals. Anal. Found (calcd): C, 51.01 (51.32); H, 3.02 (3.08); N, 1.85 (2.14). ^{1}H NMR (CD_2Cl_2, 23 °C, 300 MHz): δ 8.65 (d, J = 7 Hz, $H_{1'}$), 8.46 (dd, J = 6 and 1.2 Hz, H_1), 7.66 (ddd, J = 9, 7, and 1.6 Hz, 2H, $H_{3'}$ and H_3), 7.35 (ddd, J = 7, 2.3, and 1.2 Hz, 1H, $H_{2'}$), 7.30 (d, J = 8 Hz, $H_{4'}$), 7.18 (d, J = 9 Hz, H_4), 7.04 (ddd, J = 9, 6, and 1.5 Hz, H_2), 6.92 (dd, J = 10 and 8 Hz, H_b), 6.48 (d, J = 10 Hz, H_a), 3.91 (m, H_c), 3.45 (dd, J = 18 and 7 Hz, H_d or H_e), 2.64 (dd, J = 18 and 10 Hz, H_d or H_e), 1.48 (s, 15H, $C_5(CH_3)_5$). ^{13}C NMR (CD_2Cl_2, 23 °C, 75 MHz): δ 169.6 (s, C_{ipso}), 155.3 (s, C_{ipso}). 10 sp^2 carbons could be observed, but none of them could be precisely assigned: 154.16 (dd, $^1J_{C-H}$ = 181 Hz, J_{C-H} = 1.7 Hz), 150.5 (d, J_{C-H} = 177 Hz), 149.23 (dd, $^1J_{C-H}$ = 155 Hz, J_{C-H} = 1.6 Hz), 138.81 (d, J_{C-H} = 166 Hz), 138.76 (d, J_{C-H} = 166 Hz), 126.7 (d, J_{C-H} = 152 Hz), 124.7 (d, J_{C-H} = 168 Hz), 123.92 (d, J_{C-H} = 170 Hz), 123.82 (d, J_{C-H} = 169 Hz), 121.92 (d, J_{C-H} = 159 Hz), 96.1 (d, J_{Rh-C} = 6.4 Hz, $C_5(CH_3)_5$), 48.6 (t, J_{C-H} = 129 Hz, CH_2), 45.0 (dd, J_{Rh-C} = 22 Hz, J_{C-H} = 139 Hz, Rh-*C*H), 9.1 (q, J_{C-H} = 128 Hz, $C_5(CH_3)_5$).

Acknowledgment. This work was supported by the National Science Foundation (Grant CHE-8705534) and duPont (H. E. Bryndza). S.S.-E. acknowledges partial support from a CNRS-NSF grant. We also thank Johnson Matthey for a loan of $RhCl_3$.

Supplementary Material Available: Tables of full GC data for (1) dimerization of MA (940 equiv) using **7** under 1 atm of H_2 at 25 °C (run 1), (2) dimerization of MA (2270 equiv) using **7** under 1 atm of H_2 at 25 °C (run 2), (3) dimerization of MA (7000 equiv) using **7** under 1 atm of H_2 at 25 °C (run 3), (4) dimerization of MA (2270 equiv) using **7** under 1 atm of N_2 at 25 °C, and (5) dimerization of MA (2270 equiv) using **11** as a catalyst precursor under 1 atm of N_2 at 25 °C, and of X-ray data for **9**, **10**, **23a**, and one isomer of $Cp^*Rh(MA)_2$, including fractional coordinates, isotropic thermal parameters, anisotropic thermal parameters, interatomic distances, intramolecular angles, intramolecular nonbonding distances, and intermolecular distances (38 pages). This material is contained in many libraries on microfiche, immediately follows this article in the microfilm version of the journal, and can be ordered from the ACS; see any current masthead page for ordering information.